

**An Accelerated Test Method for Predicting the Useful Life of an LED  
Driver**

by  
Lei Han

A Thesis Submitted to the Graduate  
Faculty of Rensselaer Polytechnic Institute  
in Partial Fulfillment of the  
Requirements for the Degree of  
MASTER OF SCIENCE  
Major Subject: LIGHTING

Approved:

---

Nadarajah Narendran, Ph.D., Thesis Adviser

---

Jean Paul Freyssinier, M.S., Member

Rensselaer Polytechnic Institute  
Troy, New York  
December, 2009

# CONTENTS

LIST OF TABLES.....	v
LIST OF FIGURES.....	vi
ACKNOWLEDGMENT.....	x
ABSTRACT.....	xi
1. Introduction.....	1
2. Literature Review.....	3
2.1 LED Electrical Characteristics.....	3
2.2 LED Current Control Method.....	5
2.3 Switch-Mode Power Supply Failure Analysis.....	10
2.4 Electrolytic Capacitors.....	11
2.5 Capacitor Ripple.....	17
2.6 Accelerated Life Test Methods.....	20
2.7 Literature Review Summary.....	22
3. Pilot Studies.....	23
3.1 LED Driver Topology Analysis.....	23
3.2 Estimation of LED Driver Component Failure Rate.....	25
3.3 Estimation of Impact of Degrading Electrolytic Capacitor on LED Driver Performance.....	26
3.4 Current Ripple.....	36
3.4.1 Impact of Current Ripple on LED Performance.....	36
3.4.2 End-of-life Criterion.....	38
4. Hypothesis.....	41
4.1 Thesis Objective.....	41
4.2 Term Definitions.....	41
4.3 Hypothesis 1.....	43
4.4 Hypothesis 2.....	44

4.5	Hypothesis 3.....	44
5.	Experimental Design .....	46
5.1	Experiment Variables.....	46
5.1.1	Hypothesis 1 Experiment Variables.....	46
5.1.2	Hypothesis 2 Experiment Variables.....	47
5.1.3	Hypothesis 3 Experiment Variables.....	47
5.2	Experimental Setup .....	48
5.3	Experimental Procedures .....	53
5.3.1	Experiment 1 Procedure.....	53
5.3.2	Experiment 2 Procedure.....	54
5.3.3	Experiment 3 Procedure.....	54
6.	Results.....	56
6.1	Experiment 1 Results .....	56
6.1.1	Measurement Repeatability.....	56
6.1.2	Sample to Sample Data .....	60
6.1.3	Data Processing Method .....	63
6.1.4	Hypothesis 1 Verification .....	66
6.1.5	Summary of Experiment 1 Results .....	66
6.2	Experiment 2 Results .....	67
6.2.1	Data Processing Method .....	67
6.2.2	Hypothesis 2 Verification .....	68
6.2.3	Summary of Experiment 2 Results .....	68
6.3	Experiment 3 Results .....	69
6.3.1	Data Processing Method .....	69
6.3.2	Hypothesis 3 Verification .....	77
6.3.3	Curve Fitting and Extrapolation for Lifetime Prediction.....	77
6.3.4	Summary of Experiment 3 Results .....	81

7. Discussion.....	82
7.1 Comparison of Impact of ESR and Capacitance Change on Output Current Ripple .....	82
7.2 Impact of Topologies of LED Drivers on Output Current Ripple .....	84
7.3 Component Lifetime vs. Application Lifetime .....	85
7.4 Limitations and Proposed Future Study.....	85
8. Summary.....	87
9. References.....	88
10. Appendix A: Statistical Analysis.....	93

## LIST OF TABLES

Table 5-1 Selection of the external resistance for LED driver A .....	49
Table 5-2 Selection of the external resistance for LED driver B .....	50
Table 5-3 Selection of the capacitance values for LED driver A .....	51
Table 5-4 Selection of the capacitance values for LED driver B .....	51

## LIST OF FIGURES

Fig 2-1 Typical forward voltage of different colored LEDs (Philips Lumileds, 2007) .....	4
Fig 2-2 Relative luminous flux vs. forward current for cool-white, neutral-white and warm-white, thermal pad = 25°C maintained (Philips Lumileds, 2009).....	4
Fig 2-3 Buck based non-isolated constant current regulator topology (Broeck, 2007) .....	6
Fig 2-4 Boost based non-isolated constant current regulator topology (Broeck, 2007) .....	7
Fig 2-5 Buck-boost based non-isolated constant current regulator topology (Broeck, 2007).....	7
Fig 2-6 Flyback based isolated constant current regulator topology (Broeck, 2007)	9
Fig 2-7 Distribution of failure for each power component in switch-mode power supplies (Imam, 2005) .....	11
Fig 2-8 Structure diagram of an electrolytic capacitor (Figure extracted from Precision Graphics).....	12
Fig 2-9 Equivalent circuit of an electrolytic capacitor (Imam, 2005) .....	13
Fig 2-10 An electrolytic capacitor’s typical impedance vs. frequency relationship (CDE, 2000).....	15
Fig 2-11 Change of capacitance & ESR during degradation process of an electrolytic capacitor (Evox Rifa, 2001).....	16
Fig 2-12 Output voltage AC portion waveforms with a good capacitor (Lahyani, 1998).....	18
Fig 2-13 Output voltage AC portion waveforms with a degrading capacitor (Lahyani, 1998).....	19
Fig 3-1 LED Driver A topology diagram (Standard flyback) .....	24
Fig 3-2 LED Driver B topology diagram (Single-stage PFC based flyback).....	24
Fig 3-3 An electrolytic capacitor at output stage of LED driver B .....	25
Fig 3-4 Distribution of failure for each power component of LED driver A & LED driver B .....	26
Fig 3-5 Simplified schematic of LED driver A power stage for PSpice simulation	29

Fig 3-6 LED driver A output current waveform simulation with A food capacitor (ESR = 0.72 $\Omega$ , capacitance = 100 $\mu$ F, $I_{pkpk}$ = 65 mA) .....	30
Fig 3-7 LED driver A output current waveform simulation with A degrading capacitor (ESR = 1.44 $\Omega$ , capacitance = 80 $\mu$ F, $I_{pkpk}$ = 125 mA).....	31
Fig 3-8 Simplified schematic of LED driver B power stage for PSpice simulation	33
Fig 3-9 LED driver B output current waveform simulation with A good capacitor (ESR = 0.16 $\Omega$ , capacitance = 330 $\mu$ F, $I_{pkpk}$ = 221 mA) .....	34
Fig 3-10 LED driver B output current waveform simulation with A degrading capacitor (ESR = 0.32 $\Omega$ , capacitance = 264 $\mu$ F, $I_{pkpk}$ = 279 mA).....	35
Fig 3-11 LED driver A output current ripple waveform .....	36
Fig 3-12 LED driver B output current ripple waveform.....	37
Fig 3-13 Impact of current ripple on light output & efficiency .....	37
Fig 3-14 Output current ripple trend simulation for LED driver B .....	40
Fig 3-15 An enlarged chart of output current ripple trend around transition point for LED driver B .....	40
Fig 4-1 Current ripple definition diagram .....	41
Fig 4-2 Capacitor temperature measurement location diagram.....	42
Fig 4-3 Relationship between ESR & frequency (330 $\mu$ F, Nichicon, PW(M), 50V, 5000 hrs @ 105 $^{\circ}$ C) .....	43
Fig 4-4 Output current ripple trend simulation (The solid vertical line illustrates the critical point when the end-of-life criterion is set.) .....	45
Fig 5-1 Experiment 1 setup diagram .....	48
Fig 5-2 Experiment 2 setup diagram .....	50
Fig 5-3 Experiment 3 setup diagram .....	52
Fig 6-1 Output current parameters vs. ESR for LED driver A #1 .....	56
Fig 6-2 Partial enlargement of Fig 6-1 .....	57
Fig 6-3 Standard deviation of output current parameters vs. ESR for LED driver A #1 .....	57
Fig 6-4 Output current parameters vs. ESR for LED driver A #2 .....	58
Fig 6-5 Output current parameters vs. ESR for LED driver A #3 .....	58
Fig 6-6 Output current parameters vs. ESR for LED driver B #1 .....	59

Fig 6-7 Output current parameters vs. ESR for LED driver B #2 .....	59
Fig 6-8 Output current parameters vs. ESR for LED driver B #3 .....	60
Fig 6-9 Relationship between output current mean and ESR for LED driver A #1, #2, #3 .....	61
Fig 6-10 Relationship between output current peak-to-peak and ESR for LED driver A #1, #2, #3 .....	61
Fig 6-11 Relationship between output current mean and ESR for LED driver B #1, #2, #3 .....	62
Fig 6-12 Relationship between ESR and output current peak-to-peak for LED driver B #1, #2, #3.....	63
Fig 6-13 Relationship between output current ripple and ESR of LED driver A #1 (Dotted lines represent 95% confidence level boundaries.) .....	64
Fig 6-14 Relationship between output current ripple and ESR of LED driver A #2 (Dotted lines represent 95% confidence level boundaries.) .....	64
Fig 6-15 Relationship between output current ripple and ESR of LED driver A #3 (Dotted lines represent 95% confidence level boundaries.) .....	65
Fig 6-16 Relationship between output current ripple and ESR of LED driver A (Dotted lines represent 95% confidence level boundaries.) .....	65
Fig 6-17 Relationship between output current ripple and ESR of LED driver B (Dotted lines represent 95% confidence level boundaries.) .....	66
Fig 6-18 Relationship between output current ripple and capacitance for LED driver A (Dotted lines represent 95% confidence level boundaries.) .....	67
Fig 6-19 Relationship between output current ripple and capacitance for LED driver B (Dotted lines represent 95% confidence level boundaries.).....	68
Fig 6-20 Output current parameter drift through degradation for LED driver A #3 (Tcap = 179 °C).....	70
Fig 6-21 Output current parameter drift through degradation for LED driver B #1 (Tcap = 174°C).....	71
Fig 6-22 Output current ripple and derivative for LED driver B #1 (Tcap = 174°C) .....	71

Fig 6-23 Output current ripple trends at different temperature cases for LED driver A #3 (The diamond dots represent end-of-life points respectively.).....	73
Fig 6-24 Lifetime profile of LED driver A #1, #2, #3.....	74
Fig 6-25 Output current ripple trends at different temperature cases for LED driver B #1 (The diamond dots represent end-of-life points respectively.).....	75
Fig 6-26 Lifetime profile of LED Driver B #1, #2, #3.....	76
Fig 6-27 LED drive A lifetime profile with piecewise exponential curve fitting ...	78
Fig 6-28 LED driver A lifetime prediction (Derating factor: 59 % / 10 °C).....	79
Fig 6-29 LED drive B lifetime profile with piecewise exponential curve fitting....	80
Fig 6-30 LED driver B lifetime prediction (Derating factor: 53 % / 10 °C).....	81
Fig 7-1 Capacitance change after 1800 hours exposed at 130 °C for LED driver B (decreased by 18%).....	83
Fig 7-2 ESR change after 1800 hours exposed at 130 °C for LED driver B (increased by 1360%).....	83
Fig 10-1 Relationship between output current ripple and ESR of LED driver A #1 (Dotted lines represent 95% confidence level boundaries.).....	93
Fig 10-2 Relationship between output current ripple and ESR of LED driver A #2 (Dotted lines represent 95% confidence level boundaries.).....	94
Fig 10-3 Relationship between Output Current Ripple and ESR of LED Driver A #3 (Dotted lines represent 95% confidence level boundaries.).....	95
Fig 10-4 Relationship between output current ripple and ESR of LED driver A (Dotted lines represent 95% confidence level boundaries.).....	96
Fig 10-5 Relationship between output current ripple and ESR of LED driver B (Dotted lines represent 95% confidence level boundaries.).....	96
Fig 10-6 Relationship between output current ripple and capacitance for LED driver A (Dotted lines represent 95% confidence level boundaries.).....	98
Fig 10-7 Relationship between output current ripple and capacitance for LED driver B (Dotted lines represent 95% confidence level boundaries.).....	99
Fig 10-8 Lifetime profile of LED driver A.....	100
Fig 10-9 Lifetime profile of LED driver B.....	101

## ACKNOWLEDGMENT

I'd like to express my gratitude to many people for helping me to finish this thesis at last. I am grateful to my advisor Dr. Nadarajah Narendran for his help, guide and encouragement. It is his vision and experience that helped me to pick up such a unique topic. It is his encouragement that helped me to cross the toughest hurdle in this study. He is the one who introduced me into the research realm, pushed me to challenge and refine myself. As my committee, Jean Paul Freyssinier willingly gave his time and energy to offer me precious comments and suggestions on my thesis. I am always thankful for his continuous help on my research work. I am thankful to Conan O'Rourke for his participation as my Master thesis committee despite heavy workloads. His insight and experience are most appreciated. I will always be grateful to Dr. Nadarajah Narendran, Jean Paul Freyssinier and Conan O'Rourke for all they do as my mentors, guides and friends. I happened to meet all three of you before I came to LRC and was lucky enough to complete my final assignment of LRC with your help. I also would like to thank Terry Klein for offering me suggestions and intriguing thoughts in this study. I am thankful to Jennifer Taylor for her help with my writing as she always does. I am grateful to Andrew Bierman and John Bullough for their valuable advices on statistical analysis in this study. I would like to thank my classmates and colleagues, Tianming Dong, Yiwei Liu, Yiting Zhu, Keng Chen, Yinan Wu, Rosa Capo, Daniel Miller, Xing Zhang, Dan Wang, Tracy Meyer, Oindrila and so on for their continuous encouragement and help. I am especially grateful to the LRC's directors Mark Rea and Russell Leslie and to LRC director of research Nadarajah Narendran and all LRCers for providing such a supportive atmosphere for me to study and do research here. I would like to thank NYSTAR and Future Energy Systems Center for Advanced Technology, and the ASSIST program sponsors for providing financial support for this study.

## ABSTRACT

This study demonstrated an accelerated life test method for off-line LED drivers that use electrolytic capacitors at the output stage. Estimating the failure rate of power components suggests that the electrolytic capacitor used at the output stage of an off-line light emitting diode (LED) driver is the weakest link among all components. As an electrolytic capacitor degrades, its capacitance decreases and its equivalent series resistance (ESR) increases, both effects contributing to the increase of output current ripple of the LED drivers. Thus, the amplitude of the output current ripple is a good indicator of the degradation level of the output electrolytic capacitor. This study focuses on the parametric type of failure of the LED driver. In this study, temperature was selected as the acceleration factor because LED drivers are usually exposed to elevated temperatures in typical application environments. The current ripple is experimentally found to have a negative impact on light output and efficacy. So the useful life for LED drivers is proposed as the time it takes to reach a point when the rate of change of output current ripple reaches a maximum. Then the relationship between the capacitor's positive pin temperature and the useful life of the LED driver was established using the proposed useful life definition. The accelerated life test shows that the LED driver's useful life is shortened exponentially as the output electrolytic capacitor's operating temperature increases. Although this method may not be applicable to every LED driver on the market, it begins to identify methods that can be used for predicting the useful life of LED drivers of similar topologies.

## 1. Introduction

Lighting emitting diodes (LED) are beginning to experience widespread use in many lighting applications. One of the promises it offers is long operating life. A few commercial high power (HP) LEDs have achieved over 100 lm/W in luminous efficacy, and a guaranteed 50,000 hours of lifetime, which are competent enough to challenge traditional light sources. As an example, Cree's XP-G LEDs (2009) have minimum efficacy of 114 lm/W. However, LED itself cannot be directly used in lighting applications. An LED is a low voltage (2.5 V – 4.0 V) direct current (DC) driven semiconductor component. In most cases, the available power source such as 120V AC (Alternating Current) is not suitable to drive LEDs directly. Therefore, an LED lighting system requires a driver to handle the power conversion from AC unregulated voltage input to DC regulated current output.

An LED lighting system is composed of LED light sources, LED drivers, secondary optics, and heat sinks all working together to deliver the required lighting goals. The reliability of an LED lighting system depends on the weakest component of the system. Even though an LED light source's lifetime can be very long, typically about 50,000 hours (Philips Lumileds, 2009), the LED driver lifetime can be shorter and therefore shorten the lifetime of the whole system.

The goal of this thesis is to develop an accelerated test method that could be used for predicting the useful life of an LED driver in typical application environments. The temperatures seen in application environments range from 25°C in the non-insulated ceiling condition to up to around 100°C in the insulated ceiling condition (Jayasinghe, 2006). The scope of work in this study is limited to ambient temperatures greater than 25°C.

An LED driver can be built as an independent power supply or as being integrated into luminaires. This study mainly focuses on the type of LED drivers that is considered as an independent power supply. They are known as discrete offline LED drivers, which

can be directly powered by the grid (120V AC), convert AC to DC, and deliver constant current output that is suitable for driving a string (or strings) of LEDs.

An LED driver will either fail catastrophically (no output current) or parametrically. Parametric failure for LED drivers means driver parameters shift from original designed value. Generally, an LED driver is rated at 350 mA  $\pm$  5% for output current. For example, if this driver has an output current of 400 mA, it is considered parametrically failed. This study mainly focuses on the type of parametric failure for LED drivers.

This study first started with a comprehensive literature review to understand the LED's electrical characteristics, common off-line LED driver topologies, SMPS (Switch-Mode Power Supply) failure analysis, electrolytic capacitors and their impact on reliability of SMPS, and accelerated life test methods. Based on literature survey findings, two types of commercial LED drivers were selected to be analyzed in terms of topology and reliability. Estimations of component failure rate for the selected LED drivers were performed to understand the weakest link candidate in a driver system. A few pilot studies were conducted to understand the reliability issue of the individual component considered as the weakest link. A PSpice commercial circuit simulation software was performed to study the impact of the degradation of the weakest component in an LED driver on the driver's output current parameters. Another pilot study was conducted to evaluate how typical current ripples would influence the LED's efficacy and light output. Considering the negative impact of current ripples on LED's performance, a preliminary definition of end-of-life of the selected LED drivers was proposed based on output current parameter shift, and, several hypotheses were developed that are applicable to different LED drivers. Then a final experimental setup was made to experimentally investigate the relationship between the weakest link component in an LED driver and the driver's output current parameter shift. At the end, an accelerated life test method was developed to predict the useful lifetime of the off-line LED drivers in typical application environments.

## 2. Literature Review

### 2.1 LED Electrical Characteristics

An LED is one special type of semiconductor diodes, thus, it shares the common electrical characteristics of a typical diode, such as directional current flow capability, and exponential relationship between forward current and voltage.

A high power LED's rated forward current varies from 350 mA to 1500 mA typically, much higher than indicator type LEDs (Steigerwald, 2002). High power LEDs' forward voltage has a large manufacturing tolerance. Take the Philips Lumiled's Luxeon Rebel for example, its forward voltage ( $V_f$ ) varies from 2.55 to 3.99V for cool-white, neutral-white, warm-white, green, cyan, blue, and royal-blue types of LEDs (2009). The typical value of the forward voltage is 3.15V at 350mA. The variation of  $V_f$  is about  $\pm 27\%$ . The forward voltage is also dependent on temperature. Luxeon Rebel has a typical negative temperature coefficient of forward voltage of  $-2.0\text{mV}/^\circ\text{C}$  (Philips Lumileds, 2009). That means when the junction temperature increases from  $25^\circ\text{C}$  to  $100^\circ\text{C}$ , there is another 0.15V forward voltage drop. When the strings of a series of LEDs are used in lighting applications, these accumulative forward voltage variations are further magnified, posing serious challenge to drivers' accurate current control capabilities.

The current-voltage relationships of a typical high power LED of various colors are revealed in Fig 2-1. It shows that LED current grows exponentially with some minor increase in forward voltage, implying that a small voltage variation across an LED has a high propensity to overdrive or underdrive it.

The luminous flux of LEDs is mostly determined by the driving current at a given temperature (Fig 2-2) (Philips Lumileds, 2009). Therefore, in order to achieve uniform light output, constant current control is the preferable method to drive LEDs, especially for the color mixing lighting applications (Muthu, 2002). Using constant current driving method will avoid violating the absolute maximum current limitation and compromising

the reliability, and obtain more predictable and matched luminous intensity and chromaticity (Maxim, 2004).

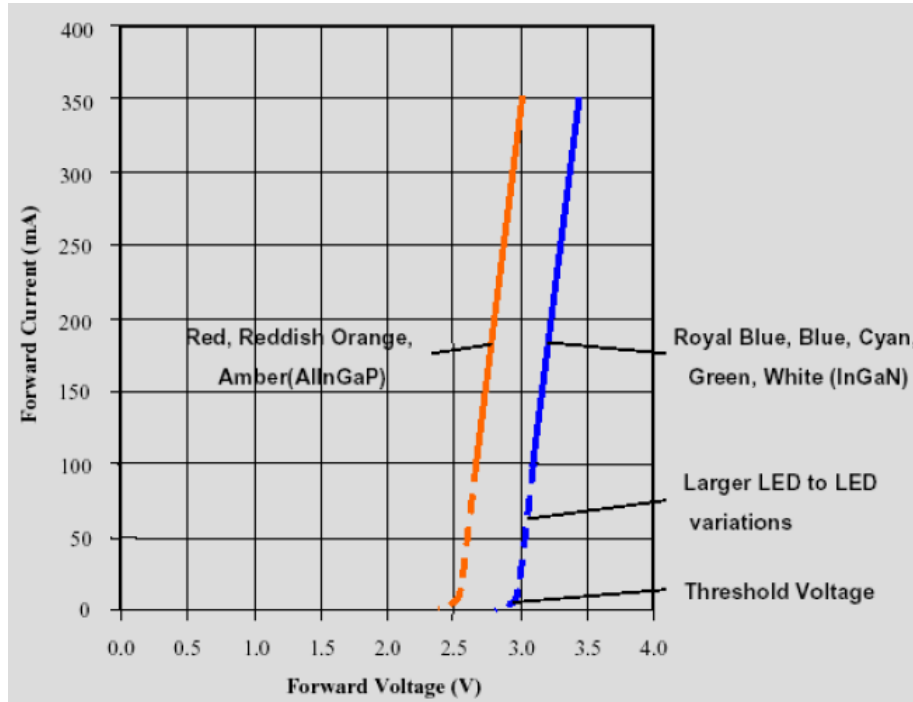


**Fig 2-1 Typical forward voltage of different colored LEDs (Philips Lumileds, 2007)**

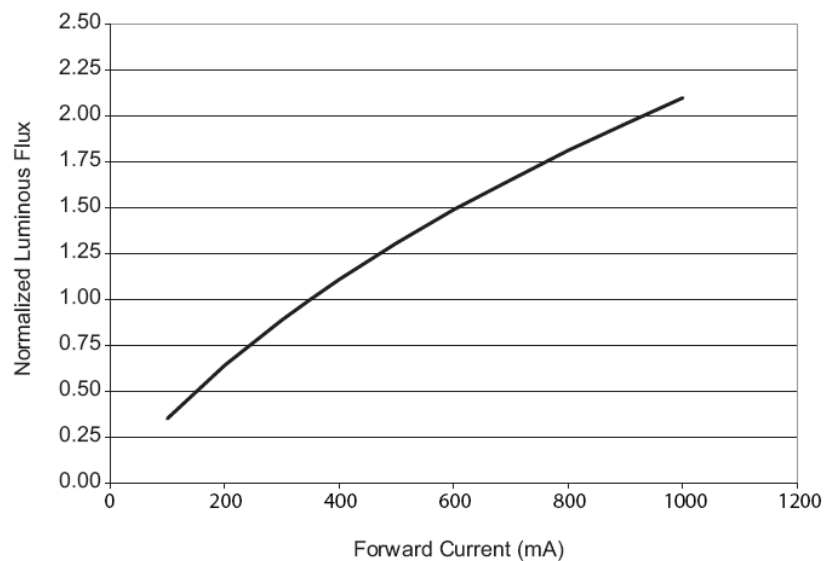


**Fig 2-2 Relative luminous flux vs. forward current for cool-white, neutral-white and warm-white, thermal pad = 25°C maintained (Philips Lumileds, 2009)**

## 2.2 LED Current Control Method

LEDs are usually characterized at one or several nominal ideal DC currents by manufacturers (Philips Lumileds, 2009; Cree, 2007; GE, 2009; Seoul Semiconductor, 2008). However, the generation of a pure DC constant current requires sophisticated and expensive power electronics technologies (Sauerlander, 2006). In fact, selecting a practical current control method and topology is a trade-off between accuracy of rated current, efficiency, reliability, cost, and component size (Ronat, 2006).

LED driver topologies differ considerably depending on the specific application requirements such as the input and output voltages, the overall power consumption, isolation for UL safety requirement, power factor correction for harmonics compliance and ENERGY STAR requirements (Department of Energy, 2008), and dimming function. The common current control methods include the use of current limiting resistors, linear voltage regulators, non-isolated switch-mode converters such as buck converters, boost converters, buck-boost converters and single ended primary inductor (SEPIC) converter, galvanic isolated switch-mode converters such as flyback converters and so on.

The use of a current limiting resistor is the simplest and cheapest current control solution, but not optimized for system efficiency. The current limiting resistor is connected in series with the LED or a string of LEDs to provide necessary extra voltage drop from the main DC voltage bus. The higher the difference between input voltage and required forward voltage, the lower the efficiency will be. This method actually does not provide constant current regulation control. If there is some forward voltage drift across LEDs, then the LEDs' operating current will accordingly shift (Broeck, 2007; Avago Technologies, 2007).

The linear voltage regulator based current control method has better current regulating performance. It acts like an active variable resistor, providing good constant current regulation performance. This kind of driver's power loss is determined by the sum of the voltage dropout between input and output of the linear regulator and the voltage drop

over the sampling resistor. Since there is usually a requirement for minimum input-output voltage drop due to the structure of linear voltage regulator, the loss over the linear regulator is phenomenal at heavy load conditions. Also, the heat dissipation problem due to its inherent relatively low efficiency performance will pose reliability issue for electronic components, and compromising driver's lifetime (Avago Technologies, 2007).

Switch-mode based topologies are known to improve system efficiency greatly (Bhandarkar, 2008). Switch-mode converters are usually designed to output stabilized voltages. However, an LED requires a stabilized constant output current. Classical non-isolated topologies such as buck, boost, and buck-boost converters can be modified for stabilizing output current. Fig 2-3, Fig 2-4 and Fig 2-5 show constant current switch-mode regulator topologies based on buck, boost, and buck-boost converters respectively. This is achieved by adding a sense resistor  $R_s$  in series to the LEDs. The forward voltage drop across the sense resistor is proportional to the LED current, and is used to provide a feedback to the comparator. Then the comparator generates an error signal to adjust the duty ratio of the Pulse Width Modulation (PWM) module to achieve stabilization of output LED current.

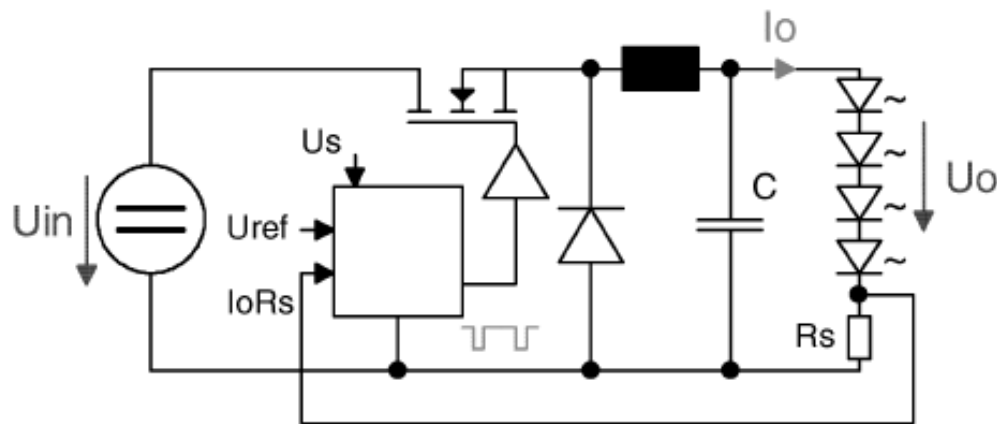


**Fig 2-3 Buck based non-isolated constant current regulator topology (Broeck, 2007)**

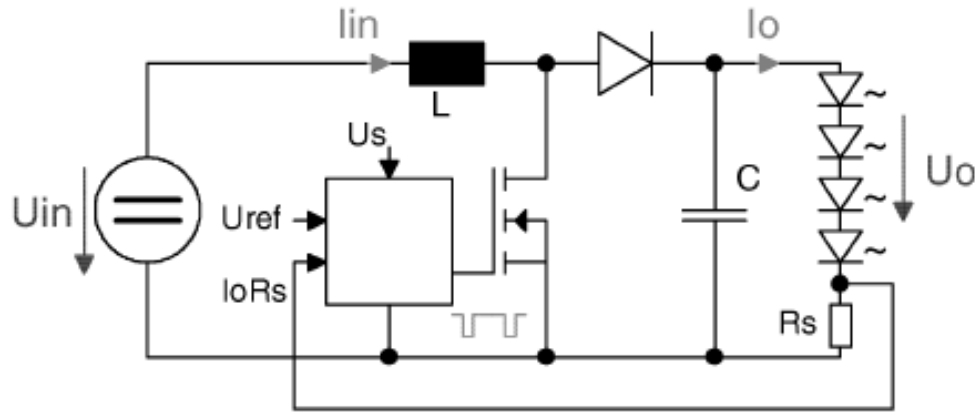


**Fig 2-4 Boost based non-isolated constant current regulator topology (Broeck, 2007)**

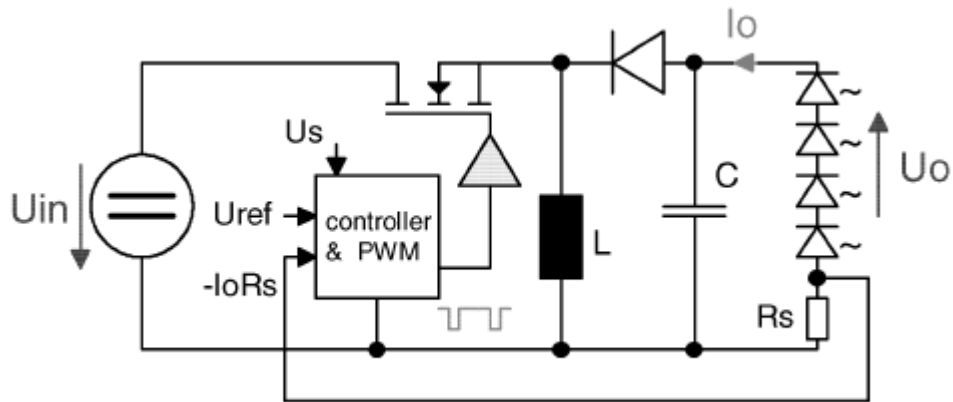


**Fig 2-5 Buck-boost based non-isolated constant current regulator topology (Broeck, 2007)**

In all of the above-mentioned cases, the measured forward voltage across the sampling resistor should be kept small relative to the total forward voltage drop of the LED or LED strings so as to minimize power losses, suggesting that the value of the sampling resistor should be as low as possible. Nevertheless, too low a value of resistance could render the feedback loop incapable of accurately responding to the change in LED current due to low Signal-to-Noise (S/N) level. An optional Op-Amp (Operational Amplifier) based amplifier stage can be added after the sampling resistor to magnify the forward voltage across the sampling resistor to increase S/N issue and provide adequate reference voltage level for feedback loop. Other power losses include forward voltage of

the freewheeling diode, conduction and switching losses over the switcher, which is usually realized by a MOSFET (Metal Oxide Semiconductor Field Effect Transistor). Off-the-shelf switch-mode voltage regulators can be configured to serve as constant current regulators by using current sensing resistors. The problem is that they are not optimized for applications such as LED drivers. The internal voltage reference is too high considering the loss over the sampling resistor under high current situations (Avago Technologies, 2007). There are new switch-mode regulators optimized for LED driver applications with extra low voltage reference requirements. The non-isolated constant current converter topologies can achieve up to 95% in terms of efficiency (National Semiconductor, 2009).

Galvanic isolated converter topologies (Fig 2-6) such as forward, flyback and push pull types can also be implemented to drive LEDs, in which the comparator and error amplifier are on the secondary side while the pulse width modulation (PWM) controller is on the primary side (Broeck, 2007). The galvanic isolated topology has the advantage of protective isolation between line voltage and the load of LEDs, but with the expenses of relatively more complicated design and conversion loss. The electrical isolation is achieved by the transformer and the optical coupler providing both power stage and feedback channels. Similarly, it also adopts a sampling resistor connected in series with the LED string to provide reference voltage proportional to the forward current of the LED string. The conversion losses include the transformer loss, power transistor's switching and conduction loss, diode forward voltage loss and so on. The typical efficiency of a galvanic isolated topology ranges from 70% to 85% (Rubinstein, 2007).

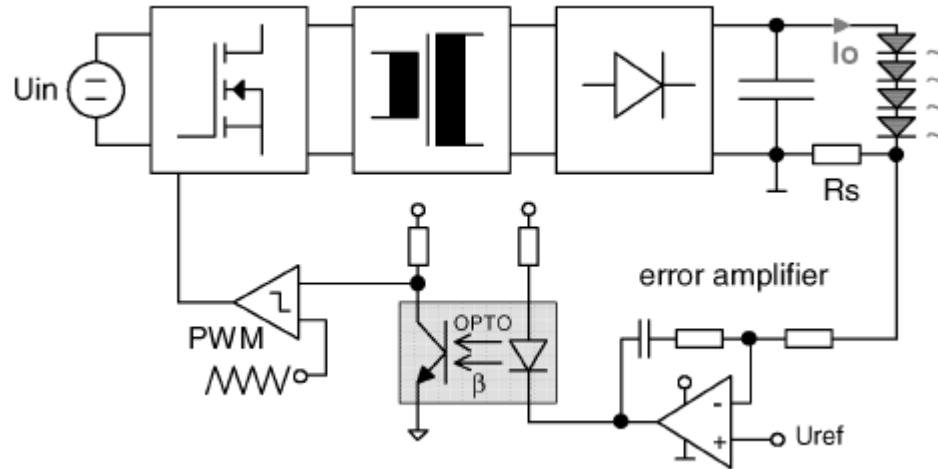


**Fig 2-6 Flyback based isolated constant current regulator topology (Broeck, 2007)**

LED lighting system can be divided into two categories, luminaires and integrated LED lamps (Green, 2009). The first category utilizes an independent off-line LED driver which requires electrical isolation and output voltage less than 60VDC or 30VAC rms according to UL8750 Class 2 limits. The second category is usually designed for retrofit use, and the LED driver circuitry is contained within sealed enclosures and is mechanically isolated so that no electrical isolation is required. The galvanic isolated topologies such as flyback converters are suitable for the first category, while the non-isolated topologies such as buck converters are more suitable to meet the second category's requirements.

In practice, the organization that sets energy standards stipulates a minimum power factor value of 0.7 for residential lighting applications and 0.9 for commercial lighting applications (Department of Energy, 2008). This requires the mandatory use of power factor correction (PFC) circuitry in the LED driver design, which would affect the off-line LED driver topologies.

Power factor correction can be realized passively by using a valley-fill filter or actively by using a PFC integrated circuit (IC) usually working as a boost converter (ON Semiconductor, 2007). Considering PFC and isolation requirements, the traditional

topology solution involves a PFC front-end stage and a cascaded flyback stage. This two-stage cascaded topology exerts excellent PFC performance with the expense of some extra conversion loss and relatively high passive component count. An improved solution takes advantage of a single-stage transition-mode PFC controller based flyback topology to realize both good current regulation and superior power factor performance and relatively lower component cost, which has been adopted by a few commercial off-line constant current LED drivers from various manufacturers.

This thesis study mainly focuses on two types of commercial off-line independent constant current LED drivers from two different manufacturers. One is a standard flyback converter, and the other is a single-stage PFC based flyback converter.

### **2.3 Switch-Mode Power Supply Failure Analysis**

The topologies of LED drivers are similar to those of switch-mode power supplies (SMPS) (Broeck, 2007). Therefore, understanding the failure modes of switch-mode power supplies helps to study LED drivers' reliability issue.

Part stress analysis method provided by Military Handbook 217F (1991) is commonly used to calculate an electronic equipment's reliability based on individual component's failure rate models. A typical example of the part failure rate model is the product of the base failure rate and several other affecting factors as shown below.

$$\lambda_p = \lambda_b \times \pi_T \times \pi_P \times \pi_A \times \pi_Q \times \pi_E \quad (\text{Eq. 2-1})$$

where  $\lambda_p$  is the part failure rate,  $\lambda_b$  is the base failure rate, and  $\pi_T$  and other  $\pi$  factors are the various acceleration factors that modify the base failure rate such as part quality, voltage stress, operating temperature, and use environment. It should be pointed out that the assumed failure modes include both catastrophic and permanent drift failures like falling out of rated tolerance bounds. And the failure rate model assumes a constant failure rate over time. (Military Handbook 217F, 1991)

Lahyani (1998), Venet (2002) and Imam (2005) among others have used this part stress analysis method in the study of static converter and switch-mode power supplies to calculate the failure rate of each power component. The results (Fig 2-7) showed that the electrolytic capacitors used to smooth the output voltage appear to have the highest probability of failure and account for over 50% of the breakdowns in switch-mode power supplies. The failure of electrolytic capacitors can often cause secondary failures such as transistor failure, regulation failure and unstable output (Fromm, 1994; Bennett, 2000).

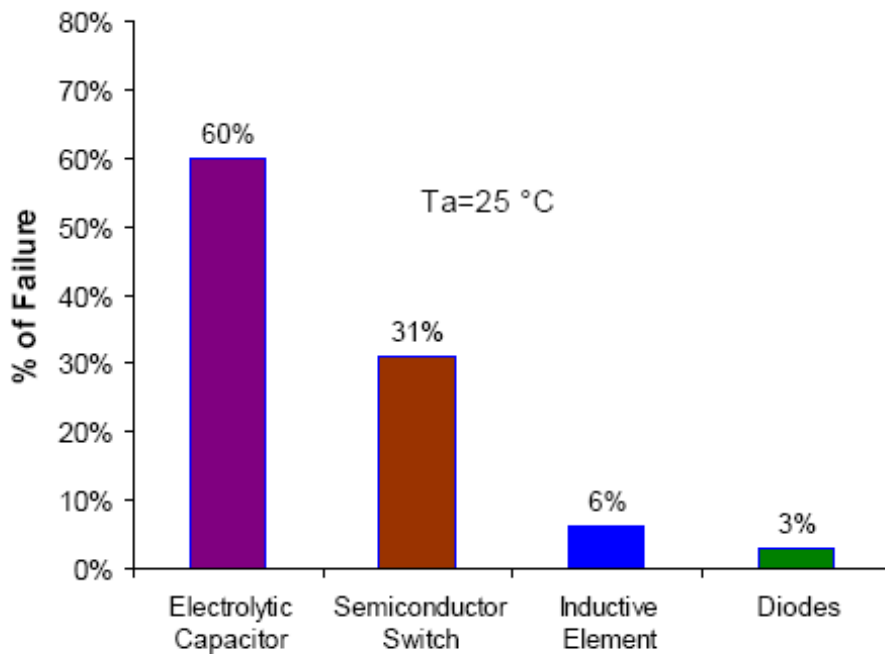


**Fig 2-7 Distribution of failure for each power component in switch-mode power supplies (Imam, 2005)**

## 2.4 Electrolytic Capacitors

Since electrolytic capacitors are estimated to be the weakest link in SMPS applications, it is worth studying the characteristics and reliability of electrolytic capacitors.

Fig 2-8 shows the structure of an electrolytic capacitor. It is composed of positive and negative charge connections, cathode aluminum foil, electrolytic paper, electrolyte, and

an aluminum oxide film acting as the dielectric which is formed on the anode foil surface. This very thin oxide film boasts superior dielectric constant and presents rectifying properties. Besides, this aluminum foil is etched so that the effective surface area is greatly enlarged (Nichicon, 2002).

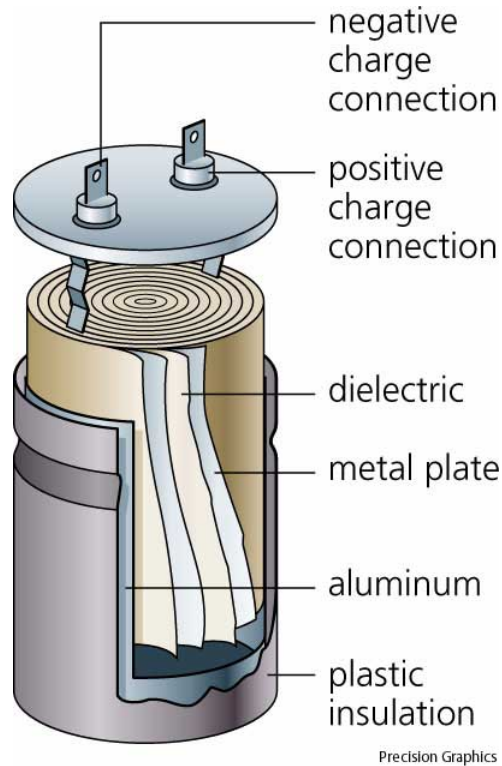


**Fig 2-8 Structure diagram of an electrolytic capacitor (Figure extracted from Precision Graphics)**

The capacitance of a given capacitor is defined by the following equation:

$$C = 8.855 \times 10^{-8} \frac{\epsilon S}{d} (\mu F) \quad (\text{Eq. 2-2})$$

where  $\epsilon$  is the dielectric constant,  $S$  is the surface area of dielectric, and  $d$  is the thickness of dielectric. Accordingly, the capacitance can be enlarged by selecting material of high dielectric constant, increasing the surface area, or decrease the thickness of the dielectric layer (United Chemi-Con, 2003).

The dielectric constant of aluminum electrolytic capacitors is not significant. However, the aluminum oxide dielectric layer can be controlled to be very thin. And with the etching technique, the effective area of the aluminum foil can be 100 times larger than the apparent area for low voltage capacitors and 40 times for middle and high voltage capacitors (Nichicon, 2002; United Chemi-Con, 2003). Therefore, the aluminum capacitor has higher capacitance per unit volume than other types of capacitors like film, ceramic and tantalum capacitors. This is why electrolytic capacitors are often the preferred choice in power electronics applications where high capacitance and limited physical dimension are required.

An actual electrolytic capacitor can be equivalent to an ideal capacitor connected in series with some resistive part and some inductive part, as shown in Fig 2-9.

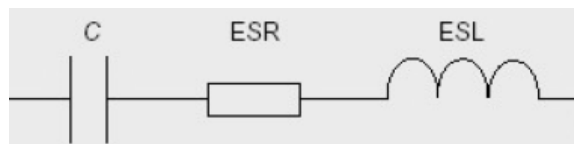


**Fig 2-9 Equivalent circuit of an electrolytic capacitor (Imam, 2005)**

The equivalent series resistance (ESR) is the sum of electrolytic resistance, dielectric loss and electrode resistance (Harada, 1993). ESR decreases as frequency of measurement or temperature increases, and increases with rated voltage (Gasperi, 1996; CDE, 2000; United Chemi-Con, 2003). According to CDE's (2000) application guide, ESR decreases steadily with increasing frequency, and then crosses over to a constant value. The crossover frequency is typically below 10kHz for aluminum electrolytic capacitors. This crossover frequency is inversely proportional to capacitance, so that the ESR of high-capacitance capacitors doesn't change much with increasing frequency. Typical values of ESR vary from 0.01  $\Omega$  to 1  $\Omega$ . For a given rated voltage, ESR is inversely proportional to capacitance due to the physical construction of an electrolytic capacitor (CDE, 2000; United Chemi-Con, 2003).

ESL is the equivalent series inductance of an electrolytic capacitor. ESL is mainly due to the capacitor terminal spacing and is not affected by frequency and temperature (CDE, 2000; United Chemi-Con, 2003). Typical values of ESL for radial-leaded types of aluminum electrolytic capacitors are in the range of 10nH to 30nH (CDE, 2000). The impedance of an electrolytic capacitor can be expressed by the following equation:

$$Z = \frac{1}{j\omega C} + j\omega L + R \quad (\text{Eq. 2-3})$$

where  $Z$  is the impedance,  $C$  is the capacitance,  $L$  is the equivalent series inductance, and  $R$  is the equivalent series resistance. The absolute value of the impedance is expressed as:

$$|Z| = \sqrt{R^2 + \left(\omega L - \frac{1}{\omega C}\right)^2} \quad (\text{Eq. 2-4})$$

Fig 2-10 shows the relationship between impedance and frequency for a typical aluminum electrolytic capacitor. The impedance is dominated by the capacitance in the frequency lower than about 1kHz. In the frequency range of about 10kHz, the impedance becomes dominated by the ESR. When it comes to the frequency range higher than 100kHz, the inductive reactance becomes increasingly dominant. The lowest point is at the self-resonant frequency:

$$f = \frac{1}{2\pi\sqrt{LC}} \quad (\text{Eq. 2-5})$$

where the impedance equals to the ESR.

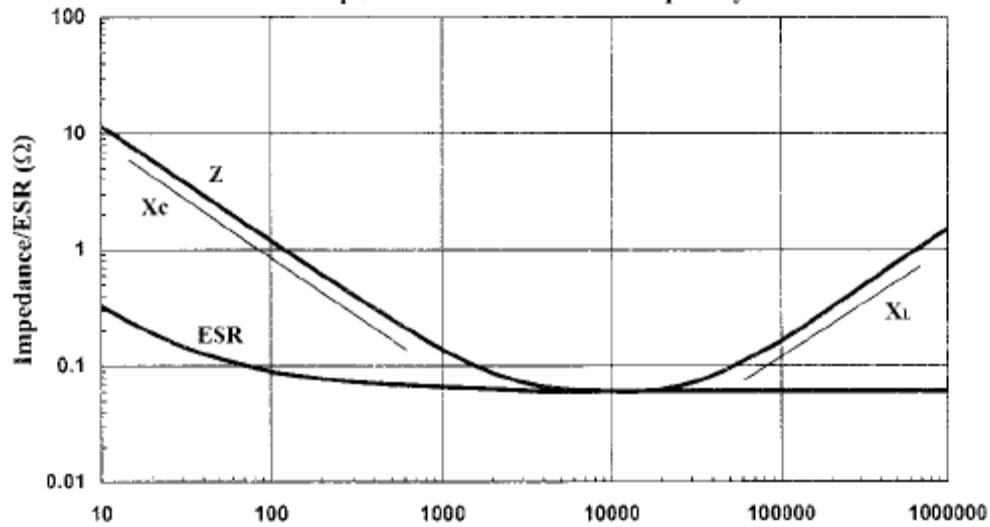


**Fig 2-10 An electrolytic capacitor's typical impedance vs. frequency relationship (CDE, 2000)**

From a design point of view, the square of RMS current multiplied by the ESR of an electrolytic capacitor results in self heating of the capacitor, which is detrimental to its reliability (Mandelcorn, 2009). So, the value of ESR for a given electrolytic capacitor is one of the critical factors that affect the lifetime of an electrolytic capacitor used in switch-mode converter applications.

The major wear-out mechanism of electrolytic capacitors is evaporation and deterioration of electrolyte due to elevated ambient temperature or internal temperature. The reduction of electrolyte volume would cause a decrease of the effective surface area, and cause the decrease of the capacitance and increase of ESR (Harada, 1993; Lahyani, 1998; Gasperi, 1996; Sankaran, 1997; Matsushita, 2000; Stevens, 2002; Evox Rifa, 2001). Fig 2-11 shows the change of capacitance and ESR respectively during degradation process of an electrolytic capacitor.

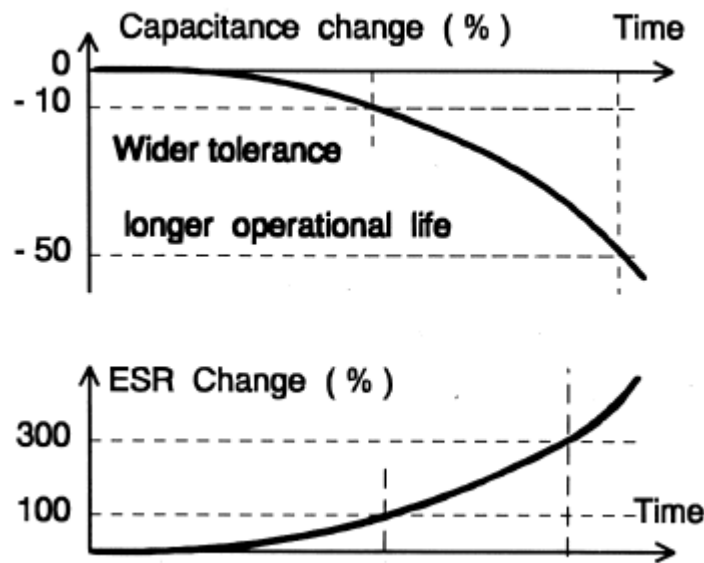


**Fig 2-11 Change of capacitance & ESR during degradation process of an electrolytic capacitor (Evox Rifa, 2001)**

Elevated ambient temperature or internal temperature will accelerate the vaporization of electrolyte. The core temperature of an electrolytic capacitor determines the lifetime of that capacitor (BHC Components, 2002). A basic rule of thumb for estimating the lifetime of an electrolytic capacitor states that life is shortened by half for every 10°C increase in operating temperature (Gasperi, 1996; Nichicon, 2002, Panasonic, 2008; CDE, 2000). In other words, the temperature derating for the lifetime of an electrolytic capacitor is 50% / 10°C.

Electrolytic Capacitor manufacturers typically define the end-of-life of an electrolytic capacitor as either a 10 - 20% of decrease in capacitance (measured at  $f = 120\text{Hz}$ ), or 200% of increase in ESR measured at 25°C (measured at  $f = 120\text{Hz}$ ) (Nichicon, 2002; BHC Components, 2002; CDE, 2000; Panasonic, 2008).

However, the end of life definition for a given electrolytic capacitor in specific application is actually governed by application requirements. Only when the increase of ESR or decrease of capacitance begins to deteriorate the application's performance can it

be considered the electrolytic capacitor in that application has been compromised. For applications where only small changes in capacitance and ESR are tolerable, the actual useful lifetime of an electrolytic capacitor could be shorter than if the applications are more tolerant.

On the other hand, a given electrolytic capacitor's degradation rate could be largely distinctive under different operating conditions. The useful lifetime of an electrolytic capacitor decreases exponentially as its core temperature increases. The core temperature is the sum of ambient temperature and an additional temperature increase caused by internal self-heating mechanism that is mainly related to the ESR and current ripple. The additional temperature increase is quantified by  $I^2R$  loss, where  $I$  is the AC current RMS (Root-Mean-Square) value, and  $R$  is the ESR of the capacitor. The heat generated due to the capacitor's ESR will contribute to the increase of the capacitor's core temperature during operation, which further deteriorate the operating condition of that capacitor and accelerate the degradation process. In a sense, both the ambient temperature and the current ripple applied to an electrolytic capacitor will accelerate the degradation rate of an electrolytic capacitor. The electrolytic capacitor's actual useful lifetime in application depends heavily on the specific application requirement and operating conditions.

## **2.5 Capacitor Ripple**

Although ESR and capacitance are two good indicators of a given electrolytic capacitor's degradation level, they are very difficult to measure directly in applications. However, capacitor current and voltage ripples are promising indirect indicators of an electrolytic capacitor's condition.

Lahyani (1998) found that electrolytic capacitors used at the output filter stage affect the performance of the static converter. ESR is the best indicator of the output filter electrolytic capacitor fault in static converter applications. And, the peak-to-peak value of the output voltage, which equals to the output capacitor voltage, increases with respect to ESR increase.

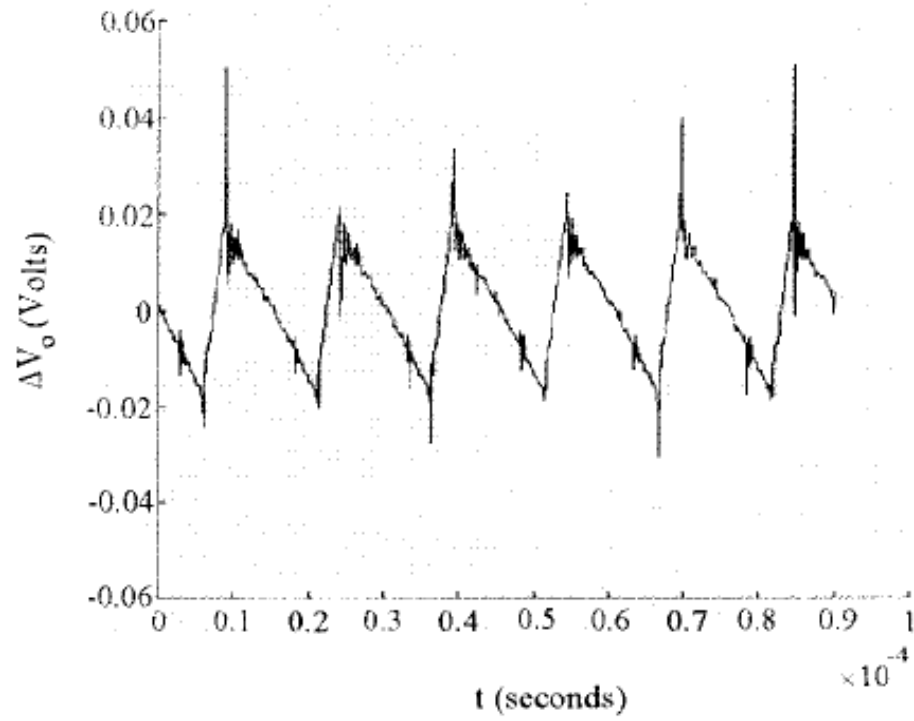


**Fig 2-12 Output voltage AC portion waveforms with a good capacitor (Lahyani, 1998)**

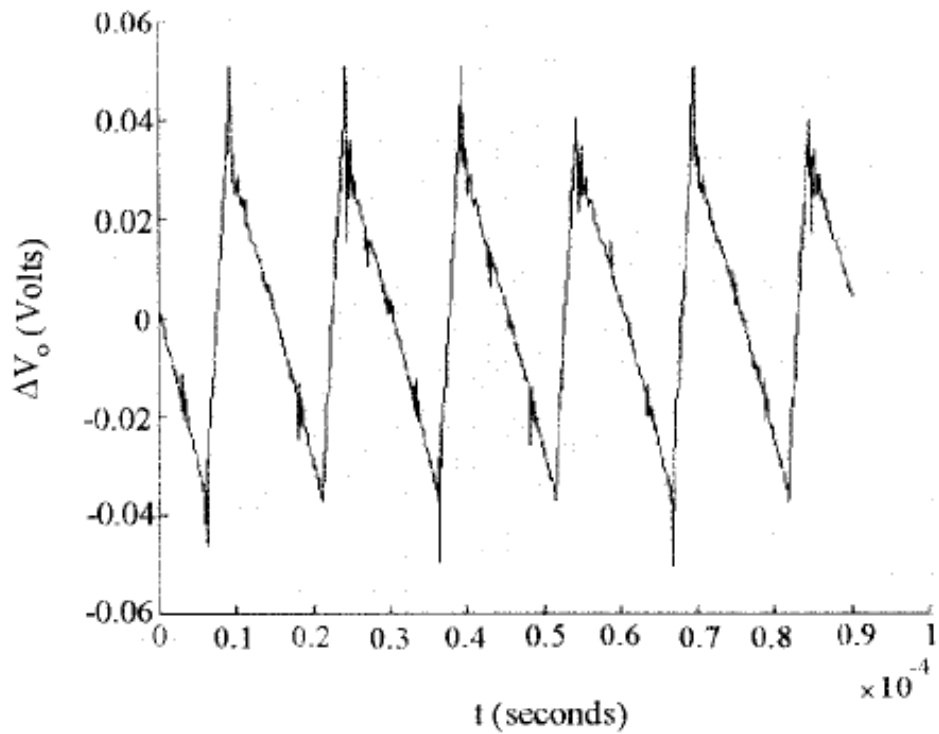


**Fig 2-13 Output voltage AC portion waveforms with a degrading capacitor (Lahyani, 1998)**

Fig 2-12 shows the AC portion of output voltage waveforms of a static converter with a good output capacitor. Fig 2-13 shows the AC portion of output voltage waveforms of a static converter with a degrading output capacitor. It is obvious that the peak-to-peak amplitude of the output voltage increases as the output capacitor degrades.

Venet (1999) showed that the degradation of the electrolytic capacitor used in static converter applications affects its filter function much more than its storage function. Since the filter function is mainly influenced by its ESR while the storage function is realized by its capacitance, Venet's finding implies that the aging caused ESR increase could be much more significant than the capacitance decrease.

Imam (2005) depicted that signatures of changes in capacitance and ESR are reflected in capacitor voltage and current ripple. He demonstrated a predictive method for the

capacitor status by analyzing capacitor voltage ripple using adaptive filter modeling technique.

These studies indicated that monitoring capacitor voltage and/or current ripple, which is a reflection of its ESR and capacitance change, is one way to indirectly predict the status of the electrolytic capacitor.

## **2.6 Accelerated Life Test Methods**

The normal degradation process of a given system could take years to see a noticeable change in practice. In order to rapidly predict the useful lifetime of a system, accelerated life tests are often used to study the characteristics of the degradation process at extreme conditions. Commonly used stress parameters include temperature, voltage, humidity, vibration and so on. The way of applying the stress parameter could be continuous or cycling (ReliaSoft, 2007).

The procedure of the accelerated life test method includes choosing the desired acceleration factor, acquiring lifetime data as a function of the selected acceleration factor, data fitting and extrapolation to typical environment in applications.

The accelerated life test method has been widely used in studying the reliability of electronic components, such as LED-based white light sources (Narendran, 2005), electrolytic capacitors in automotive applications (Sankaran, 1997), high K multilayer ceramic capacitors (Minford, 1982), and electronic power transformers (Dakin, 1965).

In Narendran's (2005) white LED reliability study, a definition of end-of-life of LEDs is proposed as light output reaches 70% of initial level. The accelerating variable here is the ambient temperature. Several LEDs were operated at their rated current but exposed to different ambient temperatures. A mathematical exponential curve fit was used to extrapolate the data and estimate life. Then the estimated life of the white LEDs as a function of the temperature at T-point where the manufacturers recommend attaching a

temperature sensor was plotted. The relationship between T-point temperature and life shows that the useful life decreases exponentially with increasing temperature.

Minford (1982) chose three manufacturers' 50 V multilayer ceramic capacitors to evaluate their lifetime. The capacitors tested were 0.22  $\mu\text{F}$  rated at 50 V dc. The accelerating variable is temperature and voltage. The voltage was increased at a rate of 10V/s. Each capacitor is connected in series with a resistor so that the voltage drop across the series resistor is measured to calculate the resistance of the capacitor. The failure criterion for the accelerated life test is when the resistance at the test temperature degraded three to four orders of magnitude below its equilibrium value at the test temperature. The acquired data sets demonstrated that the times to failure at a voltage-temperature stress conformed to a lognormal distribution with a standard deviation of about 0.5. Then the failure rate was calculated as a function of operating time at 85°C and 50Vdc by extrapolating from the results of the 0.22  $\mu\text{F}$  capacitors tested.

In Dakin's (1965) study of electronic power transformer, the principle aging factor is elevated temperature. Failure is determined by the loss of the insulation ability to function under normal operating and environmental conditions. Failure of the insulation is defined as a direct short circuit between coils or turns at normal operating voltage. The transformers used in the experiments were rated at 250 VA at 220 V rms on the primary. A thermal couple was placed between the two secondary windings, at a point found to be the hot spot. Hot spot temperatures were maintained in the transformers by the driving current. Three hot spot aging temperatures were chosen as, 200, 225, and 250°C. Ambient temperature was maintained at about 95°C in all of these tests by using a large circulating air oven. Each aging period was followed by the environmental cycle. The transformers were first cooled to room temperature and vibrated, and then followed by a cold shock for 2 hours at -55°C. It was then followed by the humidity cycle of 48 hrs. The next aging period was then started. Only the time at the controlled hot spot aging temperature was counted in the life of the transformer. Totally 5 different life test cycles and test temperatures were used, namely, including all environmental conditions, including thermal cycling, cold shock & humidity, including thermal cycling and cold

shock, including only thermal cycling, and, constant temperature aging without thermal cycling. The results follow the Arrhenius life-temperature relations. By extrapolation, an average life of the order of 60,000 hours at Class F, 155°C temperature was calculated.

## **2.7 Literature Review Summary**

It is desired to use constant current control method to drive high power LEDs in lighting applications. The constant current LED drivers' topologies are similar to those of SMPS. For SMPS applications, electrolytic capacitors are found to have the highest probability of failure. As an electrolytic capacitor degrades, the capacitance decreases while ESR increases. Heat affects an electrolytic capacitor's useful life. ESR and capacitance change are good indicators of the status of an electrolytic capacitor, and are reflected in capacitor voltage and current ripple. So, by monitoring the capacitor voltage or current ripple, it is possible to tell the degradation level of an electrolytic capacitor in application. An electronic equipment's useful life in application environments could be predicted from accelerated life testing data. However, no study was found addressing accelerated life testing or life prediction of LED drivers.

### 3. Pilot Studies

#### 3.1 LED Driver Topology Analysis

As mentioned before, two types of commercial off-line independent constant current LED drivers from two different manufacturers were selected to conduct detailed analysis in this thesis study.

LED driver A is a standard flyback converter, and its topology diagram is shown in Fig 3-1. This driver utilizes a monolithic fixed frequency current mode controller integrated with a power MOSFET to achieve a flyback topology. This design simplifies the peripheral design and reduces the number of discrete electronic components. The efficiency of this driver at full power output is about 75%. But without an active power factor controller built inside, this driver achieves a power factor value of around 0.6.

LED driver B is a single-stage PFC based flyback converter. Its topology diagram is shown in Fig 3-2. This driver is designed to use a Power Factor Correction IC (Integrated Circuit) working in critical conduction mode to serve as both a front-end power factor corrector and a flyback controller. At full power output, it is able to achieve typically 0.95 for power factor, and 80% for efficiency. The tradeoff is its relatively high output current ripple due to its slow outer feedback loop tuned to optimize the performance of power factor correction. The output current ripple can be further smoothed by using another stage of low dropout linear regulator with the sacrifice of lower efficiency and increased number of electronic components, or by using a large capacitance filter capacitor, which is the solution in LED driver B.

The flyback topology is one type of indirect converter so that an energy storage module is necessary to conduct power conversion. During the switcher on period, the input energy is stored in the primary side of the flyback transformer, while at the same time the output capacitor discharges to maintain required output power. During the switcher off period, the energy stored in the primary side is transferred to the secondary side, charging the output capacitor and providing required output power (Kassakian, 1991).

Since the secondary inductor current of a flyback converter is discontinuous, an output capacitor is necessary to realize a continuous output current. An electrolytic capacitor is used at the output stage of both of these two LED drivers (Fig 3-3).

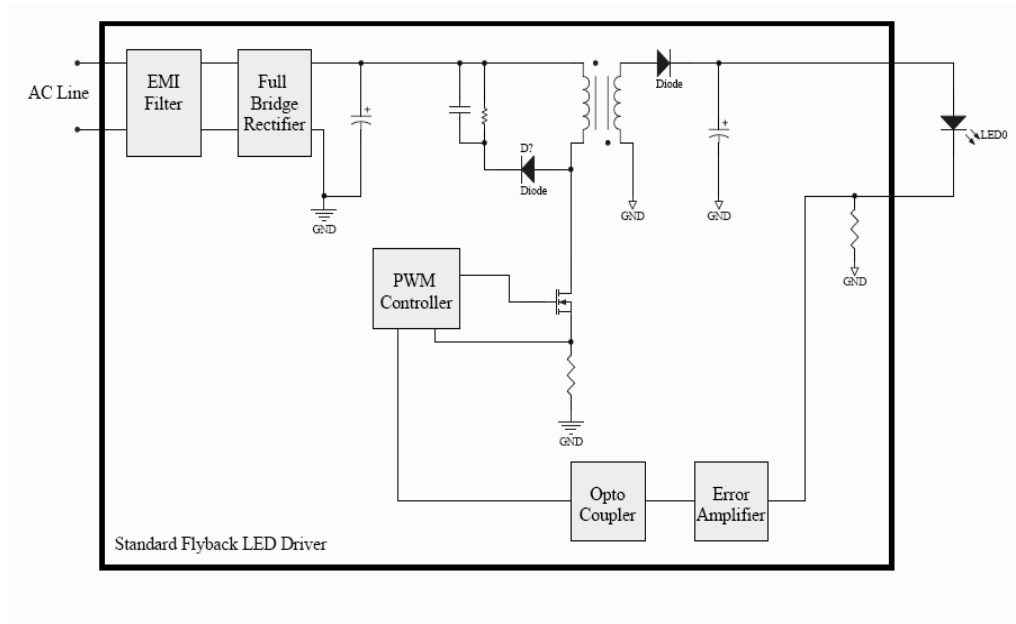


**Fig 3-1 LED Driver A topology diagram (Standard flyback)**

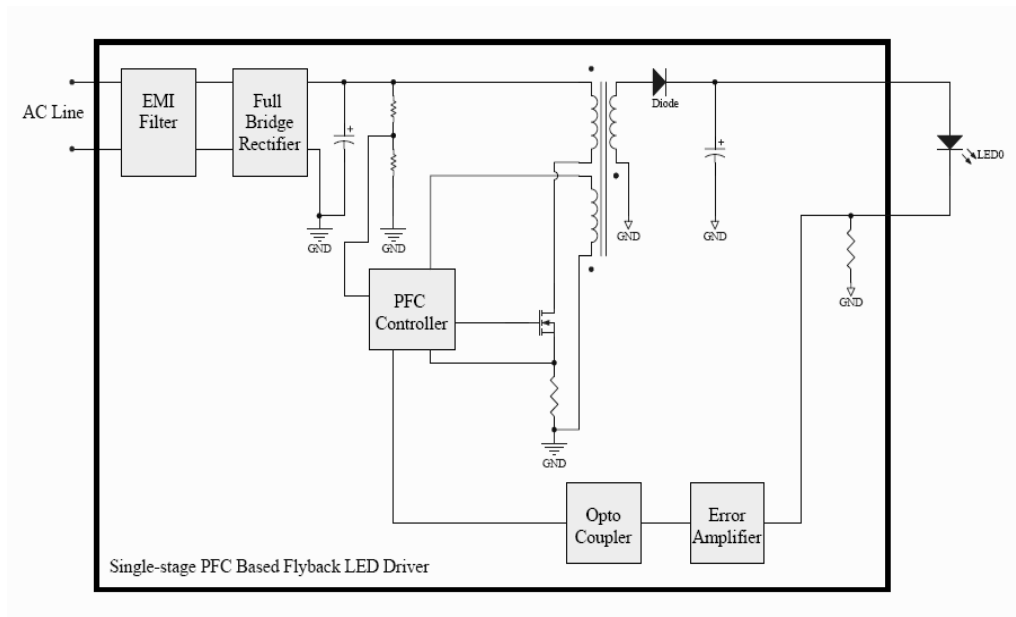


**Fig 3-2 LED Driver B topology diagram (Single-stage PFC based flyback)**



**Fig 3-3 An electrolytic capacitor at output stage of LED driver B**

### **3.2 Estimation of LED Driver Component Failure Rate**

By understanding the topologies of the LED drivers, it is possible to perform an estimation of power component failure rate using models proposed in Military Handbook 217F (1991), which was commonly used to evaluate component reliability for electronic equipments. Only power components were considered in the following estimation, because the failure rate of power circuits is found to be much higher (typically 20:1) than that of digital and linear circuits (Military Handbook 217F, 1991).

Fig 3-4 shows the calculation results of power component failure rate for both LED driver A and LED driver B. The electrolytic capacitors used at the output stage of the LED drivers appear to have the highest probability of failure and are responsible for more than half of the breakdowns in both cases. The component of the next highest

failure rate is MOSFET or flyback transformer. This is consistent with estimation results of power component failure rate of SMPS.

Although the estimation result is based on the reliability models derived from limited amount of experiments, it sheds light on the possible candidate of the weakest link in an LED driver system.

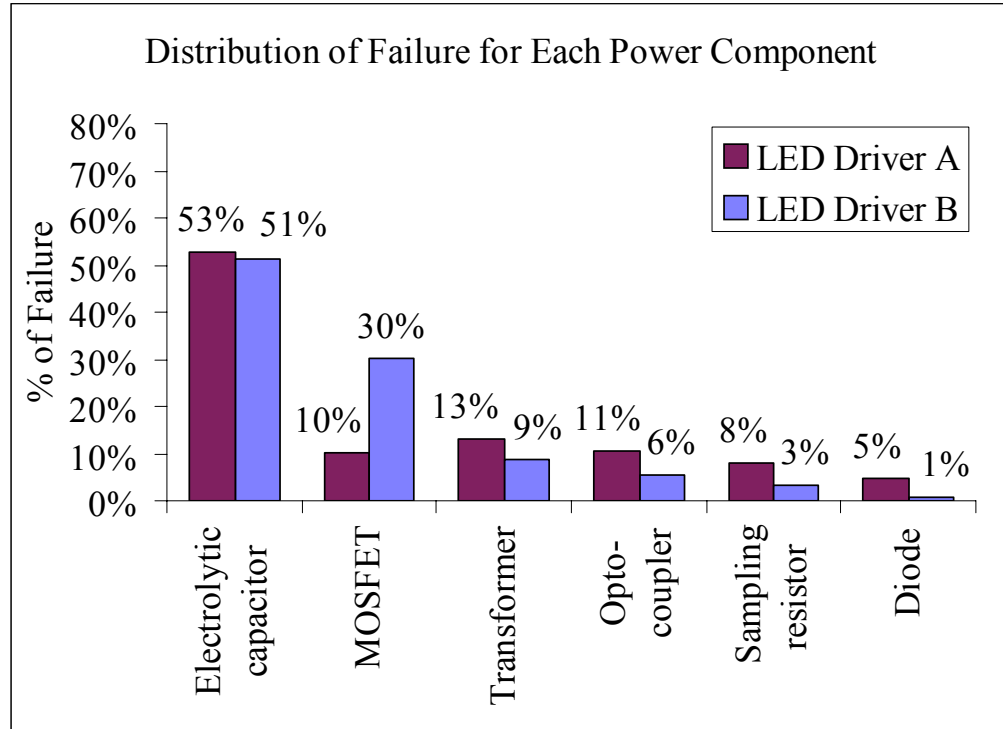


**Fig 3-4 Distribution of failure for each power component of LED driver A & LED driver B**

### **3.3 Estimation of Impact of Degrading Electrolytic Capacitor on LED Driver Performance**

Since the electrolytic capacitor used at the output stage of the two LED drivers is estimated to be the weakest link and thus it limits the life of the LED driver, it is desired to analyze the impact of the degradation of the electrolytic capacitor on the LED driver's performance. The estimation is realized by both analytical derivation and circuit simulation.

The objective of this pilot study is to derive the relationship between output current peak-to-peak amplitude and capacitance and ESR of the output filter capacitor, and to simulate output current waveforms using a good capacitor and a degrading capacitor at the output stage of LED driver A and LED driver B.

LED driver A is a standard flyback topology converter as shown in Fig 3-1. Applying charge balance analysis shows that the secondary inductor's current is the same as the load current on average. The output current ripple is mainly due to the discontinuous secondary inductor current (Kassakian, 1991). Assume that the feedback loop's bandwidth is lower than the switching frequency, and output current mean value  $I_o$  is kept constant by feedback loop. Considering the 1st order current ripple gives following equations (Kassakian, 1991).

$$V_o = \frac{D}{1-D} \cdot \frac{N_s}{N_p} \cdot V_{in} - V_D \quad (\text{Eq. 3-1})$$

$$D = \frac{V_o + V_D}{\frac{N_s}{N_p} \cdot V_{in} + V_o + V_D} \quad (\text{Eq. 3-2})$$

$$V_{o\text{pk-pk}} = \frac{I_o \cdot D}{C_o \cdot F_{sw}} \quad (\text{Eq. 3-3})$$

$$\Delta I_{o\text{pk-pk}} = \frac{I_o \cdot D}{C_o \cdot F_{sw} \cdot (R_{LED} + R_{sense})} \quad (\text{Eq. 3-4})$$

where  $V_{in}$  is the input DC bus voltage,  $V_o$  is the output voltage,  $V_{o\text{pk-pk}}$  is the output voltage peak-to-peak value,  $I_{o\text{pk-pk}}$  is the output current peak-to-peak value,  $D$  is the duty ratio,  $\frac{N_s}{N_p}$  is the turns ratio of the flyback transformer,  $V_D$  is the forward voltage drop across the flyback diode,  $F_{sw}$  is the switching frequency,  $C_o$  is the capacitance of the output filter capacitor,  $R_{LED}$  is the equivalent resistance of the LED string, and  $R_{sense}$  is the resistance of the sampling resistor connected in series with the load.

Now taking ESR into consideration gives the following modified equations (Kassakian, 1991).

$$V_o = \frac{D}{1-D} \cdot \left( \frac{N_s}{N_p} \cdot V_{in} - I_o \cdot R_{ESR} \right) - V_D \quad (\text{Eq. 3-5})$$

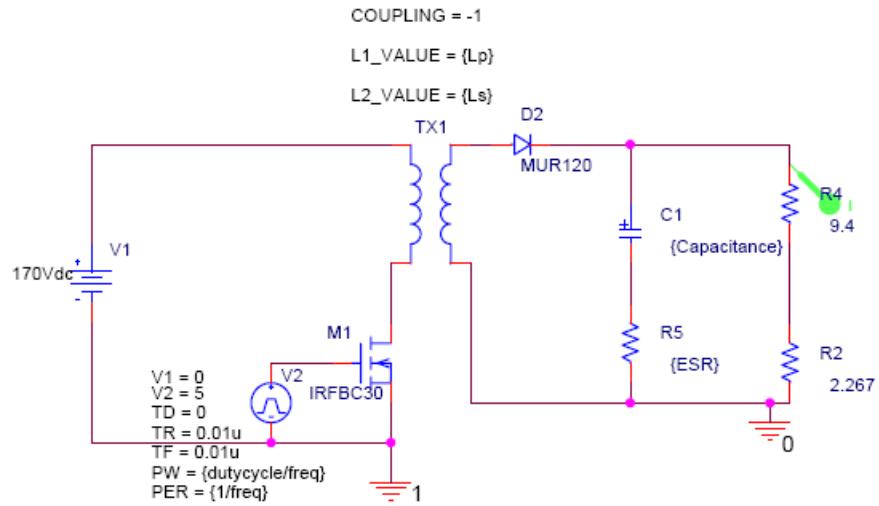
$$D = \frac{V_o + V_D}{\frac{N_s}{N_p} \cdot V_{in} - I_o \cdot R_{ESR} + V_o + V_D} \quad (\text{Eq. 3-6})$$

$$V_{o\text{pk-pk}} = \frac{I_o \cdot D}{C_o \cdot F_s} + \frac{I_o}{1-D} \cdot R_{ESR} \quad (\text{Eq. 3-7})$$

$$I_{o\text{pk-pk}} = \frac{I_o \cdot D}{C_o \cdot F_s \cdot (R_{LED} + R_{sense})} + \frac{I_o}{1-D} \cdot \frac{R_{ESR}}{R_{LED} + R_{sense}} \quad (\text{Eq. 3-8})$$

where  $R_{ESR}$  represents the equivalent series resistance of the output filter capacitor. It can be seen that as the capacitance  $C_o$  drops, the output current peak-to-peak value  $I_{o\text{pk-pk}}$  will increase. Similarly, as  $R_{ESR}$  increases, the duty ratio  $D$  will increase and the output current peak-to-peak value  $I_{o\text{pk-pk}}$  will also increase. Therefore, as the output electrolytic capacitor degrades, its capacitance decreases and its ESR increases, both causing an increase in the output current peak-to-peak value in the case of LED driver A.

Fig 3-5 shows a simplified schematic of the power stage of LED driver A for PSpice simulation (V9.2). A resistor connected in series with the output capacitor C1 was used to represent ESR part of the capacitor. A resistance of  $9.4 \Omega$  was used to represent an HP LED load at 350 mA. The switching frequency was selected at 65 kHz, which was the actual measured value for LED driver A. A transient time domain simulation was performed to observe the output current waveforms.



**PARAMETERS:**

freq = 65kHz  
duty cycle =  $\{(I_o \cdot (9.4 + 2.267) + 1) / (170 / N - I_o \cdot ESR + I_o \cdot (9.4 + 2.267) + 1)\}$   
Lp = 4mH  
Ls =  $\{L_p / (N \cdot N)\}$   
N = 8  
ESR = 0.72  
Capacitance = 100uF

**Fig 3-5 Simplified schematic of LED driver A power stage for PSpice simulation**

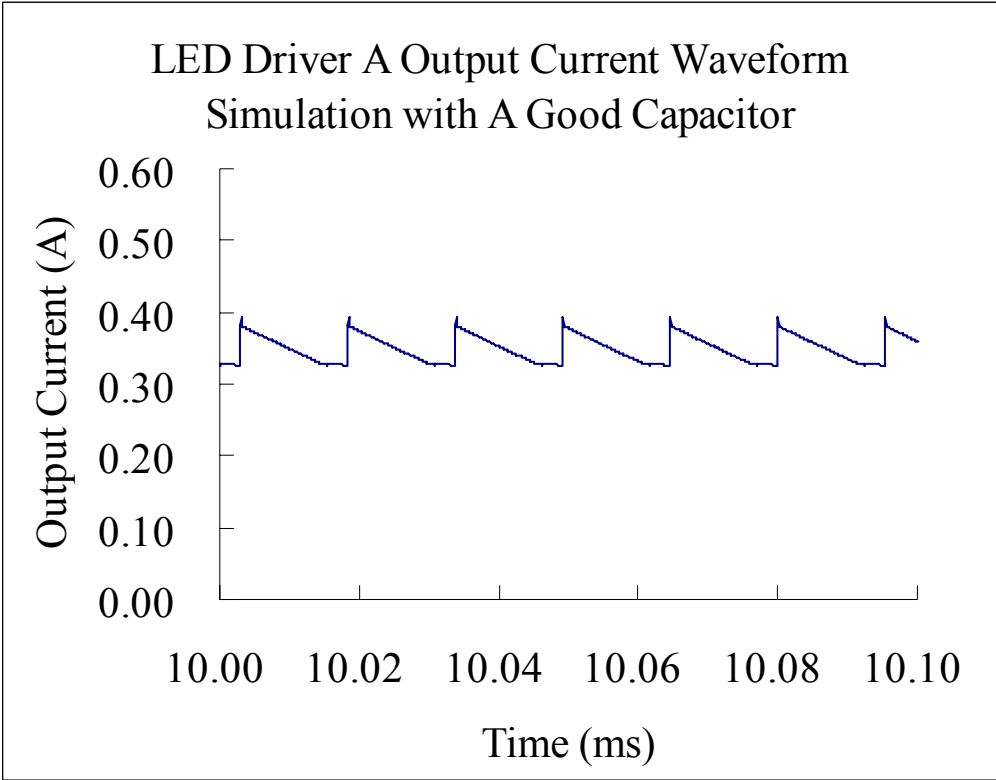


**Fig 3-6 LED driver A output current waveform simulation with A food capacitor (ESR = 0.72  $\Omega$ , capacitance = 100  $\mu$ F,  $I_{pkpk}$  = 65 mA)**

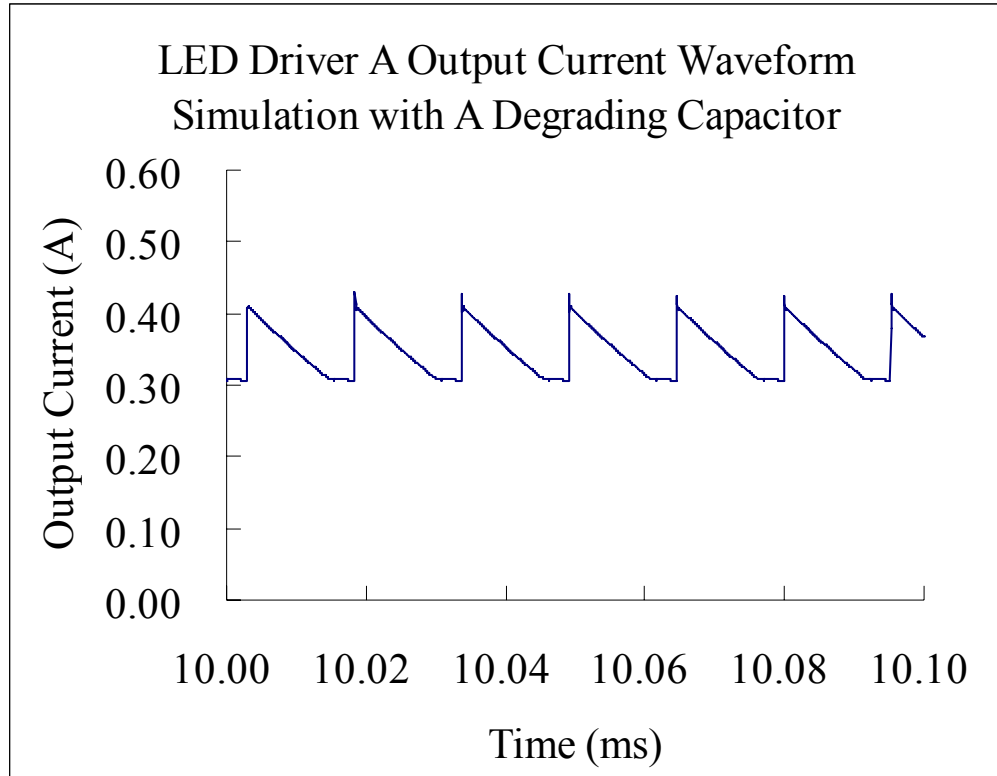


**Fig 3-7 LED driver A output current waveform simulation with A degrading capacitor (ESR = 1.44  $\Omega$ , capacitance = 80  $\mu$ F,  $I_{pkpk}$  = 125 mA)**

Fig 3-6 shows the simulated output current waveform of LED driver A with a good capacitor, whose ESR is 0.72  $\Omega$  and capacitance is 100  $\mu$ F. Under this condition, the current peak-to-peak value is 65 mA, and the current mean value is around 350 mA. Fig 3-7 shows the simulated output current waveform of LED driver A with a degrading capacitor, whose ESR is 1.44  $\Omega$  and capacitance is 80  $\mu$ F. Under this condition, the current peak-to-peak value is 125 mA, and the current mean value is still around 350 mA. The selection of the parameter change of the capacitor is based on the manufacturer's end-of-life definition: 200% of ESR increase, or capacitance drop by 20% (Nichicon, 2002; BHC Components, 2002; CDE, 2000; Panasonic, 2008). The simulation result demonstrates that, as the capacitor degrades (ESR increases and capacitance decreases), the output current peak-to-peak value increases accordingly for LED driver A. This is consistent with the analytic derivation result.

LED driver B is a single-stage PFC based flyback topology converter. This topology features both good current regulation capability and high power factor performance by using a critical conduction mode power factor controller. The output current peak-to-peak value has two components (Adragna, 2003). One is related to the high frequency switching operation and depends mostly on the ESR of the output capacitor, its maximum amplitude which occurs at the peak of the sinusoid, is:

$$I_{o1\text{ pk-pk}} = \frac{I_{PK(s)} \cdot R_{ESR}}{R_L} \quad (\text{Eq. 3-9})$$

where  $I_{PK(s)}$  is the peak amplitude of the secondary current,  $R_L$  is the resistance of the load, and  $R_{ESR}$  is the equivalent series resistance of the output capacitor.

The other component is related to the twice-mains-frequency envelop, depending mostly on the capacitance value of the output filter capacitor. For an ideal power factor correction front-end stage, the instantaneous input power undergoes a twice-mains-frequency ripple, requiring a large output capacitance to provide the storage function. The amplitude of the instantaneous input power is:

$$P_{in}(t) = I_p \sin(\omega t) \cdot V_p \sin(\omega t) = I_{rms} V_{rms} (1 - \cos(2\omega t)) \quad (\text{Eq. 3-10})$$

In order to achieve a high power factor performance, the output current feedback loop's bandwidth should be low enough to be little sensitive to the twice-mains-frequency ripple. This is why a significant twice-mains-frequency current ripple appears on the output. The amplitude of this part of the output current peak-to-peak value is:

$$I_{o2\text{ pk-pk}} = k \cdot \frac{I_{out}}{f_L \cdot C_o \cdot R_L} \quad (\text{Eq. 3-11})$$

where  $k$  is a constant,  $I_{out}$  is the output current,  $f_L$  is the mains frequency, and  $C_o$  is the capacitance of the output filter capacitor.

The amplitude of the overall output current peak-to-peak value in the case of LED driver B is:

$$I_{o\text{ pk-pk}} = \sqrt{I_{o1\text{ pk-pk}}^2 + \Delta I_{o2\text{ pk-pk}}^2} \quad (\text{Eq. 3-12})$$

The increase of the ESR of the output filter capacitor will cause an increase in high frequency part  $I_{o1\text{ pk-pk}}$ , and the decrease of its capacitance of the output filter capacitor will cause an increase in the twice-mains-frequency part  $I_{o2\text{ pk-pk}}$ . It can be seen that the degradation of the output filter capacitor is expected to cause an increase of output current peak-to-peak value for the case of LED driver B.

Fig 3-8 shows a simplified schematic of the power stage of LED driver B for PSpice simulation (V9.2). A resistor connected in series with the output capacitor C1 was used to represent ESR part of the capacitor. A resistance of 9.4  $\Omega$  was used to represent an HP LED load at 350 mA. The switching frequency was selected at 100 kHz, which was the actual measured value for LED driver B. A transient time domain simulation was performed to observe the output current waveforms.

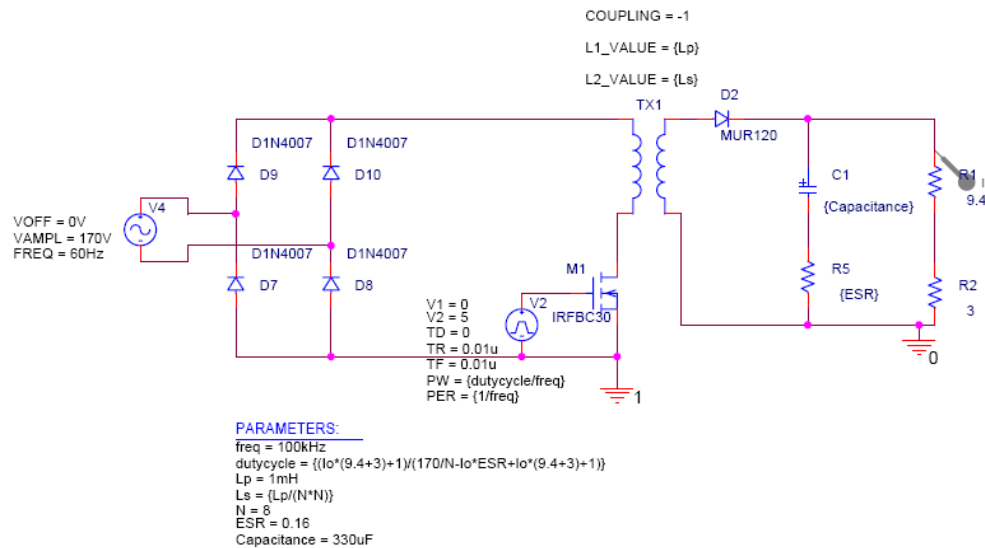


**Fig 3-8 Simplified schematic of LED driver B power stage for PSpice simulation**

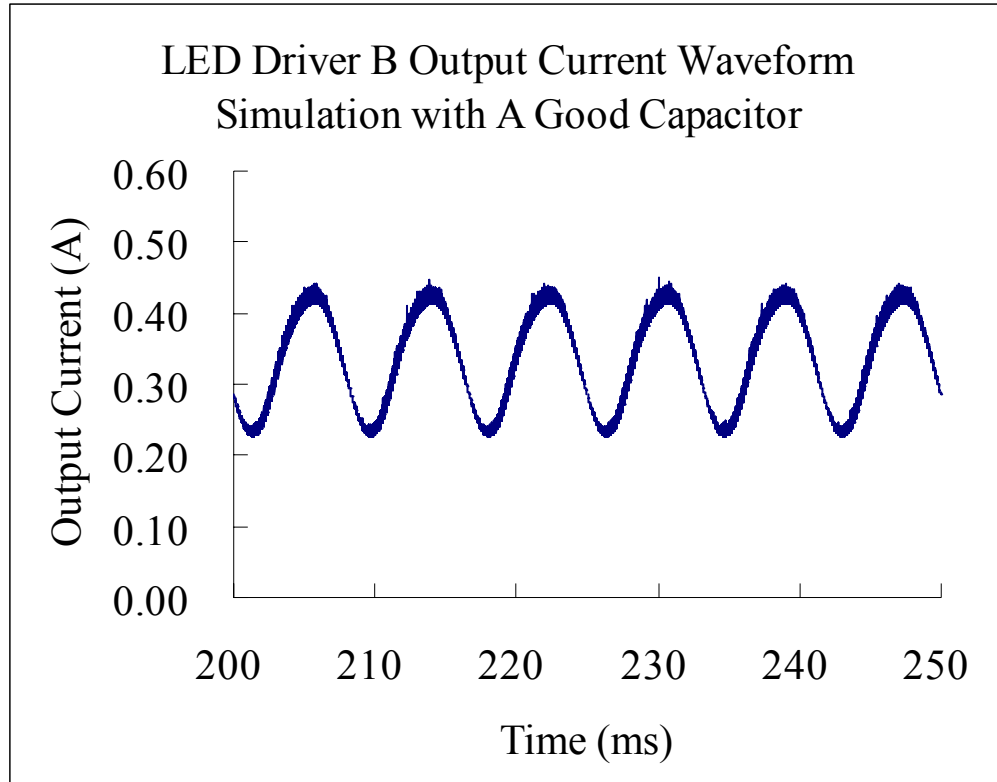


**Fig 3-9 LED driver B output current waveform simulation with A good capacitor (ESR = 0.16  $\Omega$ , capacitance = 330  $\mu$ F,  $I_{pkpk}$  = 221 mA)**

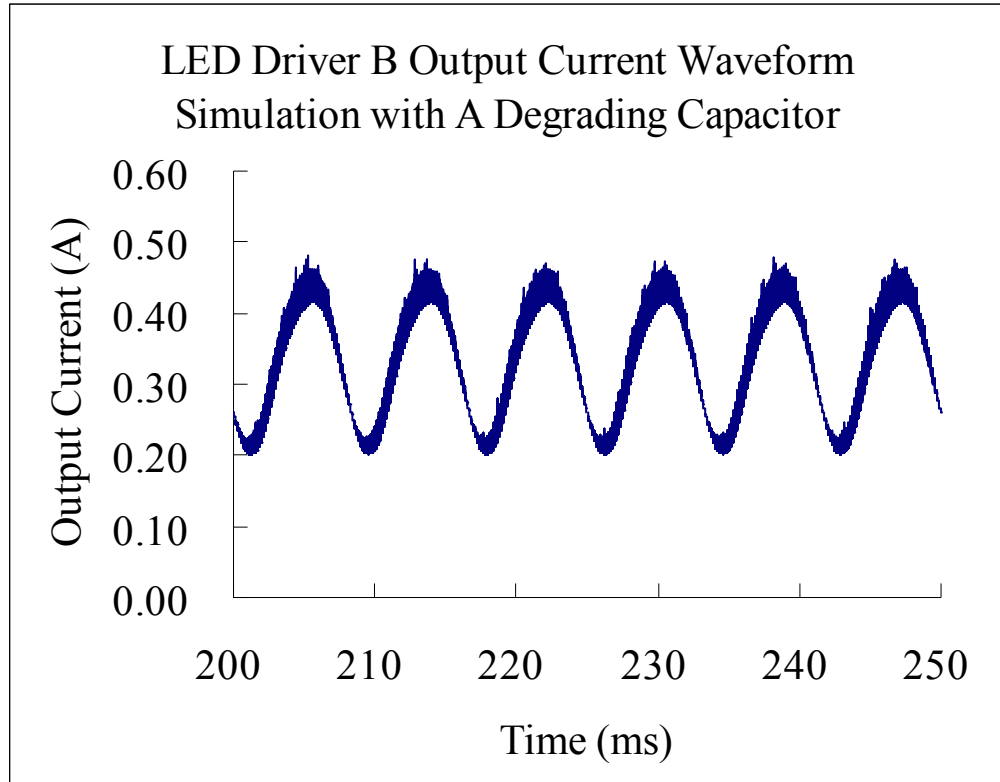


**Fig 3-10 LED driver B output current waveform simulation with A degrading capacitor (ESR = 0.32  $\Omega$ , capacitance = 264  $\mu$ F,  $I_{pkpk}$  = 279 mA)**

Fig 3-9 shows the simulated output current waveform of LED driver B with a good capacitor, whose ESR is 0.16  $\Omega$  and capacitance is 330  $\mu$ F. Under this condition, the current peak-to-peak value is 221 mA, and the current mean value is around 350 mA. Fig 3-10 shows the simulated output current waveform of LED driver B with a degrading capacitor, whose ESR is 0.32  $\Omega$  and capacitance is 264  $\mu$ F. Under this condition, the current peak-to-peak value is 279 mA, and the current mean value is still around 350 mA. The selection of the parameter change of the capacitor is based on the manufacturer's end-of-life definition: 200% of ESR increase, or capacitance drop by 20% (Nichicon, 2002; BHC Components, 2002; CDE, 2000; Panasonic, 2008). The simulation result demonstrates that, as the capacitor degrades (ESR increases and capacitance decreases), the output current peak-to-peak value increases accordingly for LED driver B. This is consistent with the analytic derivation result.

Both the analytical derivation and the simulation results show that the output current peak-to-peak amplitude is a good reflection of the output capacitor's ESR increase and capacitance decrease for two types of LED drivers. It is promising to use output current parameter shift to indirectly predict the degradation level of the output capacitor in an LED driver.

### 3.4 Current Ripple

Current ripple in this thesis study is defined as:  $\frac{\text{current peak - to - peak amplitude}}{\text{current mean amplitude}} \times 100\%$ .

Since the current ripple is an indirect indicator of an electrolytic capacitor's fault condition (Venet, 1999; Imam, 2005), it can be used to predict the degradation level of an electrolytic capacitor in application.

#### 3.4.1 Impact of Current Ripple on LED Performance

The typical output current ripple patterns are sinusoid or triangle or a combination of two. Fig 3-11 shows the measured output current ripple waveform of LED driver A. It is a typical triangular shape, and the frequency is approximately 67 kHz. Fig 3-12 shows the measured output current ripple waveform of LED driver B. It has a sinusoidal envelop of 120 Hz, and superimposed by 100 kHz high frequency triangular component.

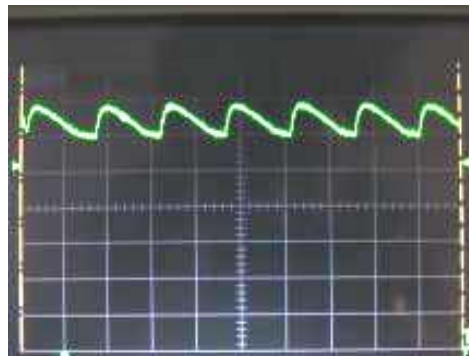


**Fig 3-11 LED driver A output current ripple waveform**

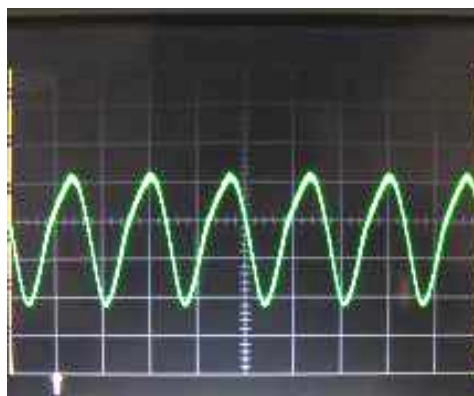


**Fig 3-12 LED driver B output current ripple waveform**

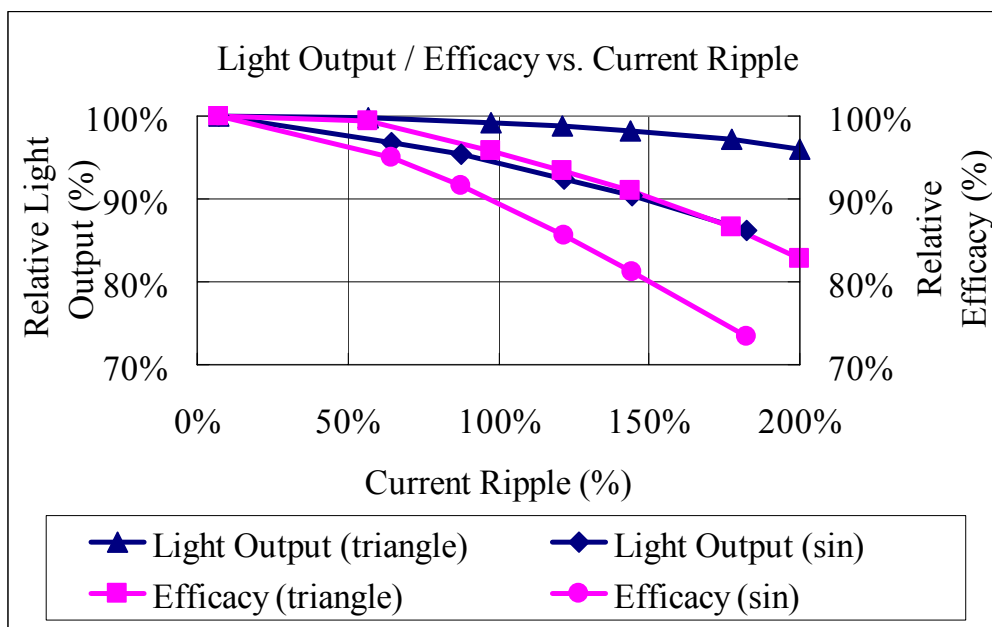


**Fig 3-13 Impact of current ripple on light output & efficiency**

A pilot study was designed to estimate the impact of typical current ripple on light output and efficacy of an LED. The typical LED driver’s output current waveforms were recreated by using a function generator and a voltage-current converter. The output current mean value was kept constant at 350 mA while the current ripple was variable. A 3W white HP LED was selected to serve as the load to the constant current source. The independent variable was current ripple patterns (triangle at 10kHz, and sinusoid at 120

Hz) and the amplitude of the current ripple (from 0% to 200%); the dependent variable was relative light output.

Fig 3-13 shows the relationship between current ripple amplitude and relative light output and relative efficacy compared to the condition with no current ripple component. It can be seen that, as current ripple increases while current mean value was maintained, both light output and efficacy of the LED decrease. For sinusoidal current ripple waveforms, when the current ripple reaches 150%, the light output was derated by 10% compared to the condition with no current ripple, and the efficacy was derated by 20%. For triangular current ripple waveforms, when the current ripple reaches 150%, the light output was derated by 3% and the efficacy was derated by 10%. As the current ripple further increases, both light output and efficacy would suffer from more derating.

The light output and efficacy derating caused by the current ripple implies that: LED light out is not only determined by current mean value, but also affected by current waveform patterns because of the non-linear relationship between light output and forward current. As the current ripple increases while current mean value is kept constant, more power will be delivered to the LED but less light output will be expected probably due to the thermal derating caused by increased input power. This will cause a decrease in system efficacy, and possibly renders the system no longer qualified for application requirements. The output current ripple is found to be one of the critical parameters that affect an LED lighting system's performance.

### **3.4.2 End-of-life Criterion**

Using the analytical and simulation methods detailed in section 3.3 above, it is possible to obtain the LED driver's output current ripple trend.

As an electrolytic capacitor degrades, its ESR increases and capacitance decreases. A good prediction model of ESR as a function of time is the linear inversed model demonstrated by Gasperi (1996), Rhoades (1984) and Jones (1987), and verified

experimentally by Lahyani (1998). For a given rated voltage, ESR is found to be inversely proportional to capacitance (CDE, 2000; United Chemi-Con, 2003). With these models, it is possible to establish ESR and capacitance trend to simulate an electrolytic capacitor's degradation process. Since we have also identified the relationship between ESR/capacitance and output current ripple as indicated by

$$I_{o\text{pk-pk}} = \frac{I_o \cdot D}{C_o \cdot F_s \cdot (R_{LED} + R_{sense})} + \frac{I_o}{1-D} \cdot \frac{R_{ESR}}{R_{LED} + R_{sense}} \quad (\text{Eq. 3-8})$$

$$\text{and } I_{o\text{pk-pk}} = \sqrt{I_{o1\text{pk-pk}}^2 + \Delta I_{o2\text{pk-pk}}^2} \quad (\text{Eq. 3-12})$$

3-12, it is possible to calculate the output current ripple as a function of time.

Fig 3-14 shows the simulated output current ripple trend at 105°C of capacitor temperature for LED driver B. The solid line represents the output current ripple in percentage. The output current ripple increases slowly and steadily at first, then at some point it starts to take off and continue to increase at a much higher rate. The transition point where the output current ripple experiences the most of the rate of change is the preferred point for end-of-life definition of the LED drivers. This is because the rate of change of output current ripple peaks at this point, implying a most unstable degradation period. And when it passes this point, the output current ripple exhibits a sharp increase within a short period of time, which is close to possible catastrophic failure. This point is a good indicative of the approaching of catastrophic failure. Fig 3-15 shows an enlarged chart of output current ripple trend around the transition point. The dotted line shows the 2<sup>nd</sup> derivative of the output current ripple. The transition point corresponds to the point where the 2<sup>nd</sup> derivative of the output current ripple reaches a maximum. Notice that at this transition point the current ripple is about 250%, at which the light output and efficacy of the LED would have suffered significantly as indicated in section 3.4.1. So, this point is used as the end-of-life criterion for the LED drivers in the following experiments and analysis.

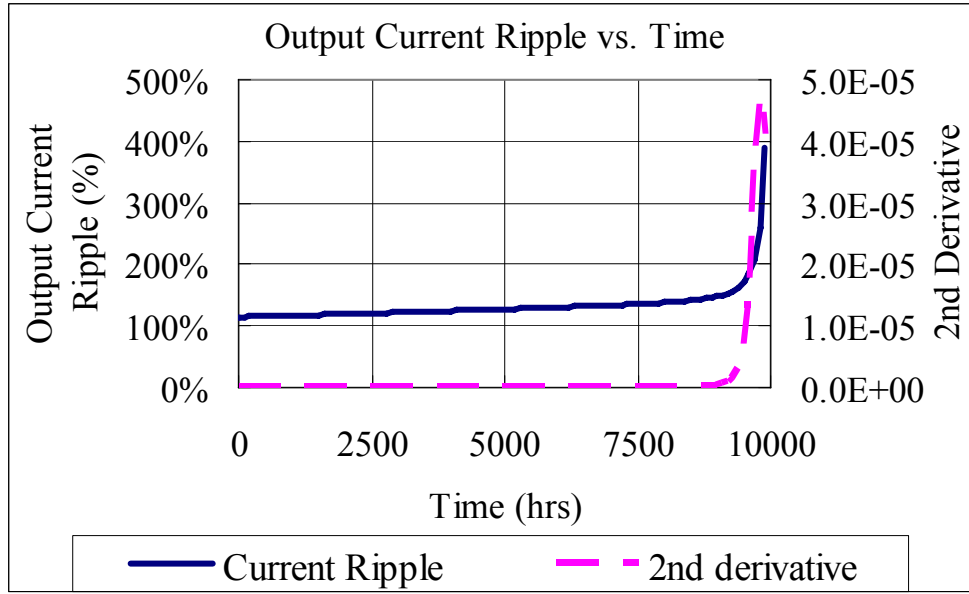


**Fig 3-14 Output current ripple trend simulation for LED driver B**

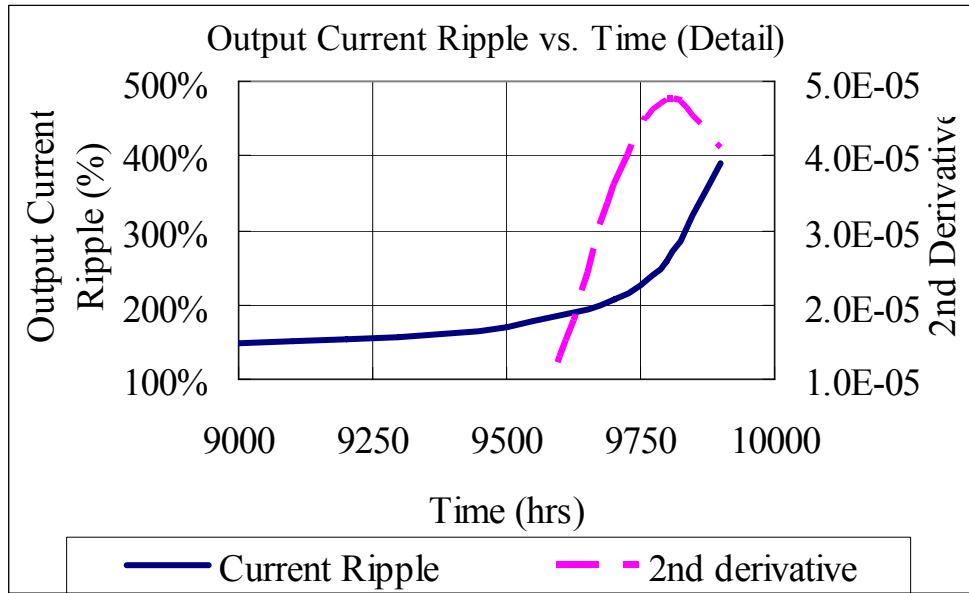


**Fig 3-15 An enlarged chart of output current ripple trend around transition point for LED driver B**

## 4. Hypotheses

### 4.1 Thesis Objective

The objective of this thesis is to experimentally investigate the relationship between output current ripple and capacitance and ESR of the output filter capacitor in an LED driver, to establish a relationship between capacitor temperature and the LED driver output current, and to develop an end-of-life criterion for the LED driver and estimate its useful life.

### 4.2 Term Definitions

Based on the findings from the literature and the pilot studies, several hypotheses were developed specifically for the LED driver samples A and B and were verified experimentally. Before stating the hypotheses, several terms are defined for better clarification.

$$\text{Current Ripple} = \frac{\text{current peak - to - peak amplitude}}{\text{current mean amplitude}} \times 100\% \quad (\text{Eq. 4-1})$$

Refer to Fig 4-1 for detailed explanation of terms used in current ripple definition.

#### Current mean amplitude

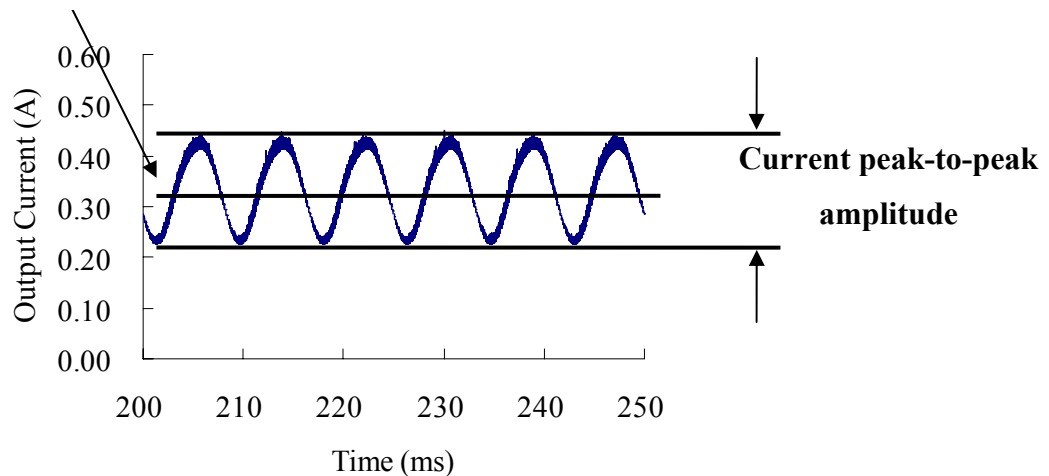


**Fig 4-1 Current ripple definition diagram**

**The LED driver** refers specifically to those independent off-line LED drivers using an electrolytic capacitor at its output stage.

**Capacitance** refers to the value of the capacitance measured at  $f = 120$  Hz using an ESR/LCR meter.

**ESR** refers to the value of the equivalent series resistance of an electrolytic capacitor measured at  $f = 120$  Hz using an ESR/LCR meter.

**Capacitor temperature** refers to the temperature measured at the root of the positive pin of an electrolytic capacitor, as shown in Fig 4-2. This is because the anode foil carries the dielectric by a formation process so that it has better contact with the electrolyte.

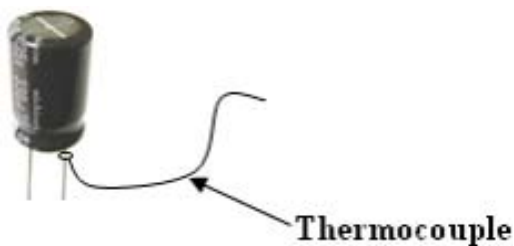


**Fig 4-2 Capacitor temperature measurement location diagram**

It should be pointed out that ESR is a function of measurement frequency. Fig 4-3 Fig 4-3 shows the relationship between ESR and frequency for an electrolytic capacitor used in LED driver B. ESR decreases steadily with increasing measurement frequency, and reaches a steady value. Generally, the constant value is reached at the measurement frequency about 10 kHz (CDE, 2000). The frequency value of 120 Hz was chosen in final measurement because that is the typical frequency the capacitor manufacturers usually use in ESR measurement. 120 Hz is also the typical frequency for rectified line voltage where the electrolytic capacitor is often used to serve the filtering purpose.

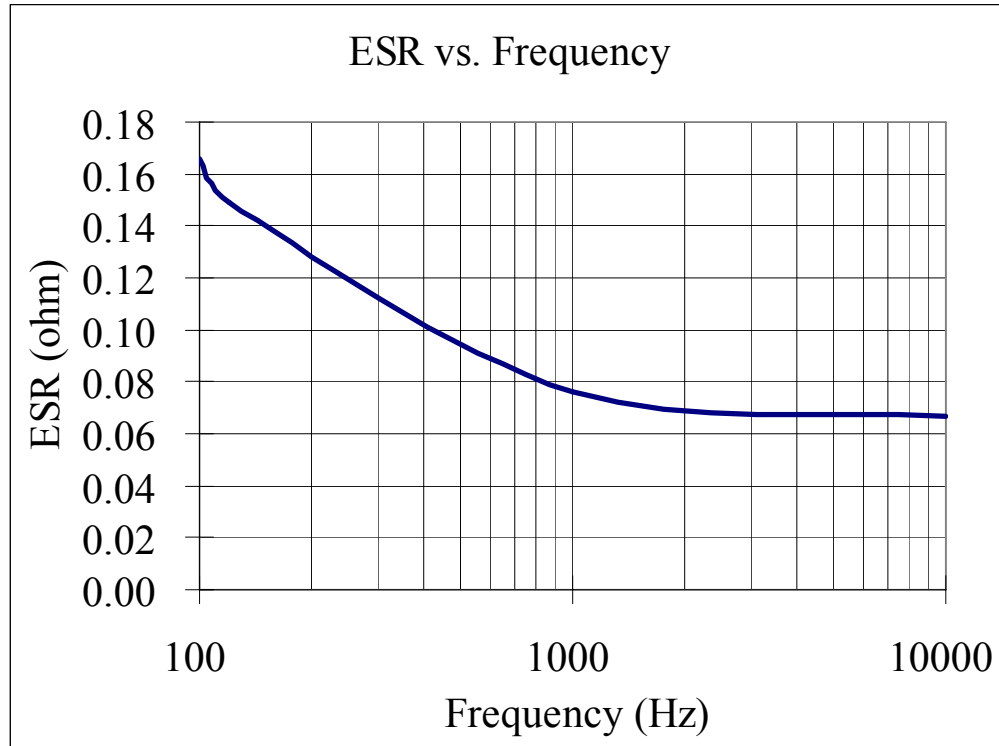


**Fig 4-3 Relationship between ESR & frequency (330  $\mu$ F, Nichicon, PW(M), 50V, 5000 hrs @ 105  $^{\circ}$ C)**

### 4.3 Hypothesis 1

*If the ESR of the output capacitor increases, then the output current ripple of the LED driver will increase.*

This hypothesis was developed based on the results observed by Harada (1993), Lahyani (1998) and major capacitor manufacturers that the ESR increase is a symbol of the degradation of an electrolytic capacitor. Theoretical analysis of the topologies of the LED drivers and PSpice simulation both predict that output current ripple is a reflection of ESR change. This hypothesis was designed to experimentally verify the impact of ESR increase on output current ripple.

## **4.4 Hypothesis 2**

*If the capacitance of the output capacitor decreases, then the output current ripple of the LED driver will increase.*

This hypothesis was developed based on the results observed by Harada (1993), Lahyani (1998) and major capacitor manufacturers that the capacitance decrease is also a symbol of the degradation of an electrolytic capacitor. Theoretical analysis of the topologies of the LED drivers and PSpice simulation both predict that output current ripple is also a reflection of capacitance change. This hypothesis was designed to experimentally verify the impact of capacitance decrease on output current ripple.

## **4.5 Hypothesis 3**

It should be emphasized that temperature will accelerate degradation of the capacitor due to evaporation of the electrolyte. The increase of capacitor temperature will increase the rate of change of ESR and capacitance.

*If the capacitor temperature increases, then the useful life of the LED driver will decrease.*

The assumption is that end-of-life criterion of the LED driver is defined as when the output current ripple of the LED driver increases to a critical point where the current ripple starts to increase significantly faster than before, as illustrated in the following Fig 4-4.

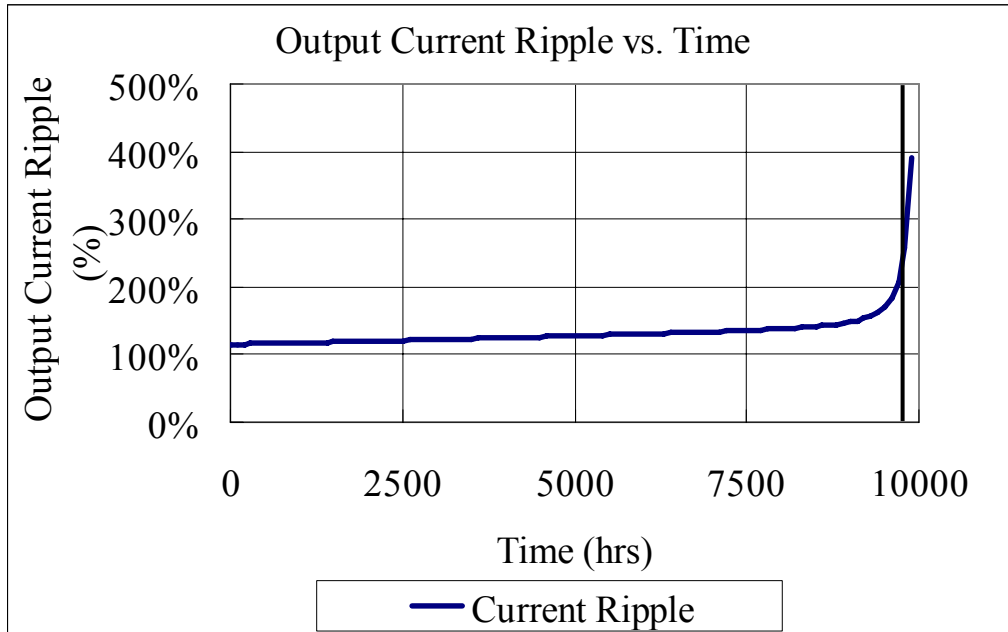


**Fig 4-4 Output current ripple trend simulation (The solid vertical line illustrates the critical point when the end-of-life criterion is set.)**

This hypothesis was developed based on the failure rate estimation results that the electrolytic capacitor used in the LED driver’s output stage has the highest probability of failure and accounts for over 50% of the breakdowns. Since an electrolytic capacitor’s lifetime is sensitive to the temperature, it is expected that the lifetime of the LED driver would be shortened if the electrolytic capacitor is exposed to elevated ambient temperature conditions.

## 5. Experimental Design

### 5.1 Experiment Variables

#### 5.1.1 Hypothesis 1 Experiment Variables

1. Independent variables:

- External resistance to simulate total ESR of the output capacitor;
- LED driver type (2 from different manufacturers).

2. Dependent variable:

- Output current.

3. Extraneous variables:

- Ambient temperature.

Since the ambient temperature will influence an electrolytic capacitor's ESR, the ambient temperature fluctuation in this experiment may affect the amplitude of the output current ripples. Therefore, the ambient temperature was controlled to remain constant during the experiment. This was achieved by the experimental room's air-conditioning system. However, there could be temperature fluctuations due to seasonal changes. Since the experimental process lasts on the order of couple of hours, the impact of seasonal changes in the air-conditioning system are kept at minimum.

- Load connected to the output

In this experiment, the load was kept constant by using a 3W high power white LED. For a given LED, the equivalent series resistance has a negative relationship with its junction temperature. In the actual experiment, the LED was mounted on a piece of heat-sink that helped to keep the junction temperature from entering into thermal run-away situation. The measurements were taken after the LED pin temperature was stabilized.

### **5.1.2 Hypothesis 2 Experiment Variables**

1. Independent variables:

- Capacitance of the output capacitor;
- LED driver type (2 from different manufacturers).

2. Dependent variable:

- Output current.

3. Extraneous variables:

- Ambient temperature.

Since the ambient temperature will influence an electrolytic capacitor's capacitance, the ambient temperature fluctuation in this experiment may affect the amplitude of the output current ripples. Therefore, the ambient temperature should be controlled to remain constant during the experiment. This is achieved by the experimental room's air-conditioning system. However, there could be temperature fluctuations due to seasonal changes. Since the experimental process lasts on the order of couple of hours, the impact of seasonal changes in the air-conditioning system are kept at minimum.

- Load connected to the output.

The same as in hypothesis 1.

### **5.1.3 Hypothesis 3 Experiment Variables**

1. Independent variables:

- Output capacitor temperature;
- LED driver type (2 from different manufacturers).

2. Dependent variable:

- Output current.

3. Extraneous variables:

- Fluctuation of the capacitor's local ambient temperature.

The local ambient temperature of the electrolytic capacitor in this experiment is kept stable by using a thermal pad and a digital temperature controller. The amplitude of the fluctuation of this local ambient temperature depends on the feedback control algorithm of the temperature controller and the input heating power. The relevant control parameters were tuned carefully in each different temperature case to minimize the fluctuation of the capacitor's local ambient temperature ( $< \pm 1.5\text{ }^{\circ}\text{C}$ ).

- Load connected to the output.

The same as in hypothesis 1.

## 5.2 Experimental Setup

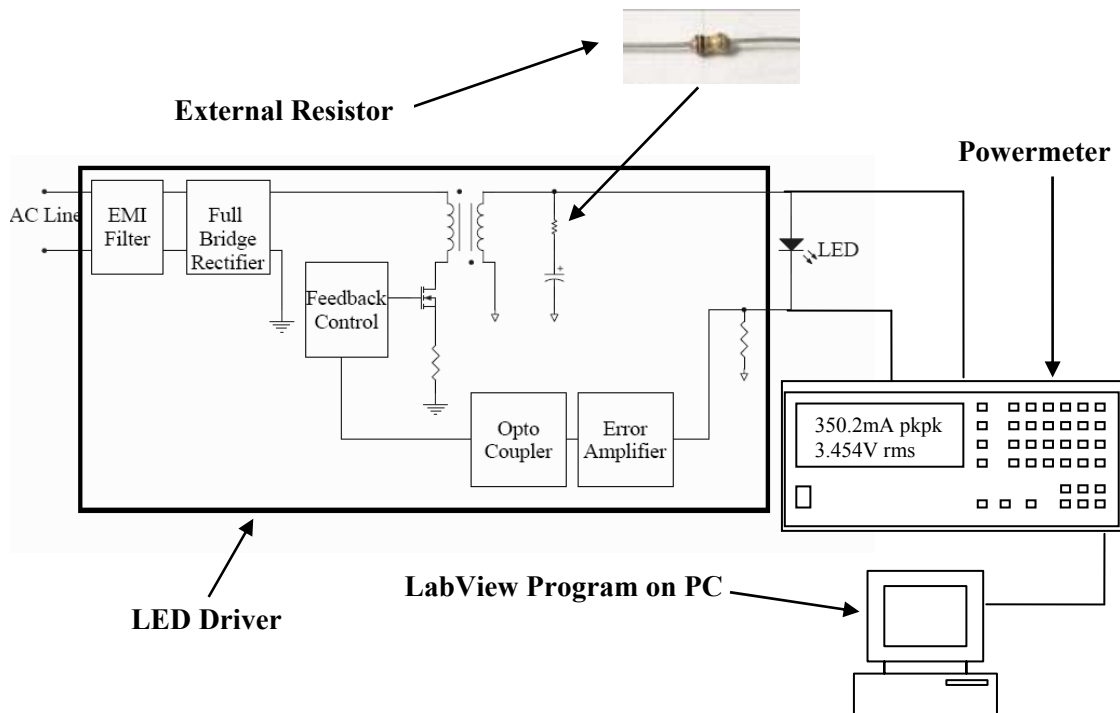


Fig 5-1 Experiment 1 setup diagram

Experiment 1 was designed for verification of hypothesis 1. Its setup is shown in Fig 5-1. The output of the LED driver was connected to a 3W high power LED. A Xitron 2503AH powermeter (from Xitron Technologies, 5959 Cornerstone Court, West Suite 100, San Diego, CA, 92121) was connected at the output of the LED driver to take measurements of current parameters such as current mean value and current peak-to-peak value. The powermeter was connected to a personal computer through the general purpose interface bus (GPIB). The measurements of the output current parameters were automatically controlled by a customized LabVIEW program running on the PC. An external resistor or a combination of resistors was connected in series with the default output electrolytic capacitor in the LED driver to simulate the changes in ESR during degradation process.

Two types of LED drivers from two different manufacturers were selected. For each type of LED drivers, 3 samples were provided for experiment 1. For LED driver A, the default output capacitor is 100  $\mu\text{F}$ . Its ESR value is measured as 0.72  $\Omega$  ( $f = 120 \text{ Hz}$ ). The selected external resistance values were listed in Table 5-1. For LED driver B, the default output capacitor was 330  $\mu\text{F}$ . Its ESR value was measured as 0.16  $\Omega$  ( $f = 120 \text{ Hz}$ ). The selected external resistance values were listed in Table 5-2. These external resistor values were chosen so that the output current ripple values of these 2 types of the LED drivers were comparable to each other.

**Table 5-1 Selection of the external resistance for LED driver A**

Driver type	A			
Capacitance (uF)	100			
Default ESR (Ohm)	0.72			
External resistance (Ohm)	0.00	0.31	0.60	1.10
Total ESR (Ohm)	0.72	1.03	1.32	1.82

**Table 5-2 Selection of the external resistance for LED driver B**

Driver type	B						
Capacitance (uF)	330						
Default ESR (Ohm)	0.16						
External resistance (Ohm)	0.00	0.19	0.30	0.60	1.10	1.59	2.09
Total ESR (Ohm)	0.16	0.35	0.46	0.76	1.26	1.75	2.25

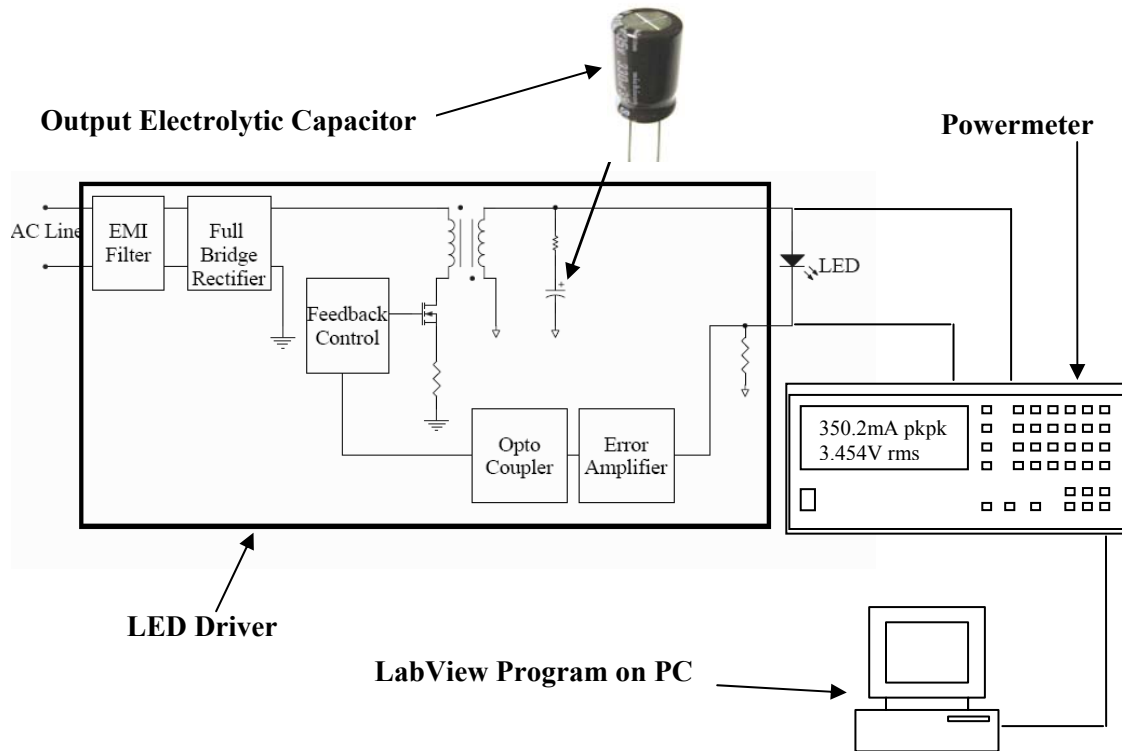


**Fig 5-2 Experiment 2 setup diagram**

Experiment 2 was designed for verification of hypothesis 2. The setup is shown in Fig 5-2. The output of the LED driver was connected to a 3W high power LED. A Xitron 2503AH powermeter was connected at the output of the LED driver to take measurements of current parameters such as current mean value and current peak-to-peak value. The powermeter was connected to a PC through GPIB. The measurements of

the output current parameters were automatically controlled by a customized LabVIEW program running on the PC. The output electrolytic capacitor in the LED driver was replaced with other electrolytic capacitors of different capacitance values to simulate the changes in capacitance during degradation process.

Two types of LED drivers from 2 different manufacturers were selected. And for each type of the LED driver, 3 samples were provided for experiment 2. For LED driver A, the default capacitor had a rated capacitance of 100  $\mu$ F. The selected capacitance values of alternative capacitors were listed in Table 5-3. For LED driver B, the default capacitor had a rated capacitance of 330  $\mu$ F. The selected capacitance values of alternative capacitors were listed in Table 5-4. The selected capacitance values were down to about 10 to 15% of its default value respectively.

**Table 5-3 Selection of the capacitance values for LED driver A**

Driver type	A						
Capacitance (uF)	100	82	56	47	33	22	10
ESR (Ohm) (120Hz)	0.50	0.49	1.09	1.44	1.31	2.53	3.42

**Table 5-4 Selection of the capacitance values for LED driver B**

Driver type	B			
Capacitance (uF)	330	220	100	47
ESR (Ohm) (120Hz)	0.16	0.40	0.73	1.05

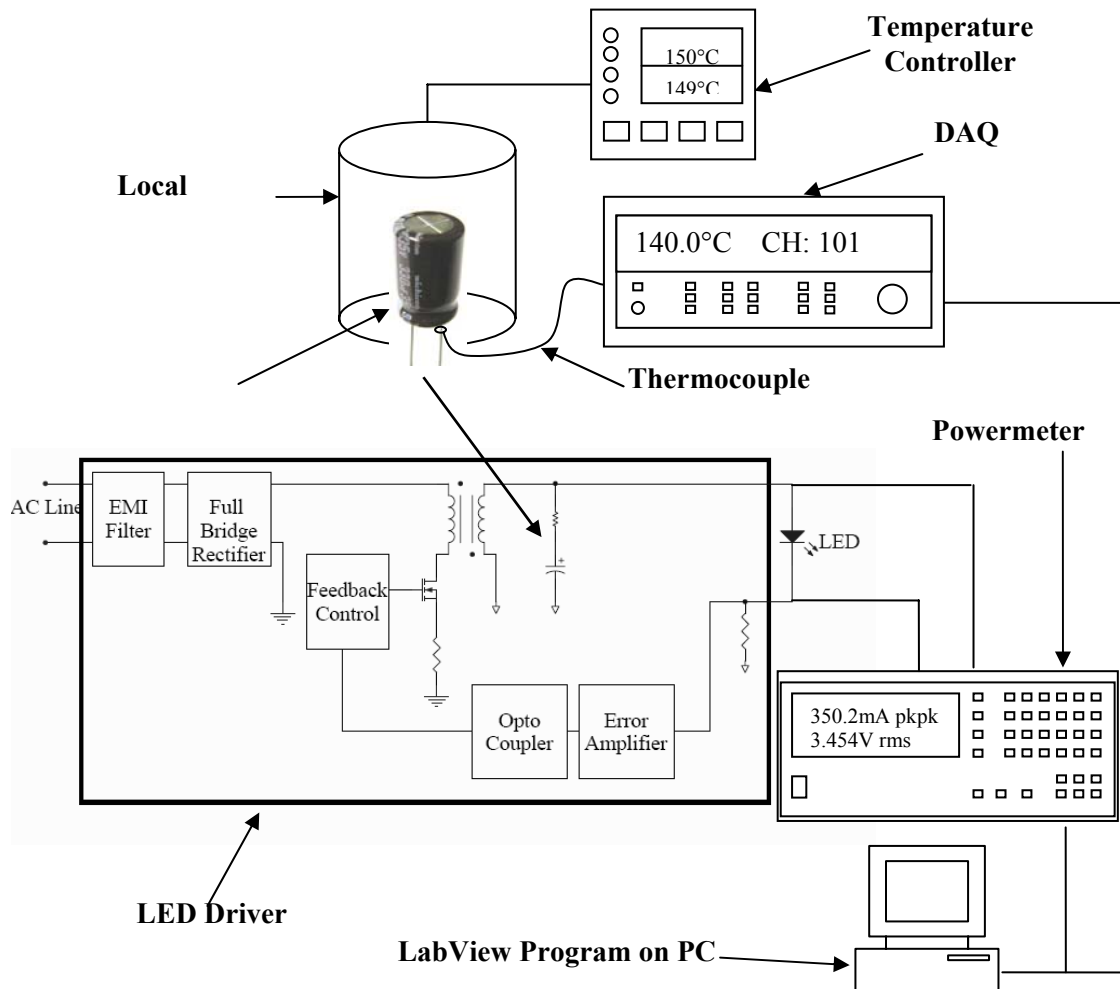


**Fig 5-3 Experiment 3 setup diagram**

Experiment 3 is designed for verification of hypothesis 3. Its setup is shown in Fig 5-3. The output of the LED driver is connected to a 3W high power LED. A Xitron 2503AH powermeter is connected at the output of the LED driver to take measurements of current parameters such as current mean value and current peak-to-peak value. The powermeter is connected to a PC through GPIB. The measurements of the output current parameters are automatically controlled by a customized LabVIEW program running on the PC. A local oven made up of a cylindrical metal case wrapped up with a piece of flexible heater is used to contain the electrolytic capacitor and to provide local ambient

temperature control. The heater is controlled by a digital temperature controller to provide stable temperature condition. The positive pin temperature of an electrolytic capacitor is found to be an indicative of the core temperature which decides the lifetime of an electrolytic capacitor. A J-type thermocouple is soldered at the root of the positive pin of the electrolytic capacitor to represent the capacitor temperature. An HP 34970A data acquisition/switch unit (DAQ) (from Hewlett Packard Co., 815 14<sup>th</sup> Street S.W., Loveland, Colorado, 80537) is used to sample the output of the thermocouple. The DAQ is also connected to the PC through GPIB. The measurement of the capacitor temperature is automatically controlled by a customized LabVIEW program running on the PC.

## **5.3 Experimental Procedures**

### **5.3.1 Experiment 1 Procedure**

- (1) The default output electrolytic capacitor is removed from the LED driver A #1's PCB (Printed Circuit Board) for initial measurement.
- (2) An ESR/LCR meter is used to take measurements of initial ESR value of the default electrolytic capacitor.
- (3) A multi-meter is used to take measurements of the values of the selected external resistors.
- (4) A default electrolytic capacitor is soldered back onto the LED driver A #1's PCB.
- (5) Connect the selected external resistor in series with the default electrolytic capacitor.
- (6) Power on the LED driver A #1 for about half an hour for stabilization.
- (7) Take measurements of output current parameters using a powermeter controlled by a LabVIEW program running on a PC. Three measurements are taken consecutively for one value of the external resistor.
- (8) Power off the LED driver A #1.
- (9) Replace with another selected external resistor.
- (10) Repeat procedure (6) (7) (8) (9) until all of the selected external resistors are used in the LED driver A #1.
- (11) Repeat procedure (6) (7) (8) (9) (10) for LED driver A #2 and LED driver A #3.

(12) Repeat procedure (1) to (11) for LED driver B #1, LED driver B #2, and LED driver B #3.

### **5.3.2 Experiment 2 Procedure**

- (1) The default output electrolytic capacitor is removed from the LED driver A #1's PCB (Printed Circuit Board) for initial measurement.
- (2) An ESR/LCR meter is used to take measurements of its capacitance values of both the default electrolytic capacitor and other alternative electrolytic capacitors.
- (3) A default electrolytic capacitor is soldered back onto the LED driver A #1's PCB.
- (4) Power on the LED driver A #1 for about half an hour for stabilization.
- (5) Take measurements of output current parameters using a powermeter controlled by a LabVIEW program running on a PC. Three measurements are taken consecutively for one electrolytic capacitor.
- (6) Power off the LED driver A #1.
- (7) Replace with another selected electrolytic capacitor.
- (8) Repeat procedure (4) (5) (6) (7) until all of the selected alternative electrolytic capacitors are used in the LED driver A #1.
- (9) Repeat procedure (4) (5) (6) (7) (8) for LED driver A #2 and LED driver A #3.
- (10) Repeat procedure (1) to (9) for LED driver B #1, LED driver B #2, and LED driver B #3.

### **5.3.3 Experiment 3 Procedure**

- (1) The default sound output electrolytic capacitor is removed from the LED driver A #1's PCB (Printed Circuit Board).
- (2) Attach a J-type thermocouple onto the root of the positive pin of the electrolytic capacitor using soldering flux.
- (3) A default electrolytic capacitor is soldered back onto the LED driver A #1's PCB.
- (4) Place the electrolytic capacitor into the local oven.
- (5) Power on the LED driver A #1.

- (6) Set the desired local oven temperature.
- (7) Take measurements of output current parameters using a powermeter and capacitor temperature controlled by a LabVIEW program running on a PC. The measurements are taken periodically every minute.
- (8) Stop the heating facility and the automatic measurements when the output current parameters have reached the proposed end-of-life criterion.
- (9) Power off the LED driver A #1.
- (10) Replace the wear-out electrolytic capacitor with a sound one of exactly the same type.
- (11) Repeat the procedure (2) to (10) at a different local oven temperature until all of the selected temperature conditions are completed.
- (12) Repeat the procedure (1) to (11) for LED driver A #2 and LED driver A #3.
- (13) Repeat the procedure (1) to (12) for LED driver B #1, LED driver B #2, and LED driver B #3.

## 6. Results

### 6.1 Experiment 1 Results

#### 6.1.1 Measurement Repeatability

At each ESR condition in experiment 1, three consecutive measurements of output current parameters were taken. Fig 6-1 shows the relationship between ESR and output current parameters with error bar at each point showing standard deviation for LED Driver A #1. The diamond dots show the output current mean values, and the triangle dots the output current peak-to-peak values. Because the standard deviation of these measurements in experiment 1 is too small to be clearly seen in Fig 6-1, a partial enlargement of Fig 6-1 centered by the third triangle point from the left is shown in Fig 6-2. Fig 6-3 shows the standard deviation value at each ESR condition for LED Dirver A #1. It can be seen that standard deviation values are all less than 4% at all different ESR conditions. Fig 6-4 to Fig 6-8 show relationship between output current parameters and ESR with error bars of standard deviation of three consecutive measurements at each ESR condition for LED driver A #2, A #3, B #1, B #2, and B #3 respectively. It can be seen that the measurement repeatability was well preserved in experiment 1.

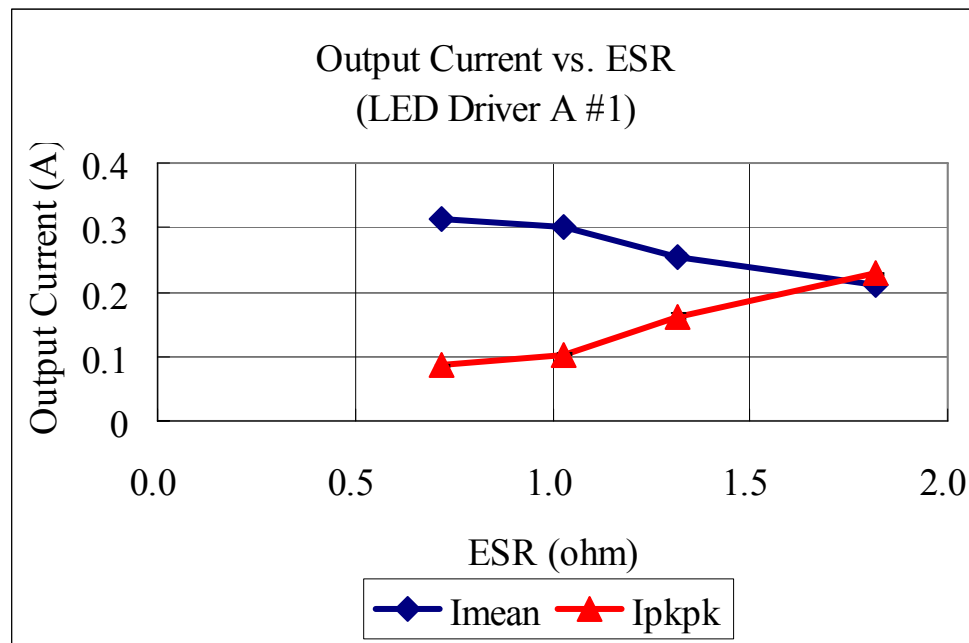


Fig 6-1 Output current parameters vs. ESR for LED driver A #1

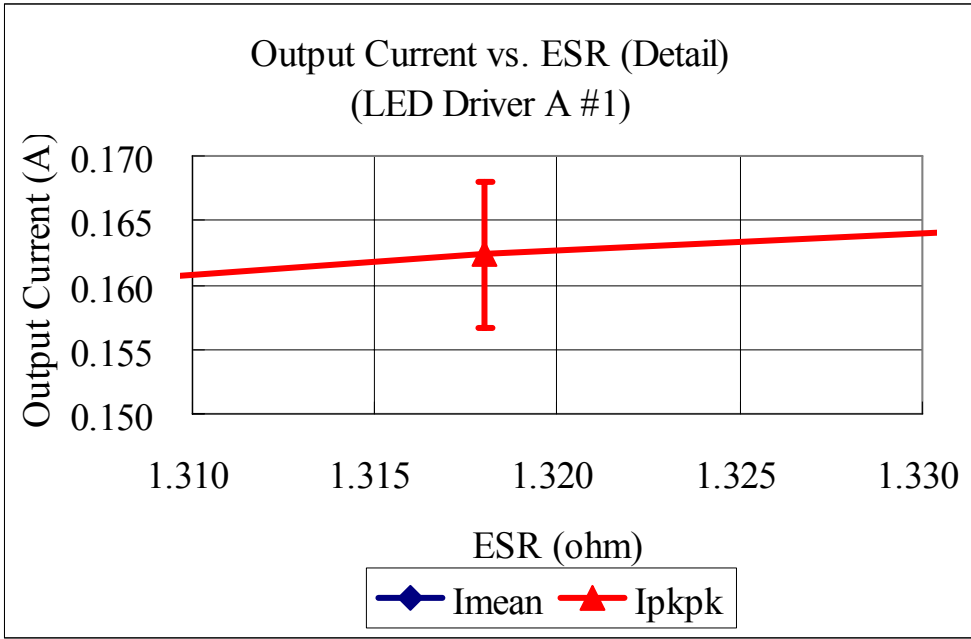


Fig 6-2 Partial enlargement of Fig 6-1

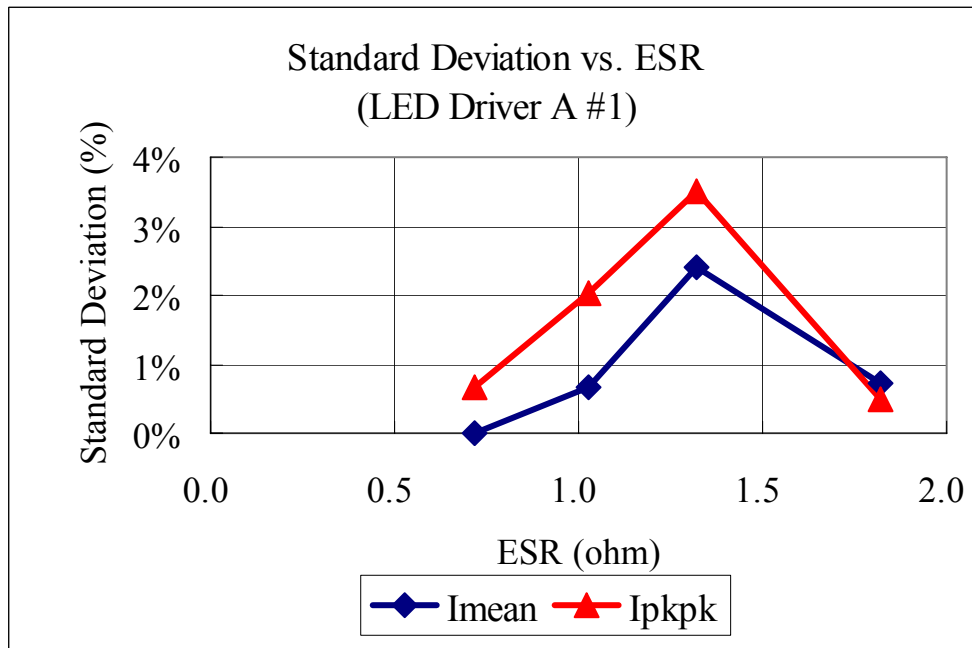
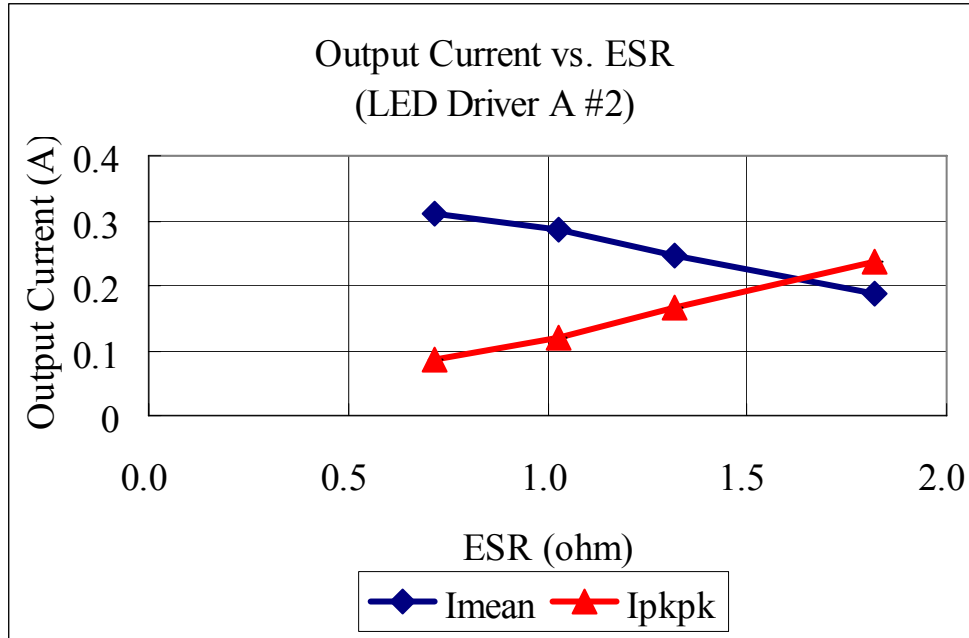
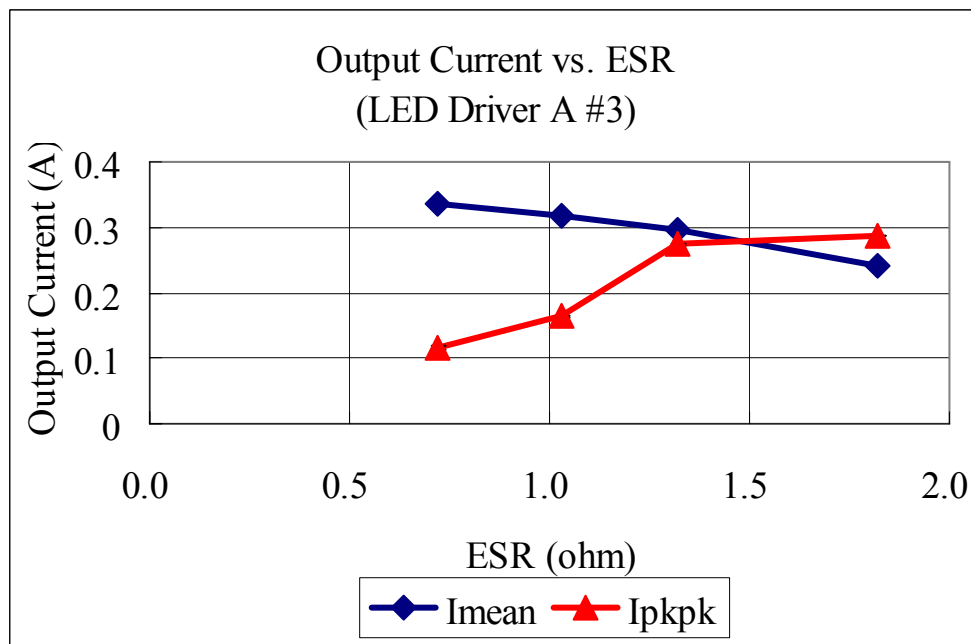


Fig 6-3 Standard deviation of output current parameters vs. ESR for LED driver A #1



**Fig 6-4 Output current parameters vs. ESR for LED driver A #2**



**Fig 6-5 Output current parameters vs. ESR for LED driver A #3**

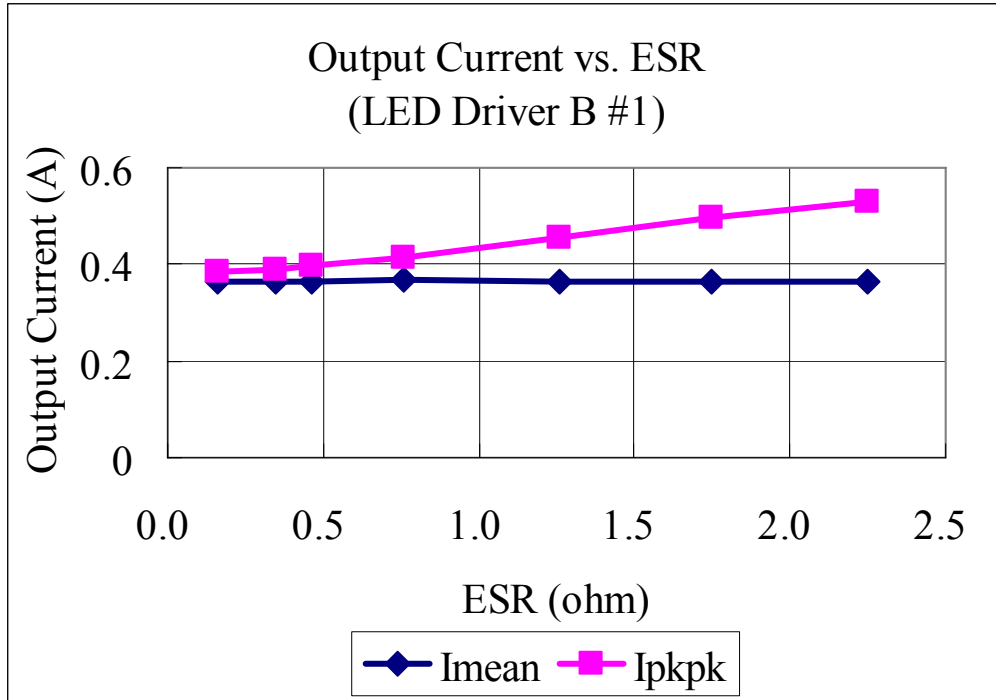


Fig 6-6 Output current parameters vs. ESR for LED driver B #1

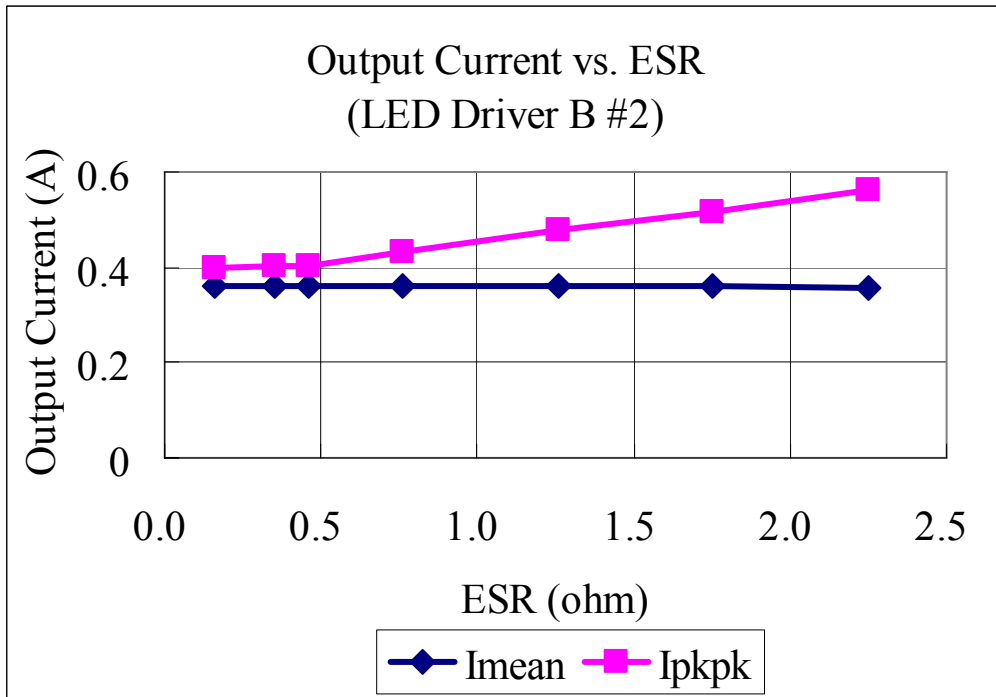
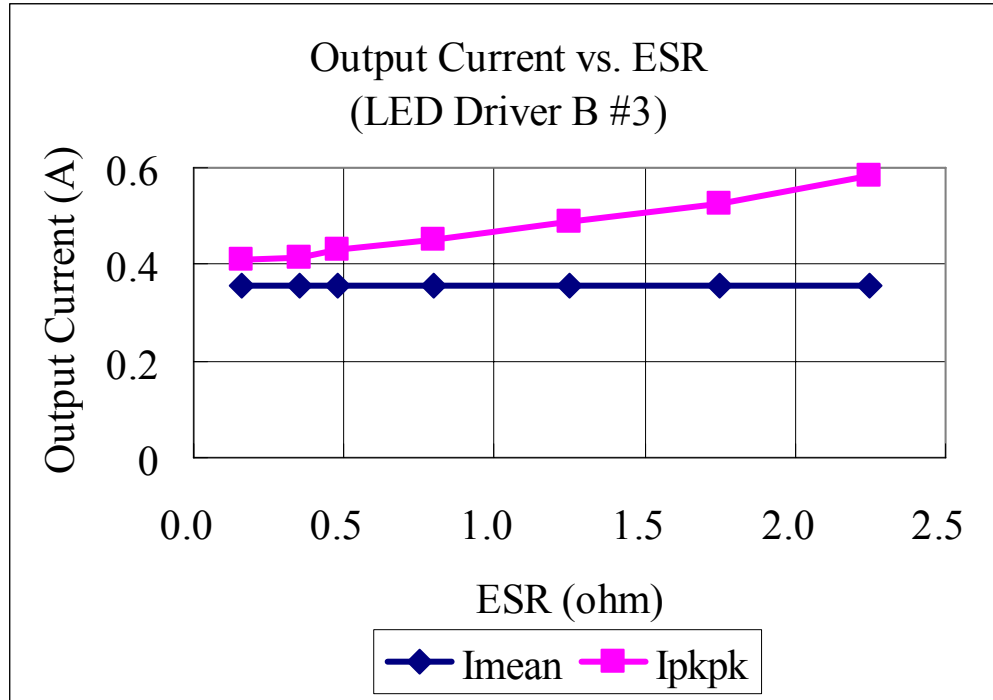


Fig 6-7 Output current parameters vs. ESR for LED driver B #2



**Fig 6-8 Output current parameters vs. ESR for LED driver B #3**

### 6.1.2 Sample to Sample Data

Plotting output current mean values of the 3 samples of LED driver A on the same chart gives Fig 6-9. It can be seen that although there is noticeable difference between samples at each ESR condition, they all show a consistent trend. That is, as ESR increases, output current mean value decreases. Fig 6-10 shows the relationship between ESR and output Current peak-to-peak value for LED driver A #1, #2, #3. Again they all show consistent trends although there is difference between samples. The trend is as ESR increases, output current peak-to-peak value increases.

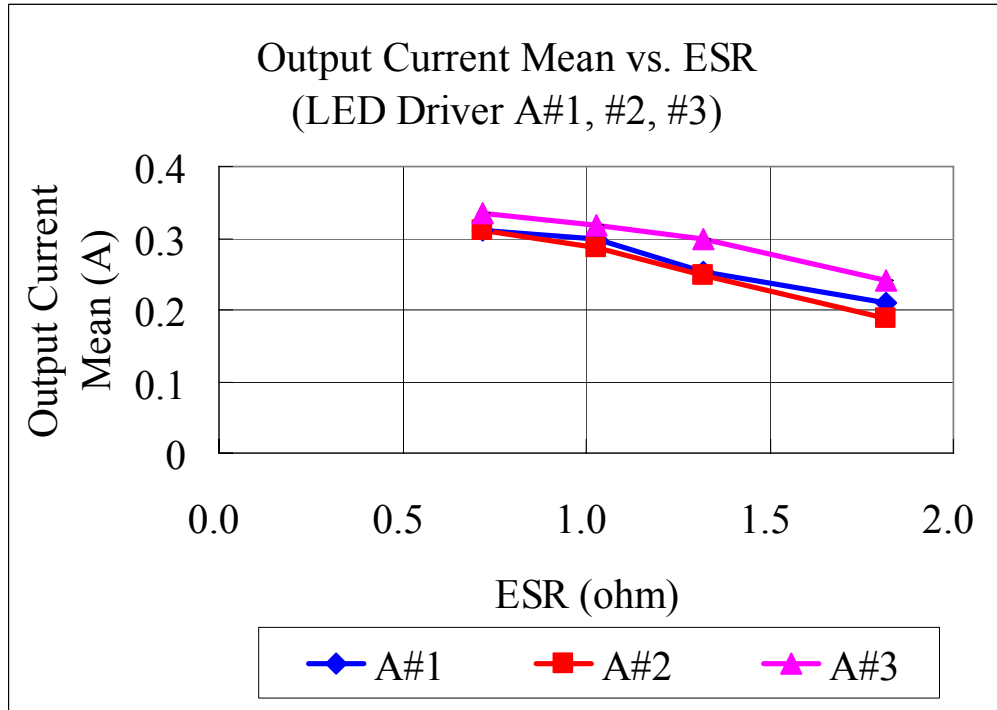


**Fig 6-9 Relationship between output current mean and ESR for LED driver A #1, #2, #3**

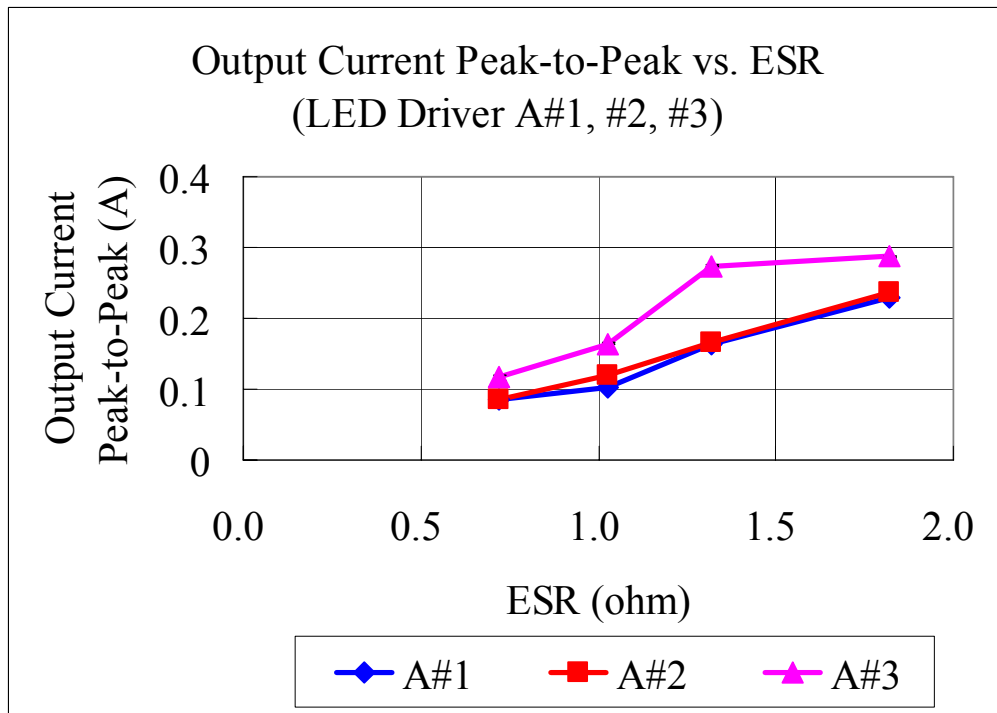


**Fig 6-10 Relationship between output current peak-to-peak and ESR for LED driver A #1, #2, #3**

Fig 6-11 shows the relationship between ESR and output current mean value for 3 samples of LED driver B. In this case, the sample to sample variation is less than 2%. The overall trend is that, the output current mean value doesn't change noticeably as ESR increases. Fig 6-12 shows the relationship between ESR and output current peak-to-peak value for 3 samples of LED driver B. Similar to the case of LED driver A, there exists difference between samples, but the overall trends are consistent. As ESR increases, output current peak-to-peak value increases.

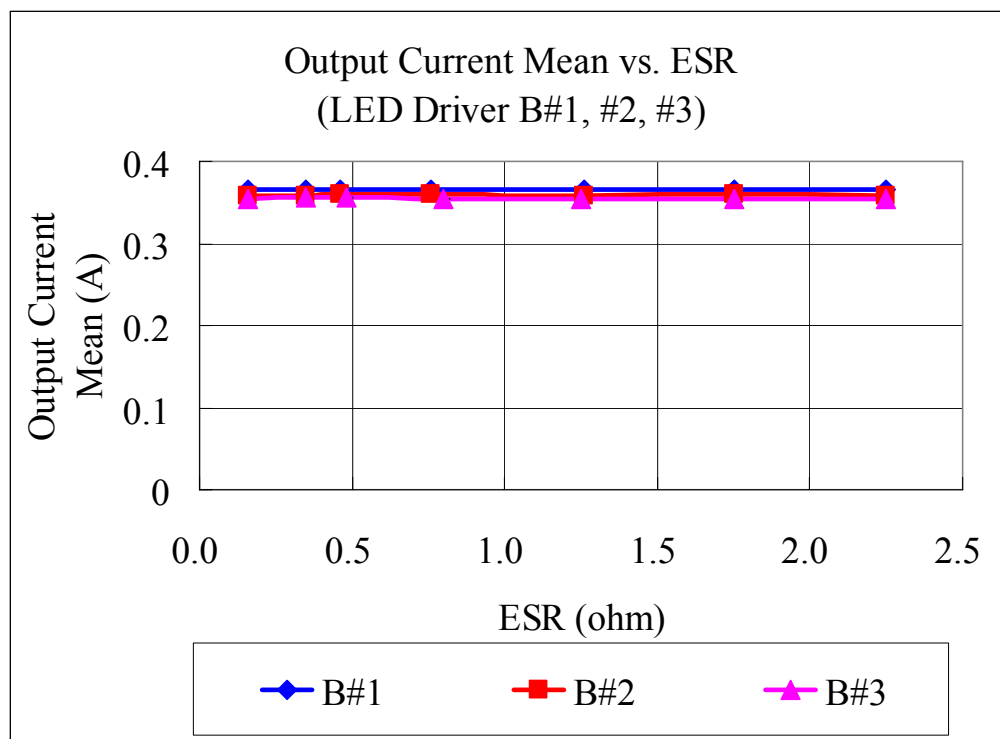


**Fig 6-11 Relationship between output current mean and ESR for LED driver B #1, #2, #3**

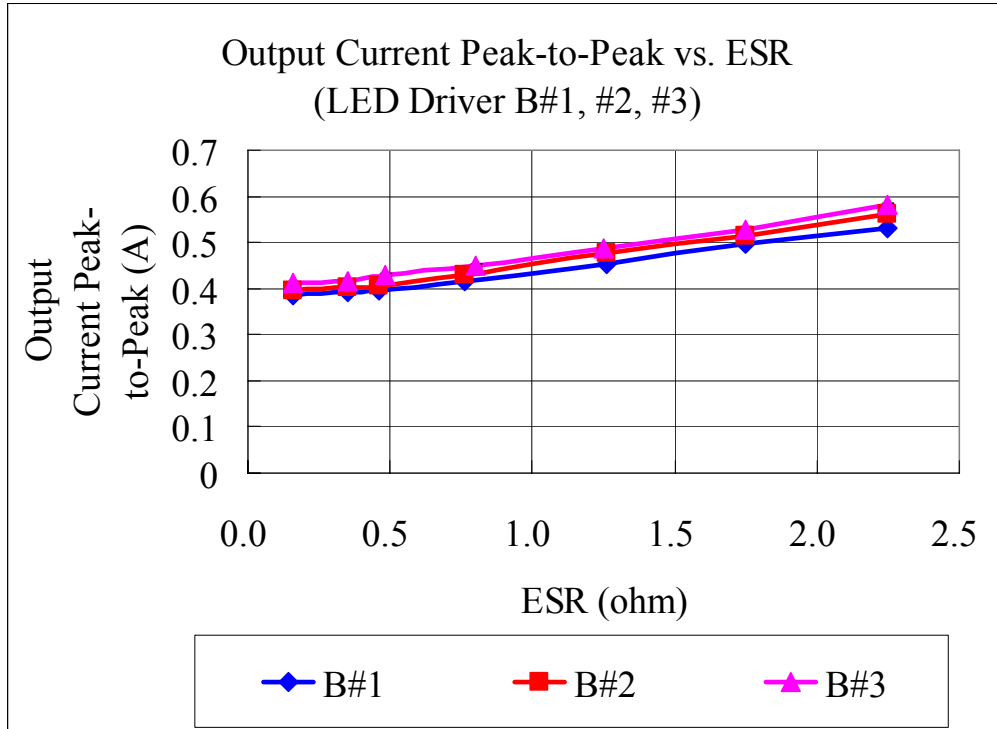


**Fig 6-12 Relationship between ESR and output current peak-to-peak for LED driver B #1, #2, #3**

### 6.1.3 Data Processing Method

By using the formula of current ripple defined in section 4.2, the relationship between output current ripple and ESR was established. Fig 6-13, Fig 6-14 and Fig 6-15 show the relationship between output current ripple and ESR of LED driver A #1, A #2 and A #3 respectively. After this positive relationship was confirmed by the statistical analysis (Appendix A) and proved to be consistent among all three samples of LED driver A, all sample data was combined and averaged to generate Fig 6-16. The positive relationship between output current ripple and ESR was again confirmed by statistical analysis (Appendix A) to the combined data of LED driver A. data of LED driver B was treated using the same data processing method. Fig 6-17 shows the relationship between output current ripple and ESR of LED driver B samples.

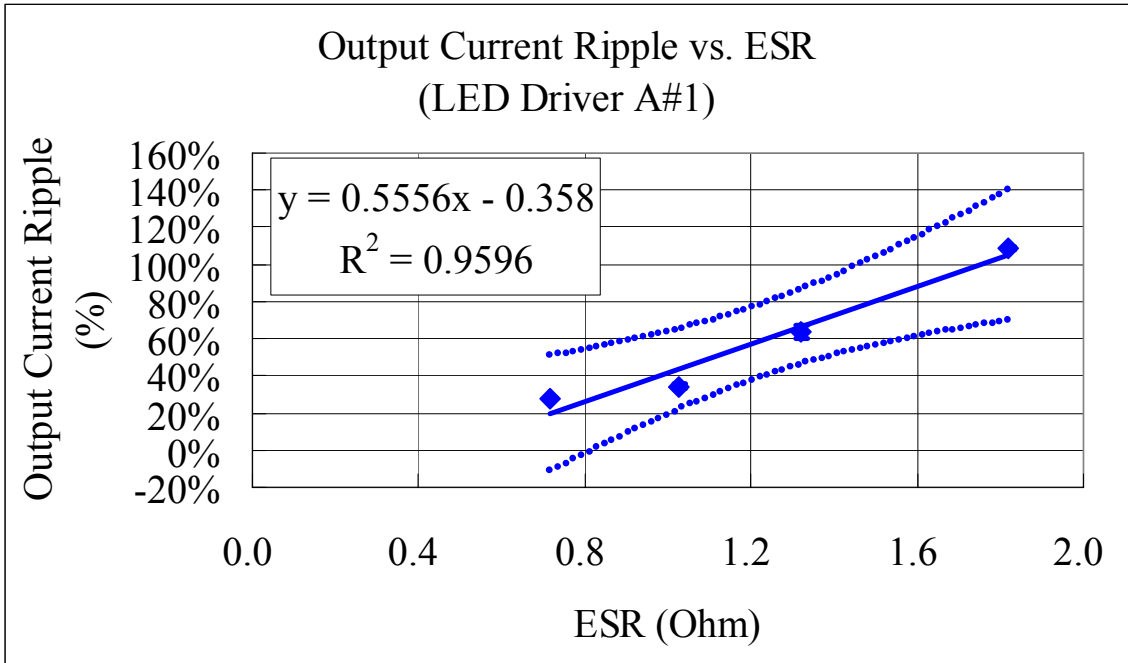


**Fig 6-13 Relationship between output current ripple and ESR of LED driver A #1  
(Dotted lines represent 95% confidence level boundaries.)**

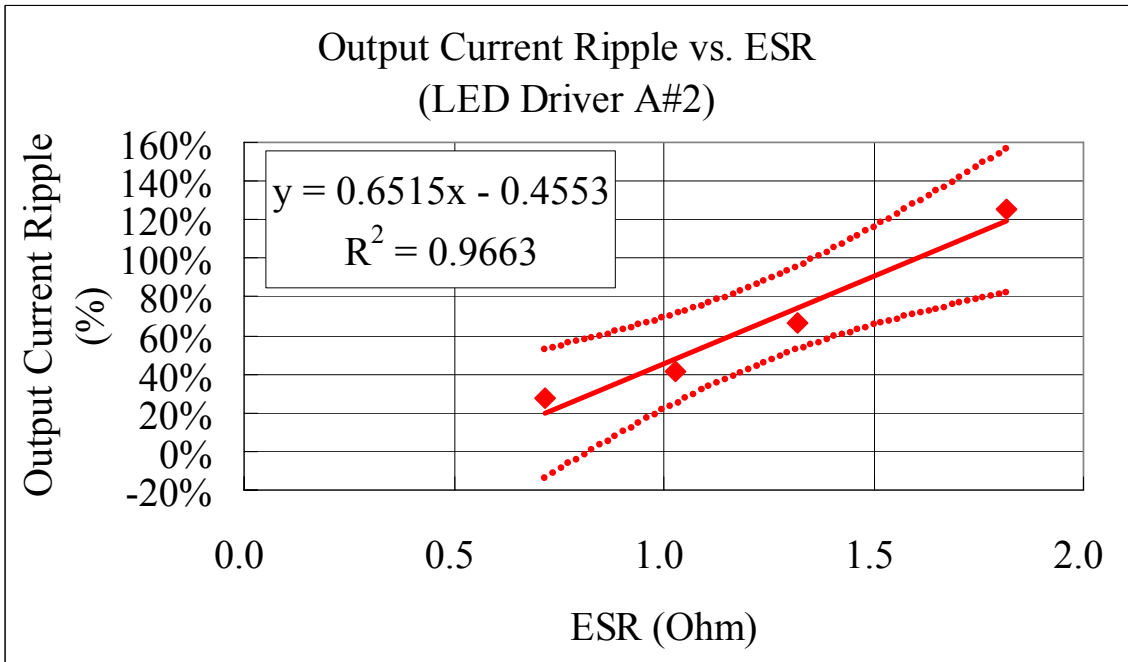


**Fig 6-14 Relationship between output current ripple and ESR of LED driver A #2  
(Dotted lines represent 95% confidence level boundaries.)**

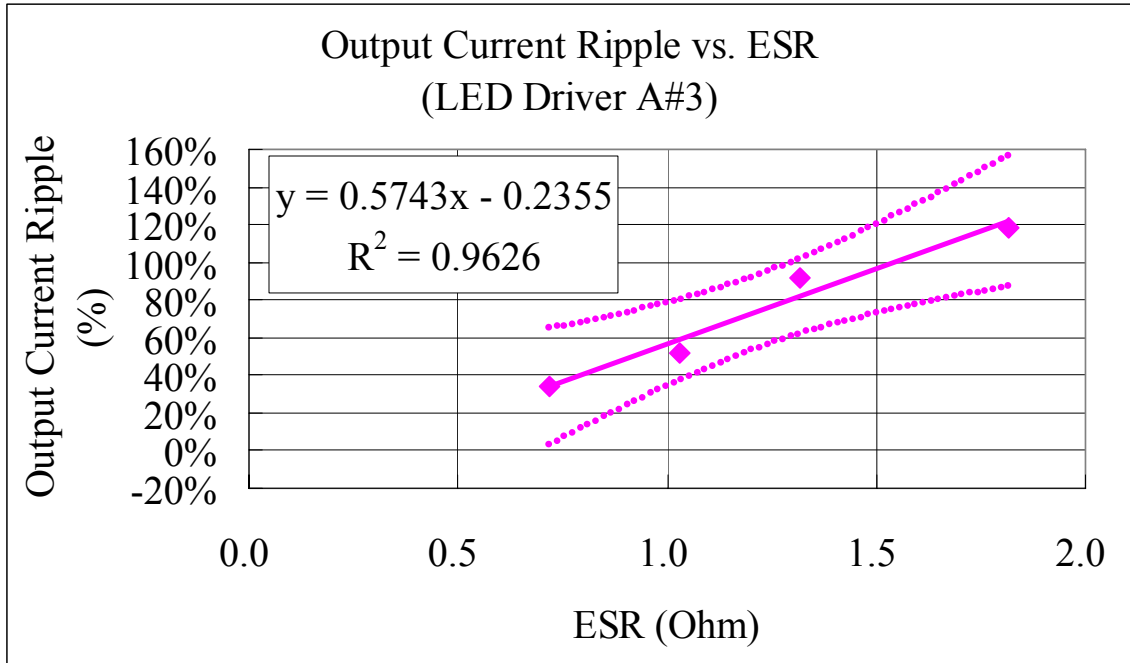


**Fig 6-15 Relationship between output current ripple and ESR of LED driver A #3  
(Dotted lines represent 95% confidence level boundaries.)**

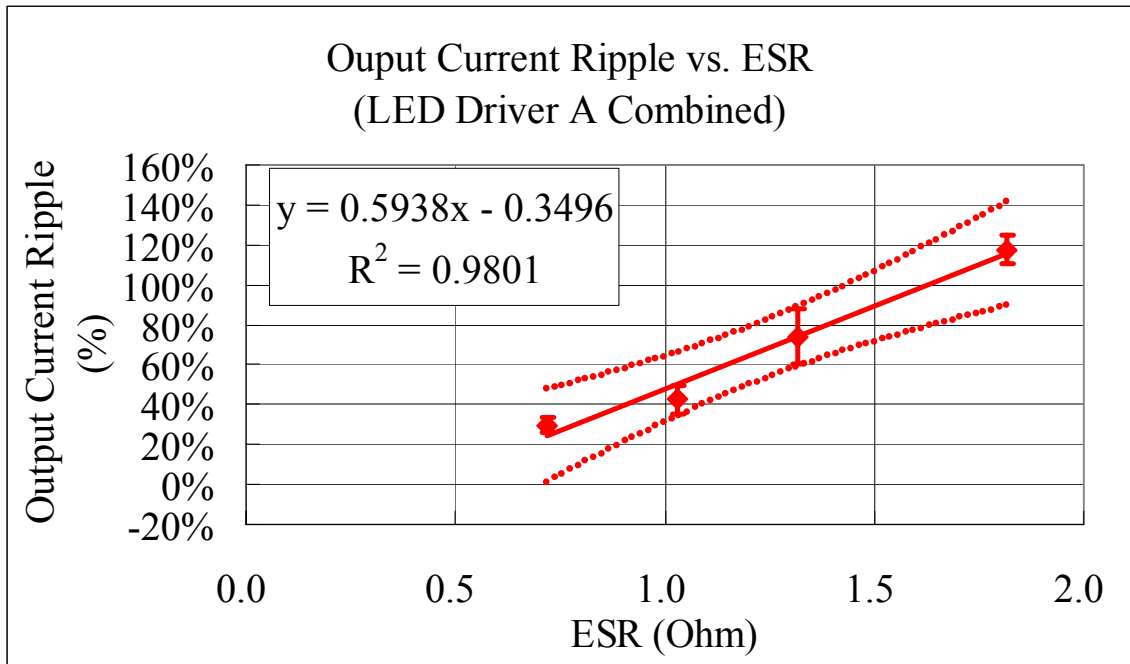


**Fig 6-16 Relationship between output current ripple and ESR of LED driver A  
(Dotted lines represent 95% confidence level boundaries.)**

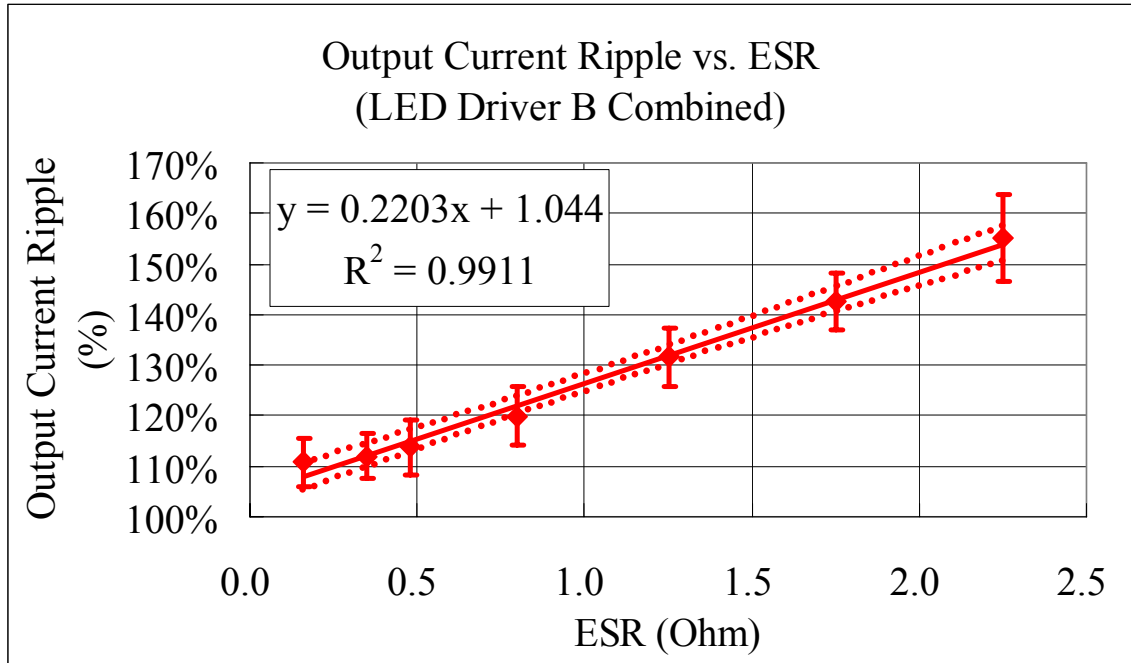


**Fig 6-17 Relationship between output current ripple and ESR of LED driver B (Dotted lines represent 95% confidence level boundaries.)**

#### 6.1.4 Hypothesis 1 Verification

Based on the results of statistical analysis (Appendix A), there is a statistically reliable positive correlation between current ripple and ESR for both LED driver A and LED driver B. So, **hypothesis 1** that states if the ESR of the output capacitor increases then the output current ripple of the LED driver will increase **is verified**.

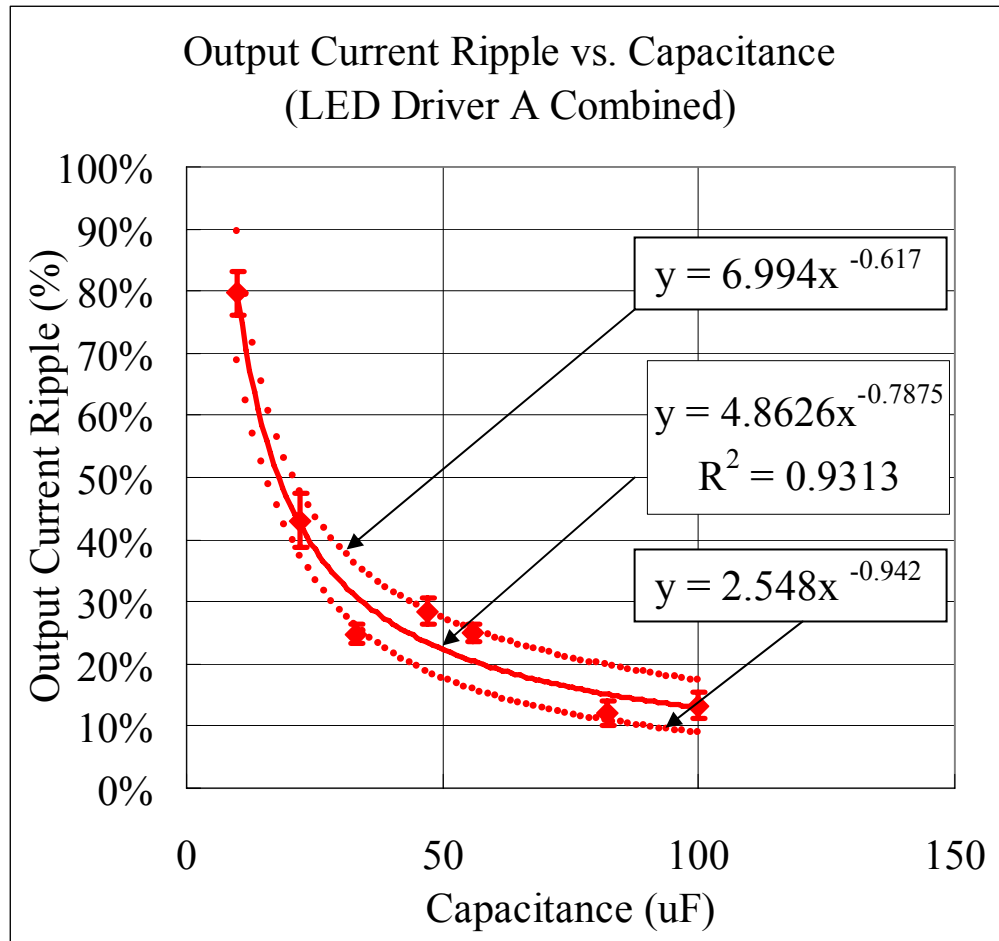
#### 6.1.5 Summary of Experiment 1 Results

As the ESR of the output capacitor increases, the output current ripple of the LED driver will accordingly increase. However, the output current ripple of LED driver A is more sensitive to ESR change than that of LED driver B. It can be calculated that LED driver A's  $\Delta$  ripple /  $\Delta$  ESR is 59% /  $\Omega$ , while LED driver B's  $\Delta$  ripple /  $\Delta$  ESR is 22% /  $\Omega$ .

## 6.2 Experiment 2 Results

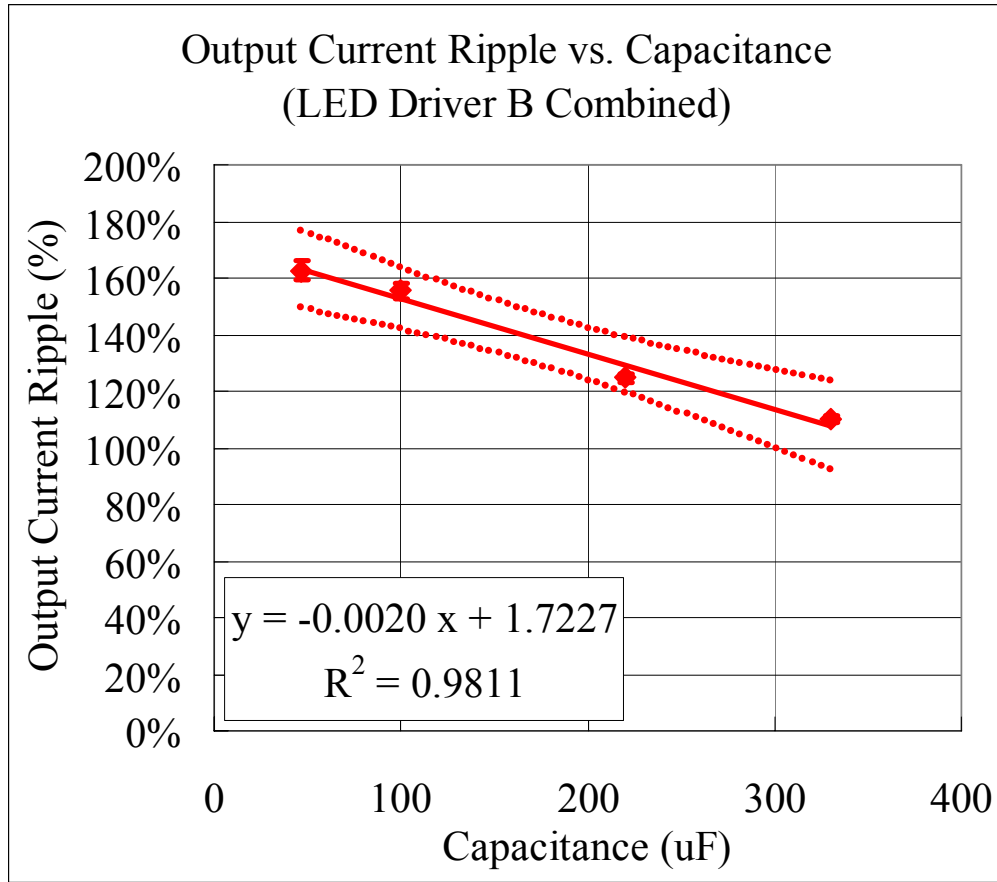
### 6.2.1 Data Processing Method

Fig 6-18 shows the relationship between capacitance and output current ripple for LED driver A. A statistical analysis (Appendix A) was conducted to the combined data of LED driver A in experiment 2.



**Fig 6-18 Relationship between output current ripple and capacitance for LED driver A (Dotted lines represent 95% confidence level boundaries.)**

Fig 6-19 shows the relationship between capacitance and output current ripple for LED driver B. A similar statistical analysis was conducted to the combined data of LED driver B in experiment 2.



**Fig 6-19 Relationship between output current ripple and capacitance for LED driver B (Dotted lines represent 95% confidence level boundaries.)**

### 6.2.2 Hypothesis 2 Verification

Based on the results of statistical analysis (Appendix A), there is a statistically reliable negative correlation between current ripple and ESR for both LED driver A and LED driver B. So, **hypothesis 2** that states if the capacitance of the output capacitor decreases then the output current ripple of the LED driver will increase **is verified**.

### 6.2.3 Summary of Experiment 2 Results

As the capacitance of the output capacitor decreases, the output current ripple of the LED driver will accordingly increase. However, the output current ripple of LED driver A is more sensitive to capacitance change than that of LED driver B. It can be calculated

that LED driver A's  $\Delta$  ripple /  $\Delta$  C is 0.74% /  $\mu$ F, while LED driver B's  $\Delta$  ripple /  $\Delta$  C is 0.20% /  $\mu$ F.

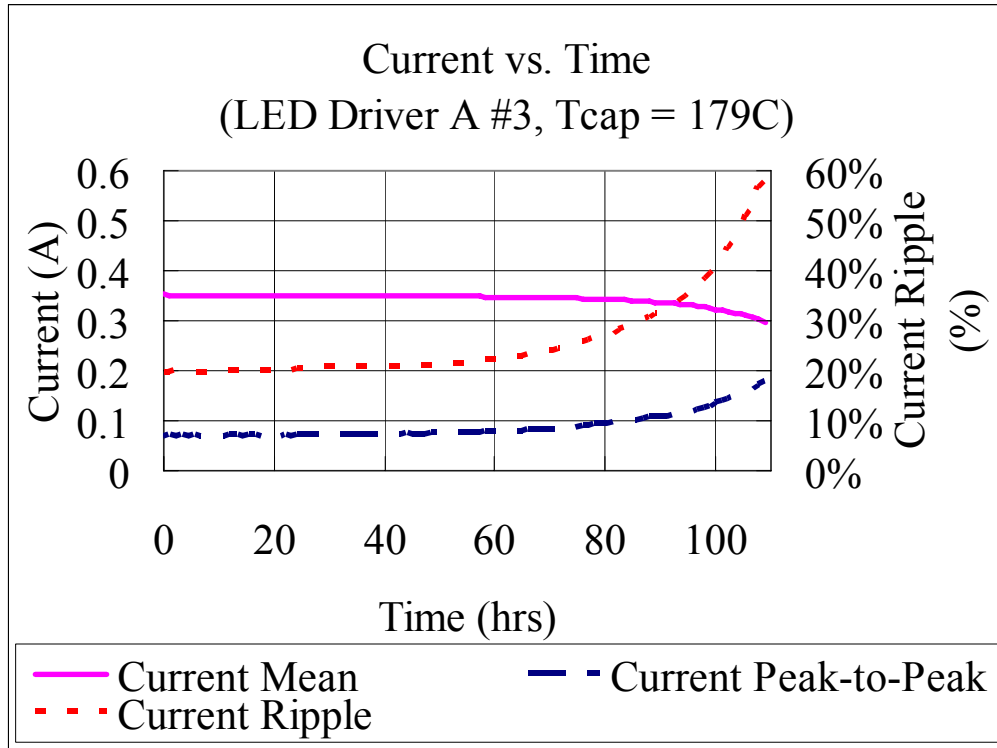
## 6.3 Experiment 3 Results

### 6.3.1 Data Processing Method

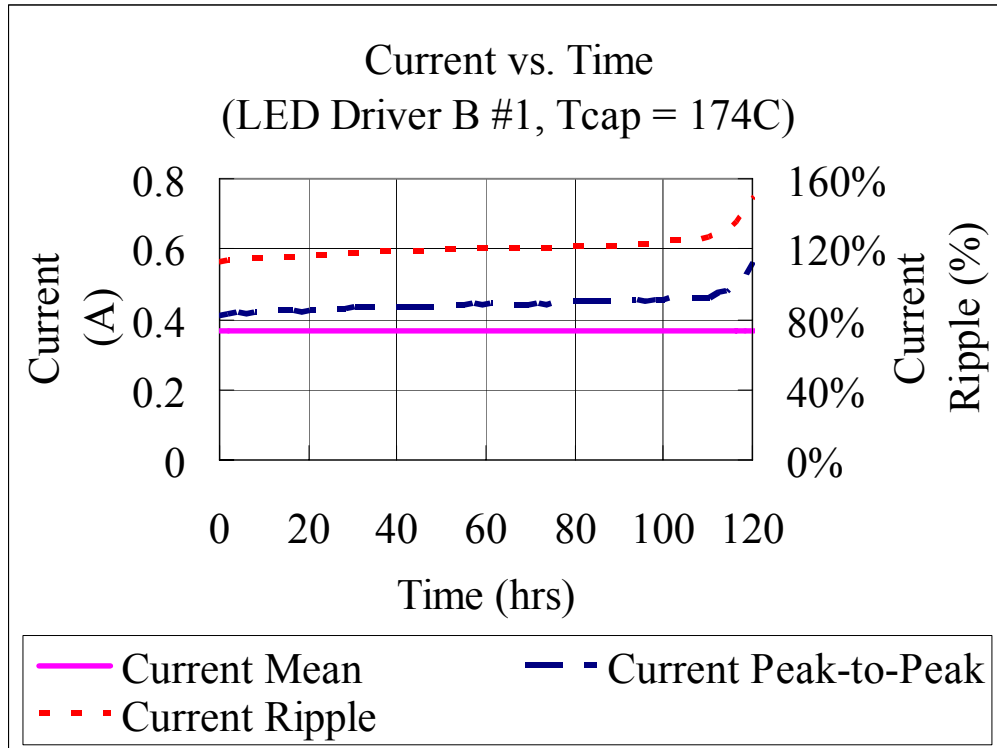
The establishment of the relationship between useful lifetime of the LED driver and the capacitor temperature involves capturing output current parameters, calculating output current ripple trends, calculating 2<sup>nd</sup> derivatives of the output current ripple and targeting its peak, estimating the time elapsed till end-of-life point for each of the capacitor temperature case.

Fig 6-20 shows the output current parameter drift through degradation for LED driver A #3 when capacitor temperature is kept at 179°C. The solid line represents the output current mean value; the dashed line represents the output current peak-to-peak value. And the dotted line shows the calculated current ripple value. It can be seen that the output current mean value decreases slowly while the output current peak-to-peak value increases with time. The combined result is that the current ripple increase slowly at first, than at some point it starts to take off, and increase more and more rapidly.

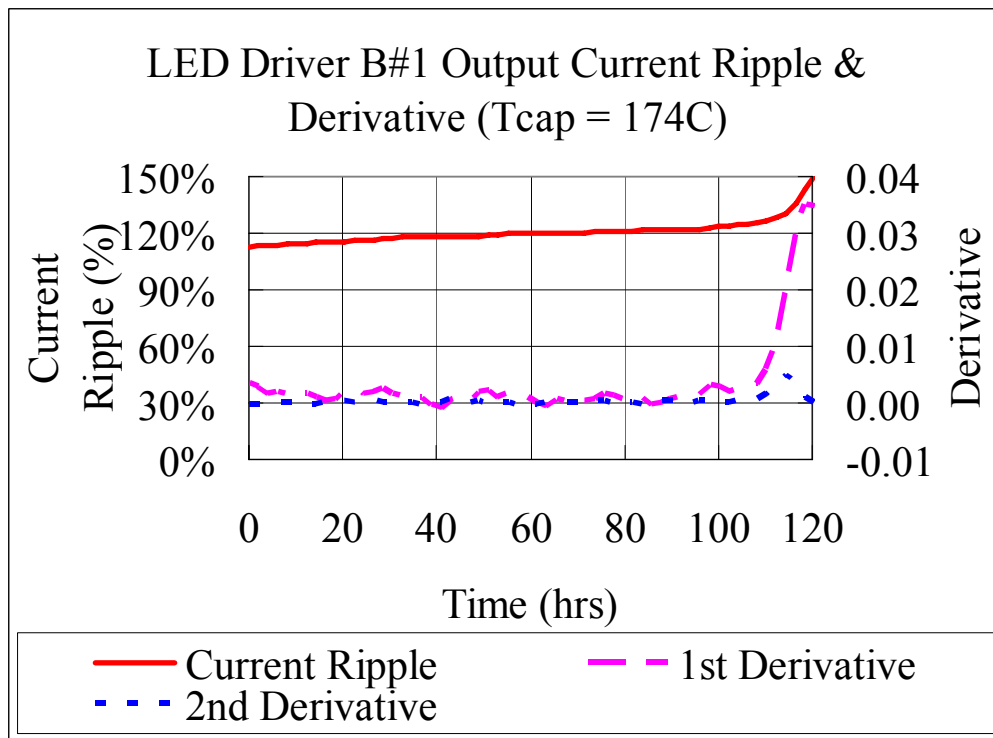
Fig 6-21 shows the output current parameter drift through degradation for LED driver B #1 when capacitor temperature is kept at 174°C. Similarly, the solid line represents the output current mean value; the dashed line represents the output current peak-to-peak value. And the dotted line is the calculated current ripple value. The difference here is that output current mean value keeps constant through the degradation process while only the output current peak-to-peak value increases with time. So, the current ripple is sheer from the contribution of current peak-to-peak amplitude. The current ripple increases at a relatively slow rate at first, and than at certain point it transit to increase at a higher and higher rate. This is very similar to the simulation results demonstrated in Fig 3-14.



**Fig 6-20 Output current parameter drift through degradation for LED driver A #3  
(Tcap = 179 °C)**



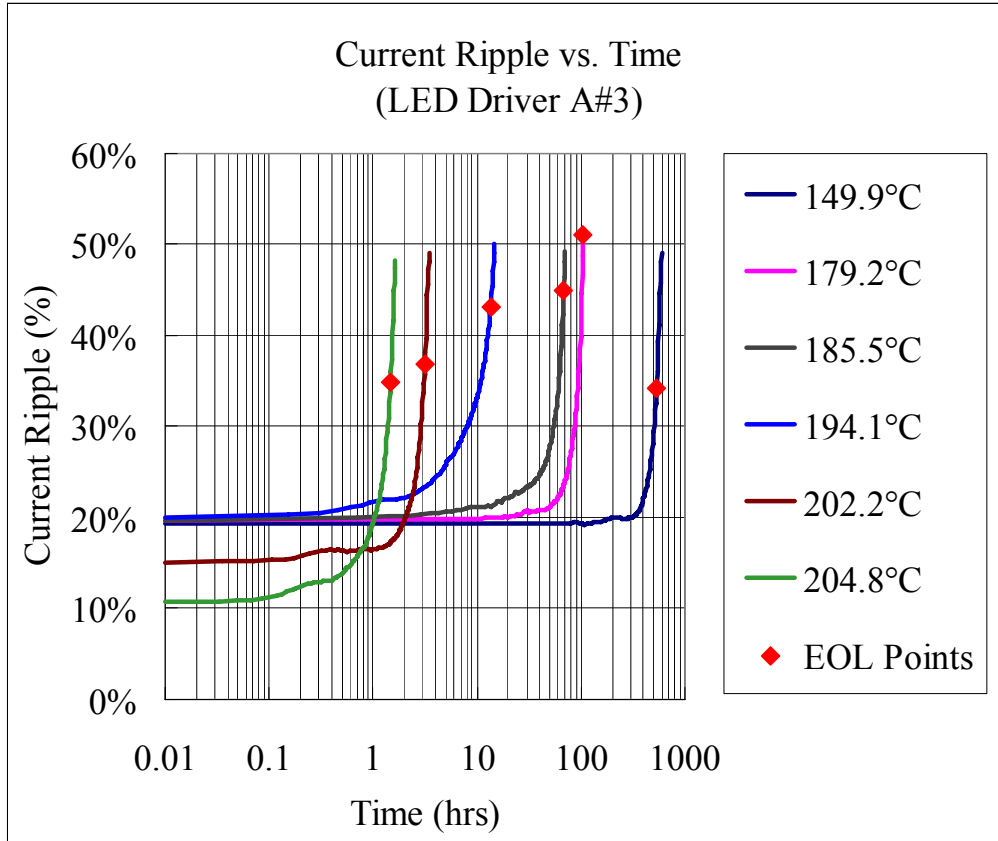
**Fig 6-21 Output current parameter drift through degradation for LED driver B #1 (Tcap = 174°C)**



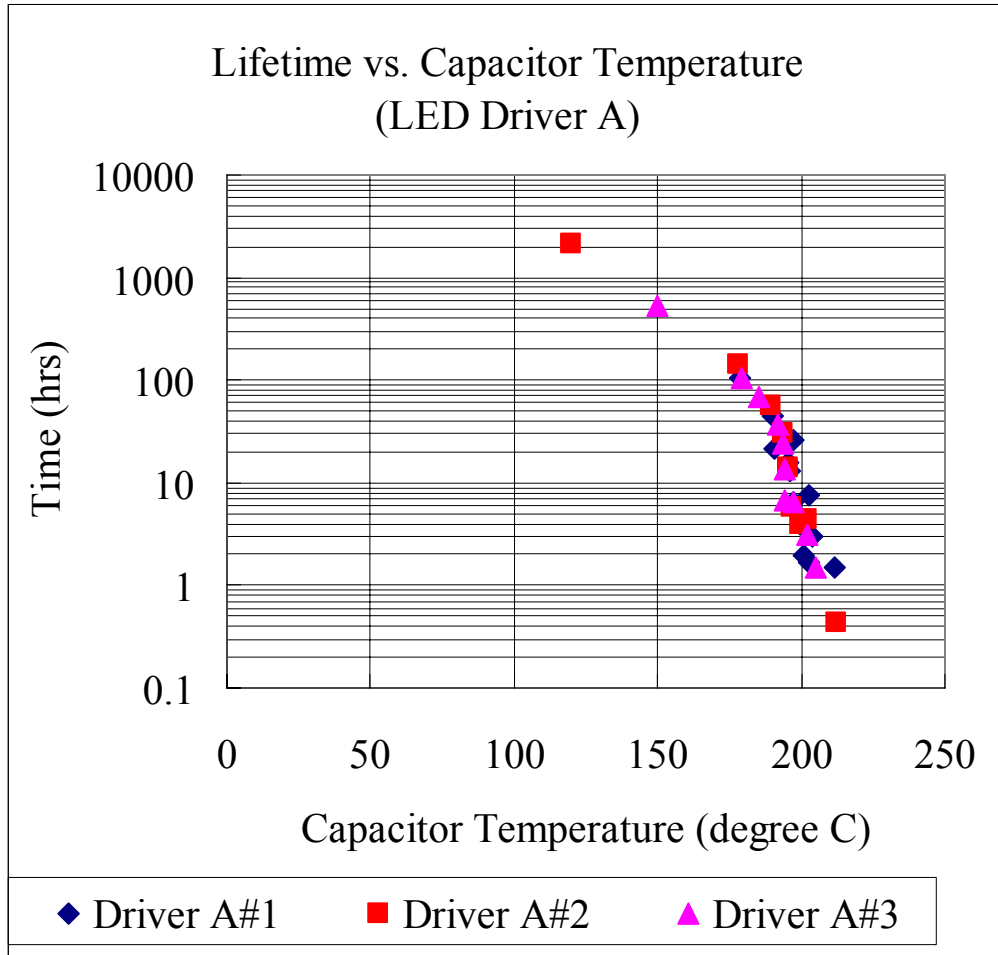
**Fig 6-22 Output current ripple and derivative for LED driver B #1 (Tcap = 174°C)**

Fig 6-22 shows an example of taking derivatives of output current ripple for one temperature case of LED drive B #1. The solid line represents the output current ripple, the dashed line is the 1<sup>st</sup> derivative of the output current ripple, and the dotted line is the 2<sup>nd</sup> derivative. The peak of the dotted line, which is the 2<sup>nd</sup> derivative of the output current ripple, is at approximately 114 hours. According to the end-of-life criterion proposed before, this is the point considered the end-of-life point of this LED driver at this particular temperature condition. So this LED driver sample's useful life at capacitor temperature of 174°C is identified at 114 hours.

Treating the data using the abovementioned data processing method for all of the temperature cases of LED driver A #3, Fig 6-23 was obtained showing a set of current ripple degradation trends at different temperature cases for LED driver A#3. The diamond dots represent the end-of-life points respectively. Then repeating the same data processing method for the data of all 3 samples of LED driver A generates a lifetime profile as a function of capacitor temperature, as depicted in Fig 6-24. Notice the vertical axis is in logarithmic scale. The diamond dots represent LED driver A #1. The square dots represent LED driver A #2. And the triangle dots represent LED driver A #3.



**Fig 6-23 Output current ripple trends at different temperature cases for LED driver A #3 (The diamond dots represent end-of-life points respectively.)**



**Fig 6-24 Lifetime profile of LED driver A #1, #2, #3**

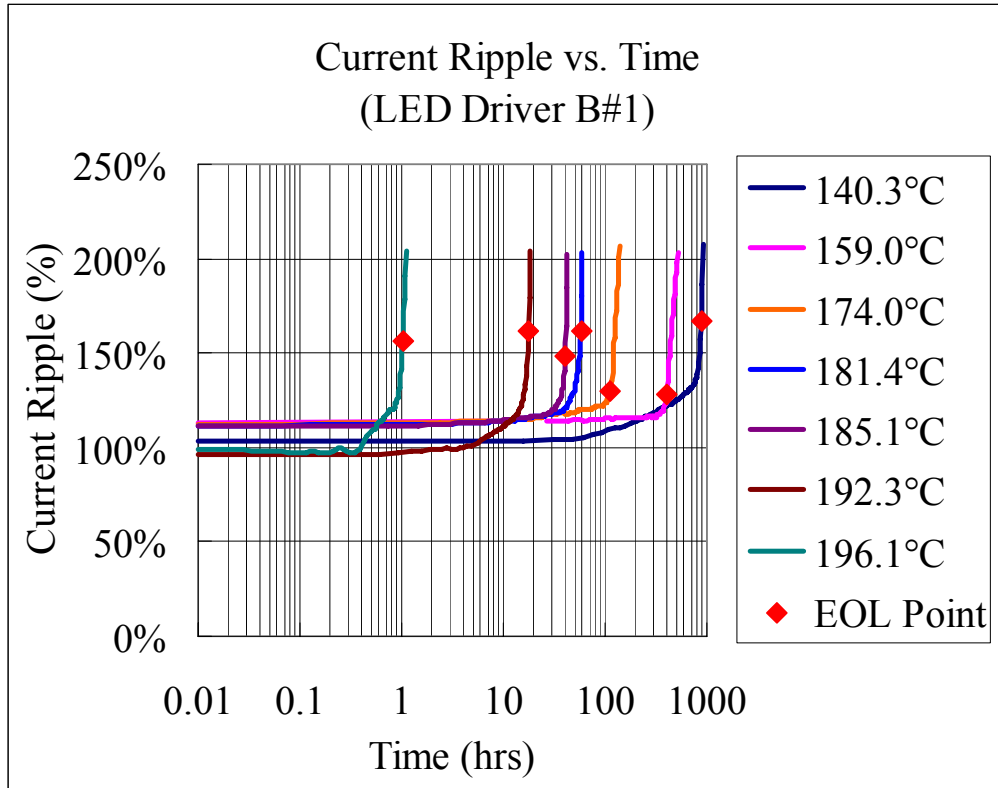


**Fig 6-25 Output current ripple trends at different temperature cases for LED driver B #1 (The diamond dots represent end-of-life points respectively.)**

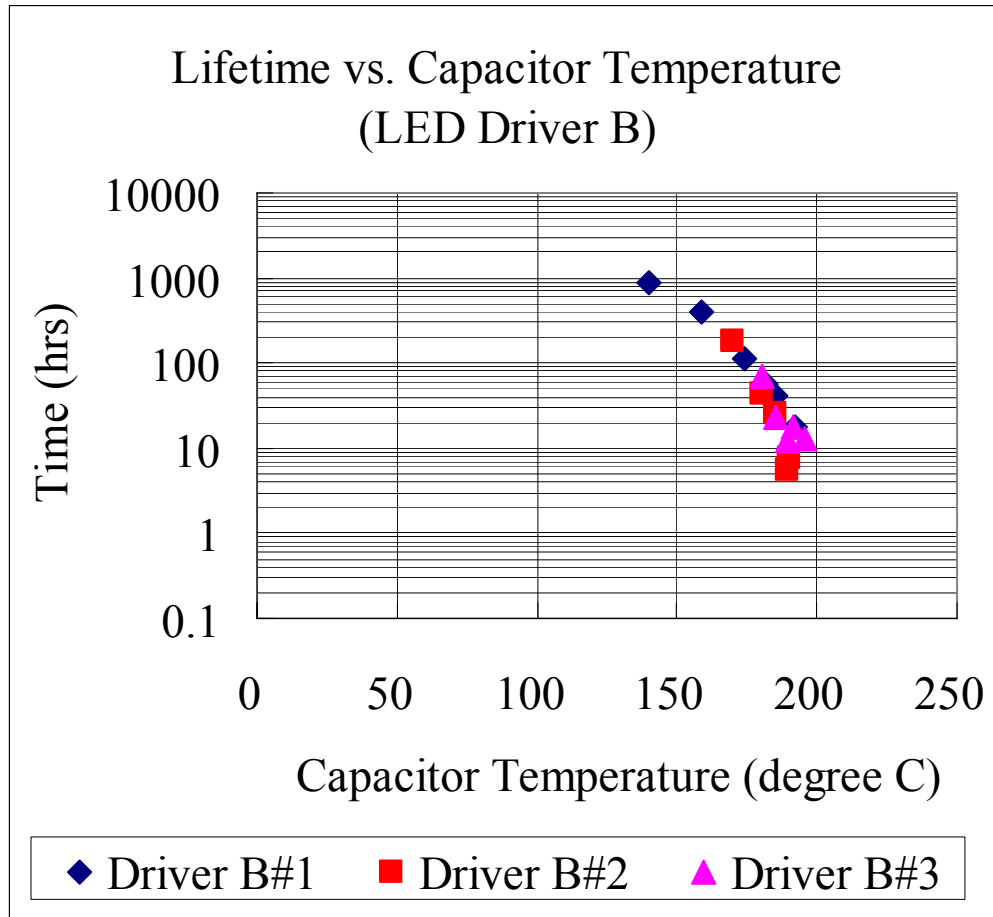


**Fig 6-26 Lifetime profile of LED Driver B #1, #2, #3**

The data of 3 samples of LED driver B was processed using the same data processing method described before. Fig 6-25 shows Output Current Ripple Trends at Different Temperature Cases for LED Driver B #1. The diamond dots represent the end-of-life points for different temperature cases. Then repeat this data processing method for the data of all 3 samples of LED driver B yields a lifetime profile as a function of capacitor temperature for LED driver B, as depicted in Fig 6-26. The diamond dots represent LED driver B #1. The square dots represent LED driver B #2. And the triangle dots represent LED driver B #3.

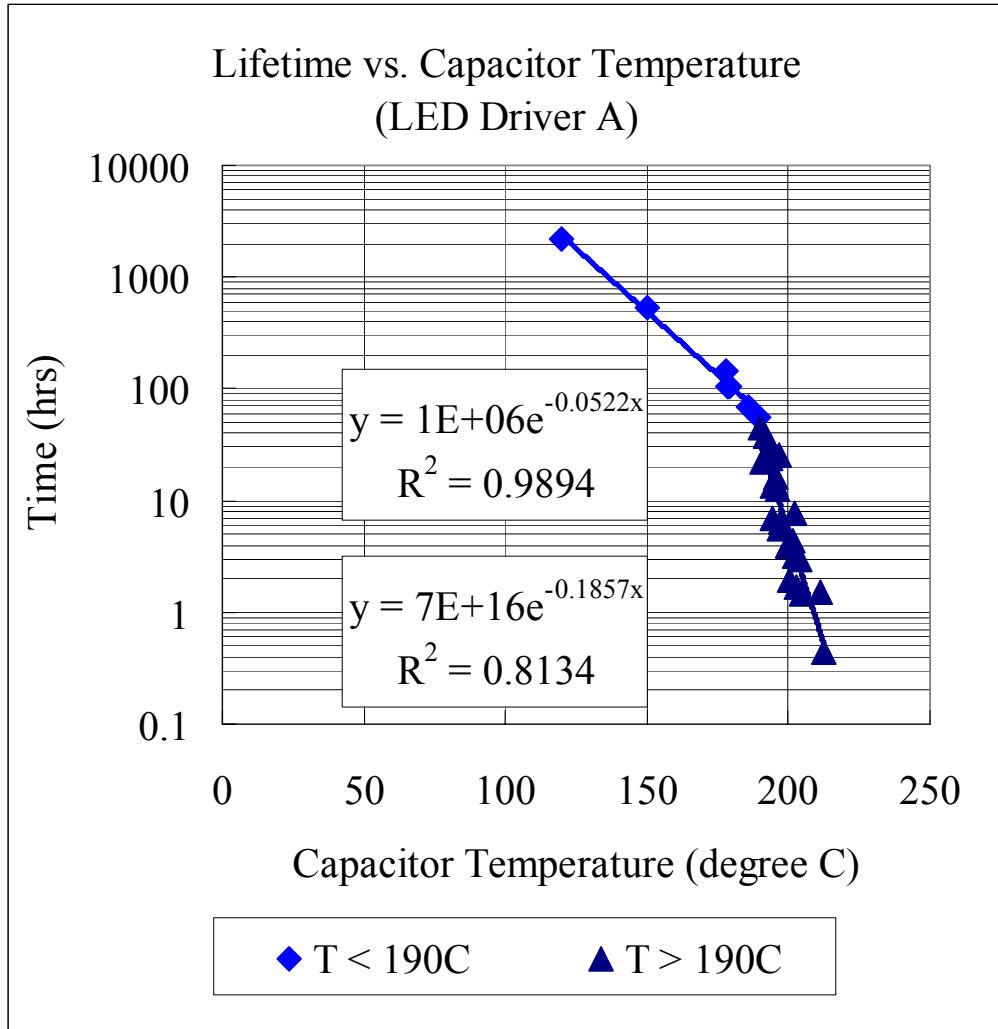
### 6.3.2 Hypothesis 3 Verification

Based on the results of statistical analysis, there is a statistically reliable relationship between useful lifetime and capacitor temperature. So, **hypothesis 3** that states if the capacitor temperature increases then the useful lifetime of the LED driver will decrease **is verified**.

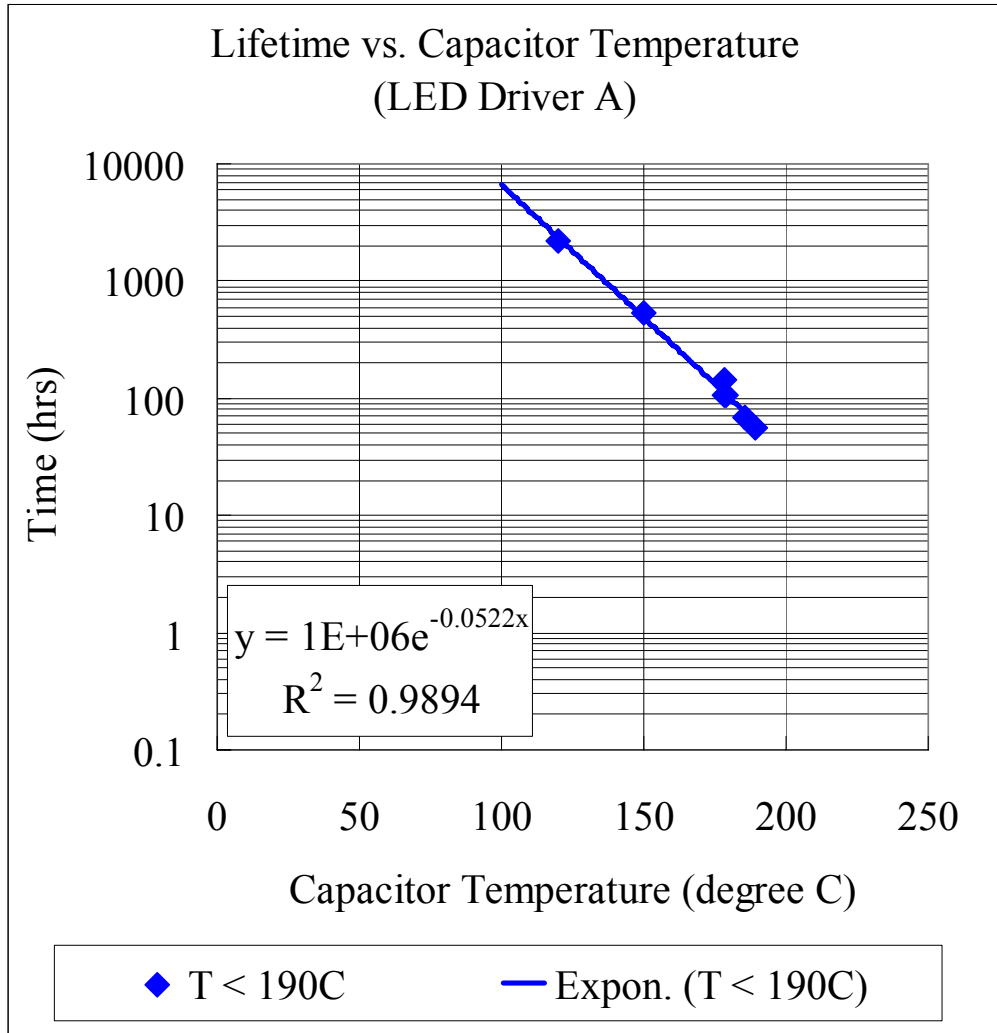
### 6.3.3 Curve Fitting and Extrapolation for Lifetime Prediction

Exponential function in the form of  $y = ae^{bx}$  was found to be a good fit to the relationship between useful lifetime of the LED driver and its output capacitor temperature. Fig 6-27 shows the piecewise exponential curve fitting for LED driver A's lifetime vs. capacitor temperature relationship. It should be pointed out that at around 190 °C, the lifetime curve bends sharply, which suggests that there exist multiple failure mechanisms. Under extremely high temperature conditions, not only the vaporization of electrolyte happens, but also the deterioration of electrolyte occurs. The chemical decomposition induced by extremely high temperature further derates the output capacitor's performance, causing a rapidly reduced useful lifetime under that condition. Therefore, only the data points below 190 °C (the diamond dots shown in Fig 6-27) should be used in extrapolation for lifetime prediction in order to avoid introducing extra failure mechanisms.

Fig 6-28 shows useful lifetime prediction for LED driver A by exponential extrapolation. For example, if the capacitor temperature is at 100 °C, the predicted useful lifetime of LED driver A is approximately 6633 hours. The useful lifetime derating caused by elevated capacitor temperature is calculated as 59% / 10°C. That means every 10°C increase in capacitor temperature will render useful life of LED driver A 59% of its original value.



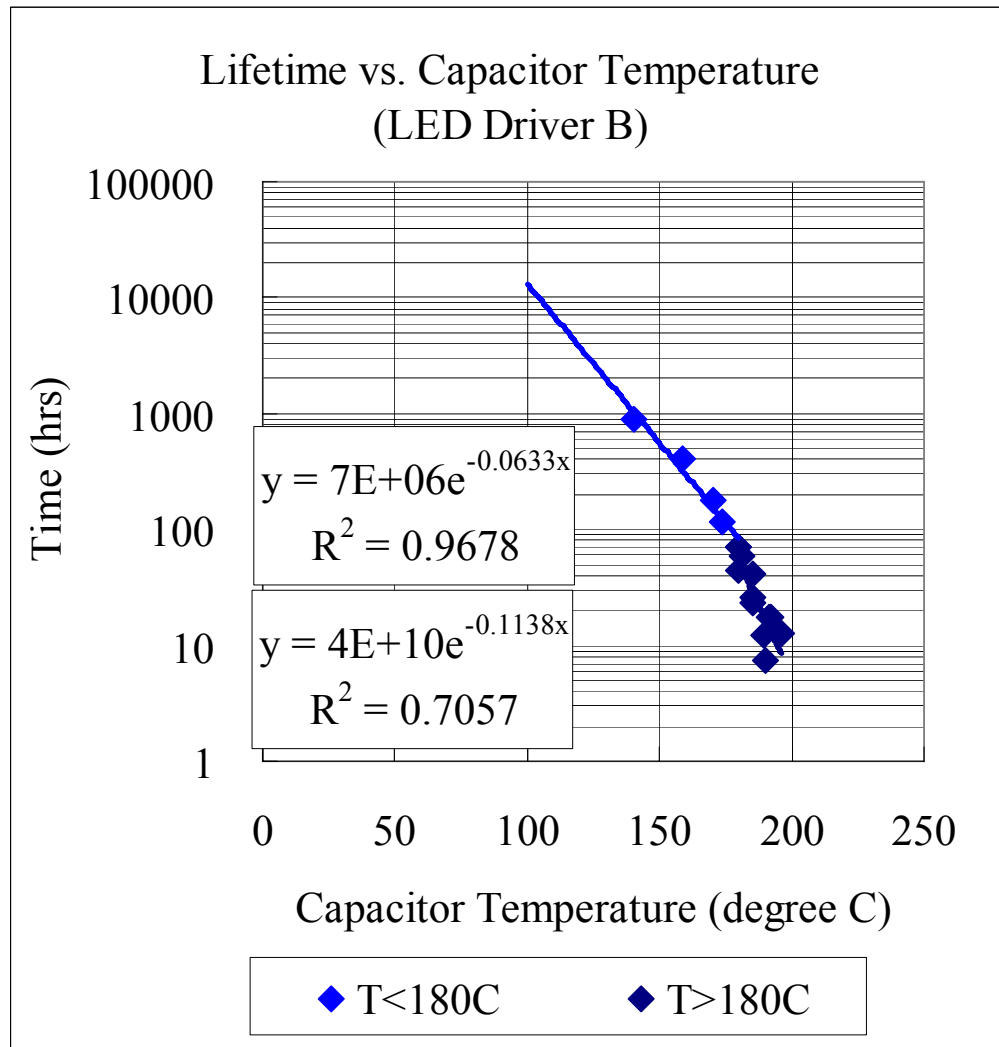
**Fig 6-27 LED drive A lifetime profile with piecewise exponential curve fitting**



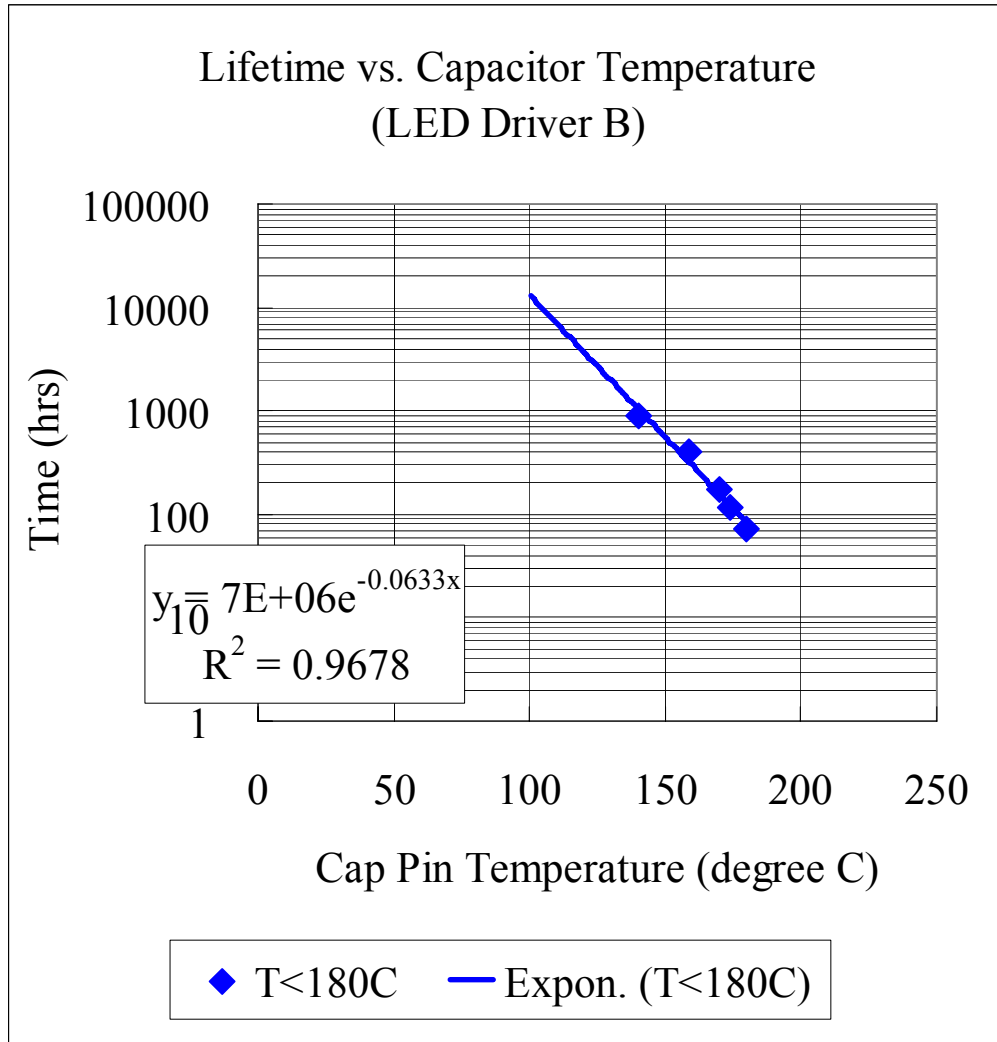
**Fig 6-28 LED driver A lifetime prediction (Derating factor: 59 % / 10 °C)**

Fig 6-29 shows the piecewise exponential curve fitting for LED driver B's lifetime vs. capacitor temperature relationship. It should be pointed out that at around 180 °C, the lifetime curve bends sharply, which also suggests the existence of multiple failure mechanisms. It is also believed that both the vaporization and the deterioration of electrolyte happen together under extremely high temperature conditions. Therefore, only the data points below 180°C (the diamond dots shown in Fig 6-29) should be used in extrapolation for lifetime prediction in order to avoid introducing extra failure mechanisms.

Fig 6-28 shows useful lifetime prediction for LED driver B by exponential extrapolation. For example, if the capacitor temperature is at 100 °C, the predicted useful lifetime of LED driver B is approximately 13169 hours. The useful lifetime derating caused by elevated capacitor temperature is calculated as 53% / 10°C. That means every 10°C increase in capacitor temperature will render useful life of LED driver A 53% of its original value.



**Fig 6-29 LED drive B lifetime profile with piecewise exponential curve fitting**



**Fig 6-30 LED driver B lifetime prediction (Derating factor: 53 % / 10 °C)**

#### 6.3.4 Summary of Experiment 3 Results

The useful lifetime of both of the 2 LED drivers used in experiment 3 decreases exponentially as its output capacitor temperature increases. LED driver A's useful life is slightly more sensitive to capacitor temperature change than that of LED driver B. The useful lifetime derating caused by capacitor temperature for LED driver A is 59% / 10°C. The useful lifetime derating caused by capacitor temperature for LED driver B is 53% / 10°C.

## 7. Discussion

### 7.1 Comparison of Impact of ESR and Capacitance Change on Output Current Ripple

Both ESR increase and capacitance decrease can cause increase of output current ripple. It is desired to further analyze which of the 2 factors that has a relatively greater impact on output current ripple increase.

Consider typical range of ESR change to evaluate its impact on output current ripple. The initial ESR value of the electrolytic capacitor used in LED driver A is about  $0.72 \Omega$ , and develops to about  $10 \Omega$  when the capacitor is degraded. LED driver A's  $\Delta$  ripple /  $\Delta$  ESR is  $59\% / \Omega$ , so a change of  $10 \Omega$  in ESR can cause 590% of its output current ripple increase. Similarly, the initial ESR value of the electrolytic capacitor used in LED driver B is about  $0.16 \Omega$ , and develops to about  $10 \Omega$  when the capacitor is degraded. LED driver B's  $\Delta$  ripple /  $\Delta$  ESR is  $22\% / \Omega$ , and a change of  $10 \Omega$  in ESR can cause 220% of its output current ripple increase.

Consider typical range of capacitance change to evaluate its impact on output current ripple. The initial capacitance of the electrolytic capacitor used in LED driver A is  $100 \mu\text{F}$ . A typical 20% drop of capacitance is expected when the capacitor is degraded. LED driver A's  $\Delta$  ripple /  $\Delta$  C is  $0.74\% / \mu\text{F}$ , so a change of  $20 \mu\text{F}$  can cause 14.8 % of its output current ripple increase. Similarly, the initial capacitance of the electrolytic capacitor used in LED driver B is  $330 \mu\text{F}$ . A typical 20% drop of capacitance is expected when the capacitor is degraded. LED driver B's  $\Delta$  ripple /  $\Delta$  C is  $0.20\% / \mu\text{F}$ , so a change of  $66 \mu\text{F}$  can cause 13% of its output current ripple increase.

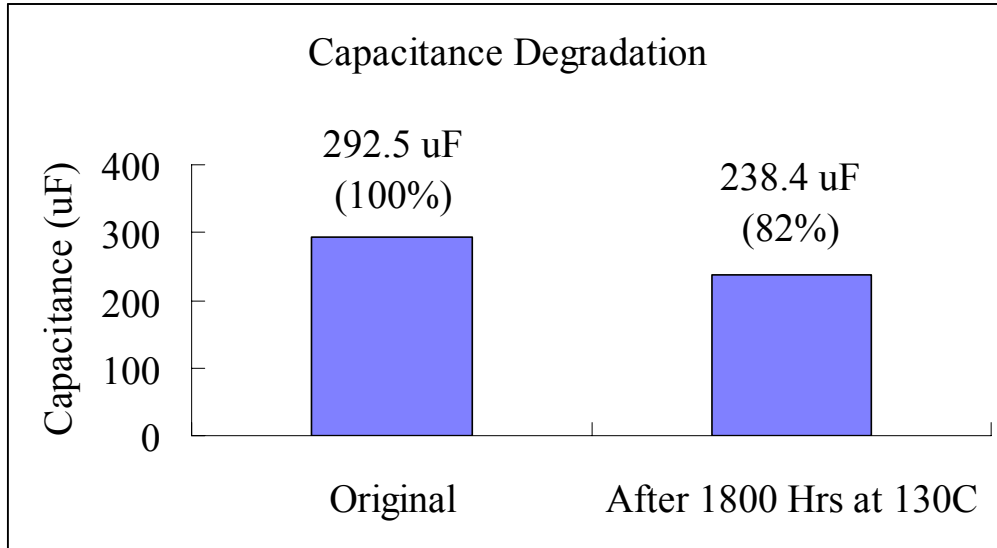


**Fig 7-1 Capacitance change after 1800 hours exposed at 130 °C for LED driver B (decreased by 18%)**

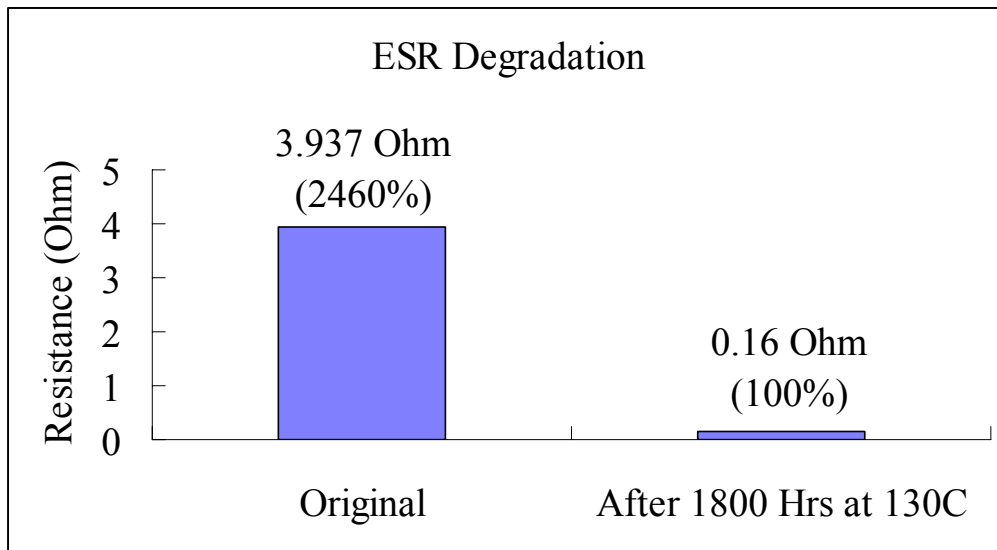


**Fig 7-2 ESR change after 1800 hours exposed at 130 °C for LED driver B (increased by 1360%)**

From the above analysis, it is obvious that current ripple development is mostly dominated by ESR than capacitance. This is consistent with Venet's (1999) findings for static converter applications. And this is also experimentally confirmed by taking measurements of the capacitance and ESR values of the electrolytic capacitor at sound

condition and at degraded condition. Fig 7-1 shows the capacitance change before the capacitor is exposed to elevated temperature condition and after 1800 hours of treatment at 130 °C. Fig 7-2 shows ESR change before and after 1800 hours of treatment at 130°C. The capacitance dropped by 18% of its initial value, while ESR increased by 2360% of its initial value. So it is the significant increase in ESR value that will dominantly affect the LED driver's output current ripple change.

ESR is a critical parameter when selecting output capacitor component. ESR is the major cause of high frequency current ripple, because at switching frequency of around 10kHz, the impedance of an electrolytic capacitor is dominated by its ESR value, and it limits the filter function of the capacitor.

## **7.2 Impact of Topologies of LED Drivers on Output Current Ripple**

The final experiments show that output current ripple of different types of LED drivers has different sensitivity to capacitance change and ESR change. This is mainly due to the difference in LED driver topology. LED driver A is a standard flyback converter so that its ripple is mainly at switching frequency which is solely dependent on ESR. LED driver B performs both current regulation as a standard flyback and power factor correction. Its output current ripple has a 120 Hz sinusoidal like ripple envelop superimposed with high frequency switching ripple. Thus, ESR change only affects the width of the ripple envelop while the amplitude of the ripple envelop is determined by the capacitance, which doesn't experience significant change compared to that of ESR. However, the downside of LED driver B is that the initial current ripple absolute value is fairly high due to the limitation of the speed of the output voltage feedback loop. Therefore, for applications using the type of LED driver B, it is important to ensure that the peak current will not exceed the LED's maximum allowable forward current for better reliability.

### **7.3 Component Lifetime vs. Application Lifetime**

The output electrolytic capacitor used in LED driver A has a component lifetime of 1000 hours @ 105°C, and the output electrolytic capacitor in LED driver B has a component lifetime of 5000 hours @ 105°C. However, given the same capacitor temperature of 100°C, LED driver A's useful life is 6633 hours while LED driver B's useful lifetime is 13169 hours. Although the component lifetime of the output electrolytic capacitor in LED driver B is 5 times of that of the output electrolytic capacitor used in LED driver A, it does not guarantee that the application lifetime of LED driver B is also 5 times that of that of LED driver A. In fact, the useful lifetime of LED driver B is 2 times that of LED driver A. This implies that the capacitor manufacturers' end-of-life definition is not always applicable to application. The component's useful lifetime in a system largely depends on application requirements and specific operating environments.

### **7.4 Limitations and Proposed Future Study**

This study only considers the type of offline LED drivers that uses an electrolytic capacitor at the output stage. For other type of LED drivers that does not have an electrolytic capacitor installed at the output stage, this study's methods and results may not be valid.

In this study, an end-of-life criterion based on the analysis of the rate of change of the output current ripple was proposed. Different end-of-life criterion may affect the predicted lifetime value. For instance, the predicted useful lifetime could be shorter in applications that have a tighter tolerance to output current ripple.

This study only considered continuous operation of the LED drivers. In real applications, the usage pattern can also impact the useful life of an off-line LED driver. The above-mentioned test method does not take switching operation into consideration. Additional studies are needed to quantify performance if frequent turning on and off operations exist.

In this study, only the output capacitor instead of the whole LED driver was treated with elevated temperature stress. This is because the potting compound which is often used for insulation purpose in commercial LED drivers will cause uncomfortable smell and smoking at temperatures above 100°C, but the accelerated life testing needs to apply temperature treatment above 100°C. So based on the literature review and component failure rate estimation results for the LED drivers, the output electrolytic capacitor was assumed to be the weakest link in an LED driver, and it was chosen to receive temperature treatment rather the whole LED driver. The next step is to develop a method so that the whole LED driver will experience the stress condition instead of a single component.

Other types of LED drivers, other acceleration patterns like cycling, other acceleration factors such as input voltage, humidity, and vibration, may also be used in this accelerated life testing study. A combination of several acceleration factors helps to rapidly identify an electronic system's weak link and reliability issue.

## **8. Summary**

The output electrolytic capacitor is estimated to have the highest failure rate in offline LED drivers. As an electrolytic capacitor degrades, its ESR increases and its capacitance decreases. The electrolytic capacitor's lifetime is sensitive to operating temperature. Heat affects the rate of change of ESR and capacitance and accelerates the degradation process. The LED driver's output current ripple increases when the output capacitor's ESR increases and its capacitance decreases. Therefore, the LED driver's output current ripple was shown to be a good predictor of the useful life of the LED drivers. For the LED drivers tested, useful lifetime decreased exponentially as capacitor temperature increased. Output current ripple is affected by LED driver topologies. Generally, ESR change has much more impact on output current shift than capacitance change. A long component lifetime of an electrolytic capacitor does not guarantee an equivalently long application lifetime. It depends on application requirements and specific operating environments.

## 9. References

Adragna, C., “AN1059 Application Note: Design Equations of High-Power-Factor Flyback Converters Based On The L6561”, [www.st.com](http://www.st.com), Sept., 2003. Date Last Accessed, 08/19/2009.

Avago Technologies, “Application Note 5310: Driving High Power and High Brightness LEDs”, [www.avagotech.com](http://www.avagotech.com), June, 2007. Date Last Accessed, 08/19/2009.

Bennett, D.N., “Off-Line SMPS Failure Modes PWM Switchers and DC-DC Converters”, <http://www.ti.com/>, 2000. Date Last Accessed, 08/19/2009.

Bhandarkar, V., Steele, B., “Driver ICs for HB LEDs: A Large and Growing Market”, *LEDs Magazine*, March 2008

BHC Components, “Aluminum Electrolytic Capacitor Application Notes”, <http://www.bhc.co.uk/literature.htm>, 2002. Date Last Accessed, 08/19/2009.

Broeck, H., Sauerlander, G., Wendt, M., “Power Driver Topologies and Control Schemes for LEDs”, *Applied Power Electronics Conference, APEC 2007 – Twenty Second Annual IEEE*, pp: 1319-1325, Feb., 2007.

CDE (Cornell Dubilier Electronics, Inc.), “Application Guide, Aluminum Electrolytic Capacitors”, <http://www.cornell-dubilier.com>, 2000. Date Last Accessed, 08/19/2009.

Cree, Inc., “Cree Xlamp XP-G LED Data Sheet”, [www.cree.com/xlamp](http://www.cree.com/xlamp), 2009. Date Last Accessed, 08/19/2009.

Dakin, T.W., Henry, E.N., Mullen, G.A., “Life Testing of Electronic Power Transformers”, *IEEE Transactions on Electrical Insulation*, Vol. 3, Issue 1, Feb., 1968.

Fromm, R., “Power Supply Repair”, <http://www.mikesarcade.com>, 1994. Date Last Accessed, 08/19/2009.

Gasperi, M.L., “Life Prediction Model for Aluminum Electrolytic Capacitors”, *Industry Applications Conference, 1996. Thirty-First IAS Annual Meeting, IAS '96 Conference Record of the 1996 IEEE*, Vol. 3, pp: 1347-1351, Oct., 1996.

GE Lighting, “Vio High Power White LED Data Sheet”, <http://www.lumination.com/product.php?id=56>, 2009. Date Last Accessed, 08/19/2009.

Harada, K., Katsuki, A., Fujiwara, M., “Use of ESR for Deterioration Diagnosis of Electrolytic Capacitor”, *IEEE Transactions on Power Electronics*, Vol. 8, No. 4, pp: 355-361, 1993.

Imam, A.M., Habetler, T.G., Harley, R.G., Divan, D.M., “LMS Based Condition Monitoring of Electrolytic Capacitor”, *Industrial Electronics Society, 2005. IECON 2005. 31<sup>st</sup> Annual Conference of IEEE*, Nov., 2005.

Jayasinghe, L., Gu, Y.M., Narendran, N., “Characterizaion of Thermal Resistance Coefficient of High-power LEDs”, *6<sup>th</sup> International Conference on Solid State Lighting, Proceeding of SPIE*, Vol. 6337, pp: 63370V.1 – 63370V.10, 2006.

Jones, J.A., Hayes, J.A., “The Parametric Drift Behavior of Aluminum Electrolytic Capacitors: An Evaluation of Four Models”, *1<sup>st</sup> European Capacitor and Resistor Technology Proceeding, U.K.*, pp: 171-179, 1987.

Kassakian, J.G., Schlecht, M.F., Verghese, G.C., *Principles of Power Electronics*, Prentice Hall, July, 1991.

Lahyani, A., Venet, P., Grellet, G., Viverge, P.J., “Failure Prediction of Electrolytic Capacitors During Operation of a Switchmode Power Supply”, *IEEE Transactions on Power Electronics*, Vol. 13, No. 6., Nov., 1998.

Mandelcorn, J., “Buck Converter: Key Is Selecting the Right Capacitor”, [www.powermanagementdesignline.com](http://www.powermanagementdesignline.com), June, 2009. Date Last Accessed, 08/19/2009.

Matsushita Electronic Components Co., LTD., “Technical Guide of Aluminum Electrolytic Capacitors”, 2000.

Maxim Integrated Products, “Application Note 3256: Why Drive White LEDs with Constant Current?”, [http://www.maxim-ic.com/appnotes.cfm/an\\_pk/3256](http://www.maxim-ic.com/appnotes.cfm/an_pk/3256), Aug., 2004. Date Last Accessed, 08/19/2009.

McGuigan, F.J., *Experimental Psychology: Method of Research*, 7<sup>th</sup> edition, Prentice Hall, 1997.

Minford, W., “Accelerated Life Testing and Reliability of High K Multilayer Ceramic Capacitors”, *IEEE Transactions on Components, Hybrids, and Manufacturing Technology*, Vol. 5, Issue 3, Sept., 1982.

Muthu, S., Schuurmans, J.P., Pashley, M.D., “Red, Green, and Blue LEDs for White Light Illumination”, *IEEE Journal of Selected Topics in Quantum Electronics*, Vol. 8, No. 2, March, 2002.

National Semiconductor, “LED Drivers for High-Brightness Lighting Solution Guide”, <http://www.national.com>, Vol. 2, 2009. Date Last Accessed, 08/19/2009.

Nichicon Inc., “General Descriptions of Aluminum Electrolytic Capacitors”, <http://www.nichicon.co.jp/english/index.html>, 2002. Date Last Accessed, 08/19/2009.

ON Semiconductor, “Power Factor Correction Handbook”, [www.onsemi.com](http://www.onsemi.com), Rev. 3, Sept., 2007. Date Last Accessed, 08/19/2009.

Panasonic Industrial Company, “Aluminum Electrolytic Capacitors”, <http://www.panasonic.com/industrial/components>, 2008. Date Last Accessed, 08/19/2009.

Philips Lumileds, “LUXEON Rebel Technical Datasheet DS64”, <http://www.philipslumileds.com/products/luxeon-rebel-white>, 2009. Date Last Accessed, 08/19/2009.

ReliaSoft Co., “Accelerated Life Testing Reference On-Line Reference”, <http://www.weibull.com/acceltestwebcontents.htm>, 2007. Date Last Accessed, 08/19/2009.

Revox Rifa, “Life-Limiting Factors in Electrolytic Capacitors”, [www.evov-rifa.com](http://www.evov-rifa.com), 2001. Date Last Accessed, 08/19/2009.

Rhoades, G.E., Smith, A.W.H., “Expected Life of Capacitors with Nonsolid Electrolyte”, *34<sup>th</sup> Component Conference Proceeding, 1984*, pp: 156-161, 1984.

Ronat, O., Green, P., Ragona, S., “Accurate Current Control to Drive High Power LED Strings”, International Rectifier, El Segundo, CA, 2006.

Rubinstein, F., “Controls for Solid-state Lighting”, Lawrence Berkeley National Laboratory, 2007.

Sankaran, V.A., Rees, F.L., Avant, C.S., “Electrolytic Capacitor Life Testing and Prediction”, *Industry Applications Conference, 1997. Thirty-Second IAS Annual Meeting, IAS '97., Conference Record of the 1997 IEEE*, Vol. 2, pp: 1058-1065, Oct., 1997.

Sauerlander, G., Hente, D., Radermacher, H., et al., “Driver Electronics for LEDs”, *Industry Applications Conference, 2006. 41<sup>st</sup> IAS Annual Meeting. Conference Record of the 2006 IEEE*, Vol. 5, pp: 2621-2626, Oct., 2006.

Seoul Semiconductor, “X41280 Technical Data Sheet”, <http://www.acriche.com/en/>, 2008. Date Last Accessed, 08/19/2009.

Steigerwald, D.A., Bhat, J.C., Collins, D., et al. “Illumination with Solid State Lighting Technology,” *IEEE Journal on Selected Topics in Quantum Electronics*, Vol. 8, No. 2, March, 2002.

Stevens, J.L., Shaffer, J.S., Vandenharn, J.T., “The Service Life of Large Aluminum Electrolytic Capacitors: Effects of Construction and Application”, *IEEE Transactions on Industry Applications*, Vol. 38, No. 5, Sept., 2002.

United Chemi-Con, “Characteristics of Aluminum Electrolytic Capacitors”, <http://www.chemi-con.com/u7002/characteristics.php>, 2003. Date Last Accessed, 08/19/2009.

U.S. Department of Defense, “Military Handbook 217F: Reliability Prediction of Electronic Equipment”, Dec., 1991.

U.S. Department of Energy, “ENERGY STAR Program Requirements for Solid State Lighting Luminaires Eligibility Criteria – Version 1.1”, Dec. 19, 2008.

Venet, P., Lahyani, A., Grellet, G., Ah-Jaco, A., “Influence of Aging on Electrolytic Capacitors Function in Static Converters: Fault Prediction Method”, *EPJ. Applied Physics*, Vol. 5, No. 1, pp: 71-83, 1999.

Venet, P., Perisse, F., El-husseini, M.H., Rojat, G., “Realization of A Smart Electrolytic Capacitor Circuit”, *IEEE Industry Applications Magazine*, Jan., 2002.

## 10. Appendix A: Statistical Analysis

The statistical analysis methods used to verify hypothesis were evaluation of correlation coefficient, and 95% confidence level calculation. The first method states that, if the calculated correlation coefficient from variable X and variable Y is found to be greater than the threshold, then there is a positive relationship between Y and X for correlation coefficient greater than 0, or there is a negative relationship between Y and X for correlation coefficient less than 0 (McGuigan, 1997). The second method involves choosing curve fitting and calculates the upper and lower boundaries of 95% confidence level. If the lower boundary curve still has an increasing trend as indicated by a positive sign of the 1<sup>st</sup> derivative of Y as a function of X, then there is a positive relationship between Y and X. Similarly, if the upper boundary curve is proved to an decreasing trend as indicated by a negative sign of the 1<sup>st</sup> derivative of Y as a function of X, then there is a negative relationship between Y and X.

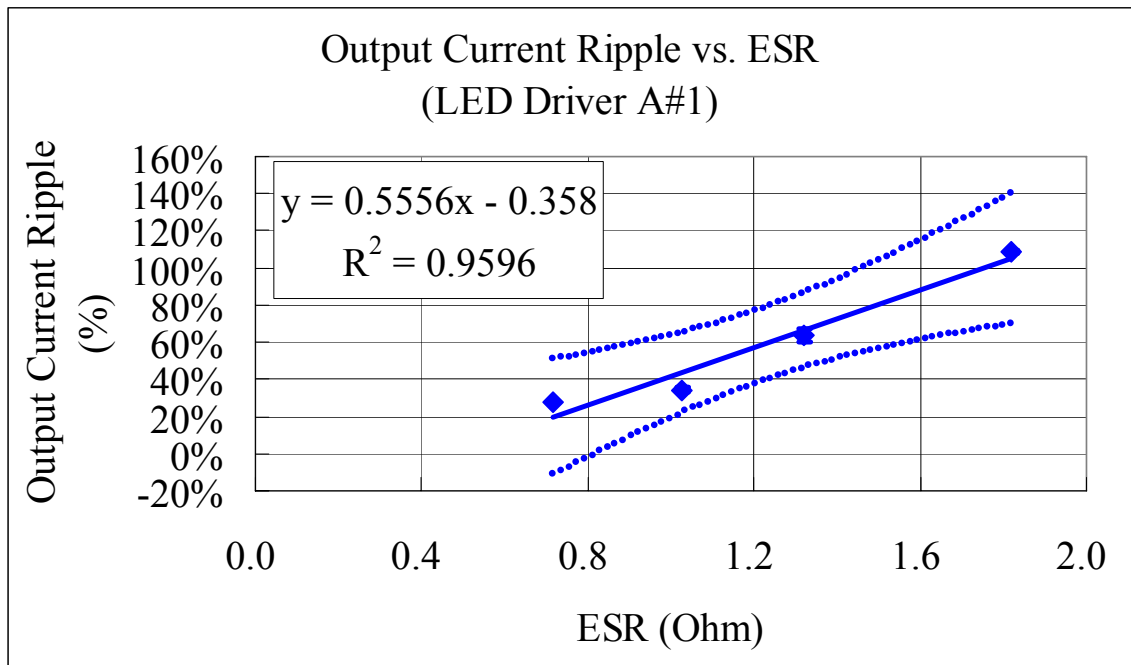


**Fig 10-1 Relationship between output current ripple and ESR of LED driver A #1 (Dotted lines represent 95% confidence level boundaries.)**

By using the formula of current ripple defined in section 4.2, the relationship between ESR and output current ripple was established. Fig 10-1 shows the relationship between ESR and output current ripple of LED driver A #1. The first statistical method shows that, the calculated R(correlation coefficient) is 0.980, whose absolute value is greater than 0.950 (threshold for  $p = 0.05$ ,  $N = 4$ ). This proves that there is a statistically reliable positive correlation between current ripple and ESR for LED driver A #1. The second statistical analysis method gives the boundaries of 95% confidence level as indicated by the 2 dotted lines shown in Fig 10-1. The slope upper limit is 1.2569, and the slope lower limit is 0.2907. Even the lower limit of the slope is positive, suggesting that as ESR increases, there is a reliable increase of the current ripple for LED driver A #1. Similar statistical methods were performed to the data of LED driver B #2, and LED driver B #3, as shown in Fig 10-2 and Fig 10-3.

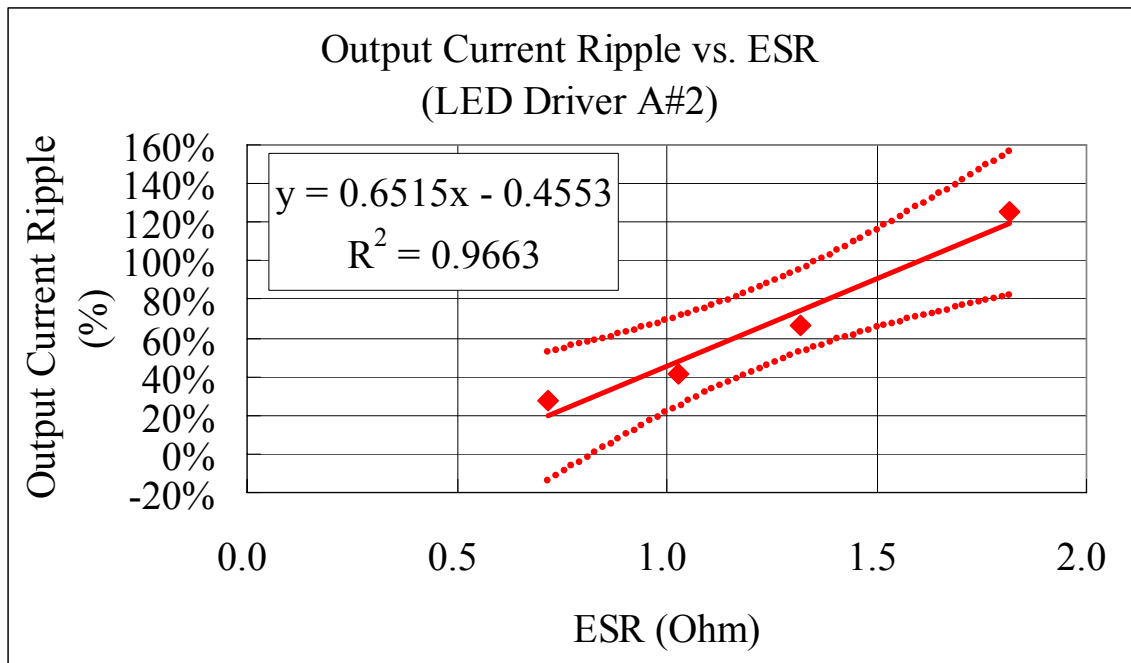


**Fig 10-2 Relationship between output current ripple and ESR of LED driver A #2 (Dotted lines represent 95% confidence level boundaries.)**

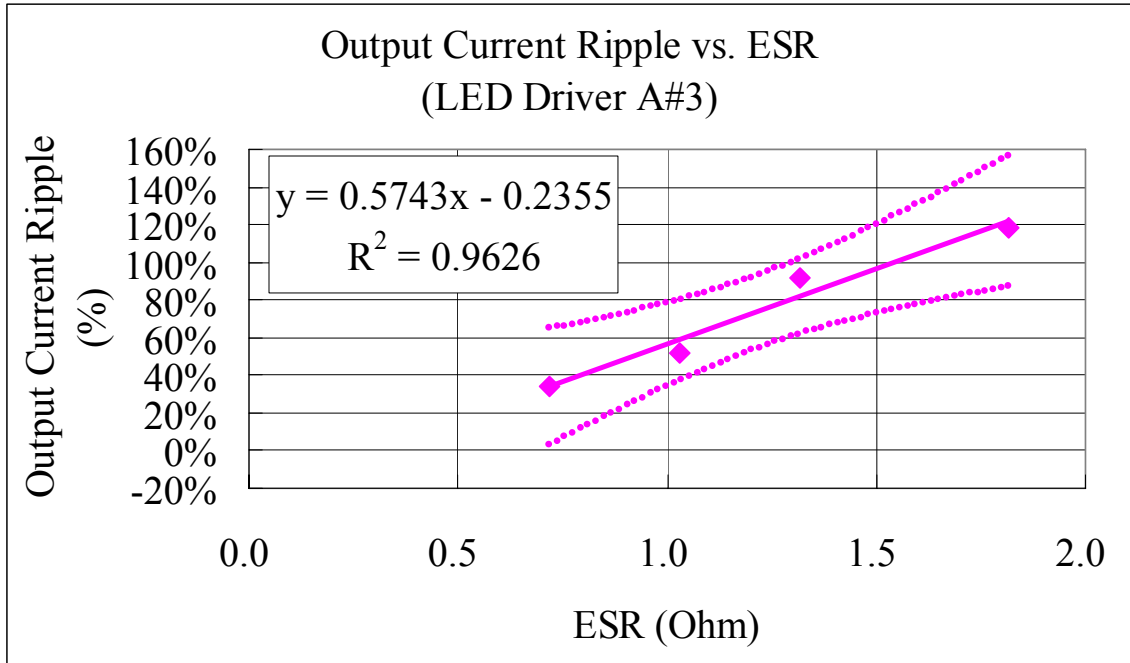


**Fig 10-3 Relationship between Output Current Ripple and ESR of LED Driver A #3 (Dotted lines represent 95% confidence level boundaries.)**

Since all of the 3 samples of LED driver A showed consistent trends and were proved to have a statistically reliable positive relationship between current ripple and ESR, the data was averaged at each ESR condition to generate Fig 10-4. A similar statistical analysis was conducted to the combined data of LED driver A in experiment 1. The calculated correlation coefficient is 0.990, which is greater than 0.950 (threshold for  $p = 0.05$ ,  $N = 4$ ). This proves that there is a statistically reliable positive correlation between current ripple and ESR for the LED driver A. 95% confidence level calculation shows that, the slope upper limit is 1.1851, and the slope lower limit is 0.4689, both of which are positive, suggesting that as ESR increases, there is a reliable increase of the current ripple for LED driver A. This verifies hypothesis 1 for LED driver A.

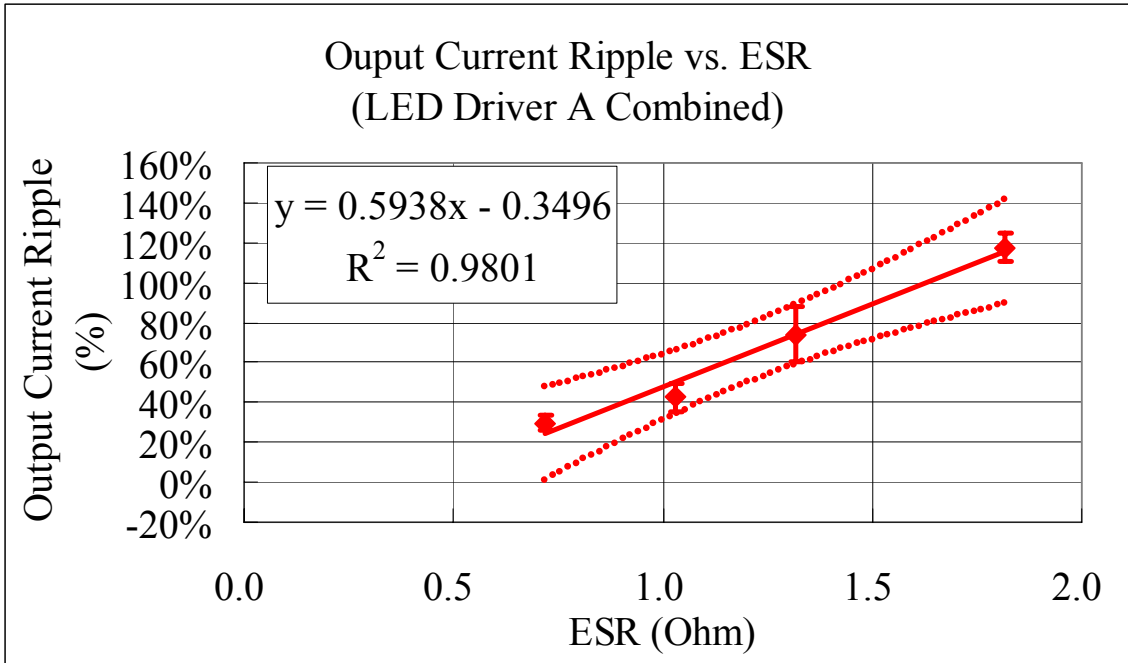


**Fig 10-4 Relationship between output current ripple and ESR of LED driver A (Dotted lines represent 95% confidence level boundaries.)**

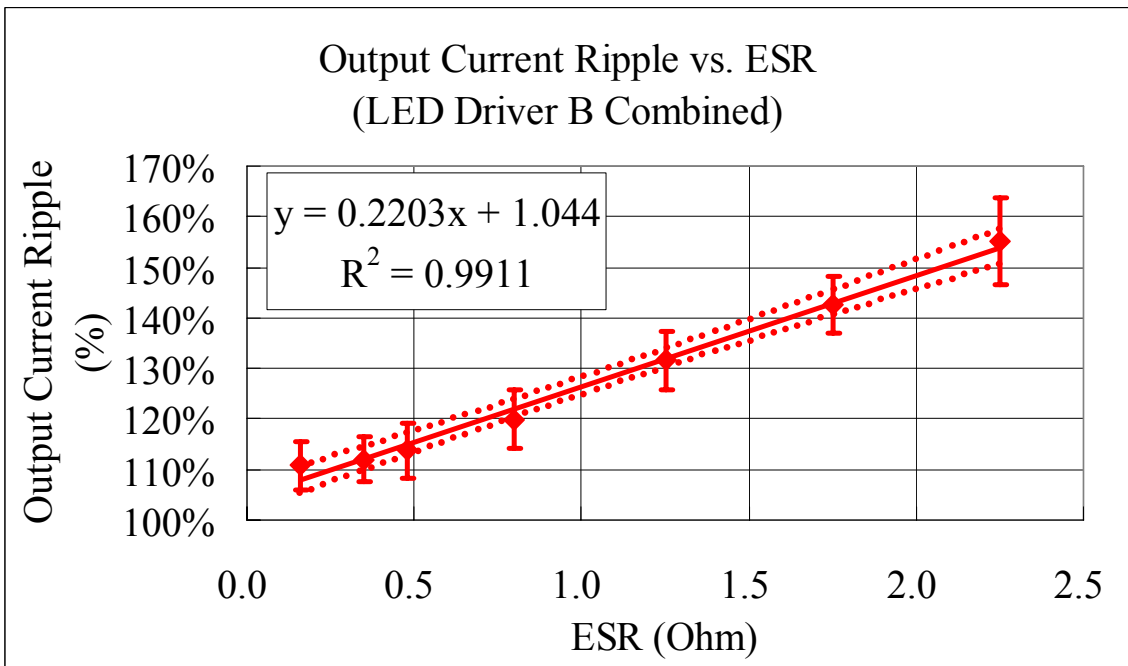


**Fig 10-5 Relationship between output current ripple and ESR of LED driver B (Dotted lines represent 95% confidence level boundaries.)**

Data of 3 samples of the LED driver B went through the same data processing procedure as described above. Fig 10-5 shows the relationship between ESR and output current ripple using combined data from 3 samples of LED driver B. A similar statistical analysis was conducted to the combined data of LED driver B in experiment 1. The calculated correlation coefficient is 0.996, which is greater than 0.754 (threshold for  $p = 0.05$ ,  $N = 7$ ). This proves that there is a statistically reliable positive correlation between current ripple and ESR for the LED driver B. 95% confidence level calculation shows that, the slope upper limit is 0.2443, and the slope lower limit is 0.1964, both of which are positive, suggesting that as ESR increases, there is a reliable increase of the current ripple for LED driver B. This verifies hypothesis 1 for LED driver B.

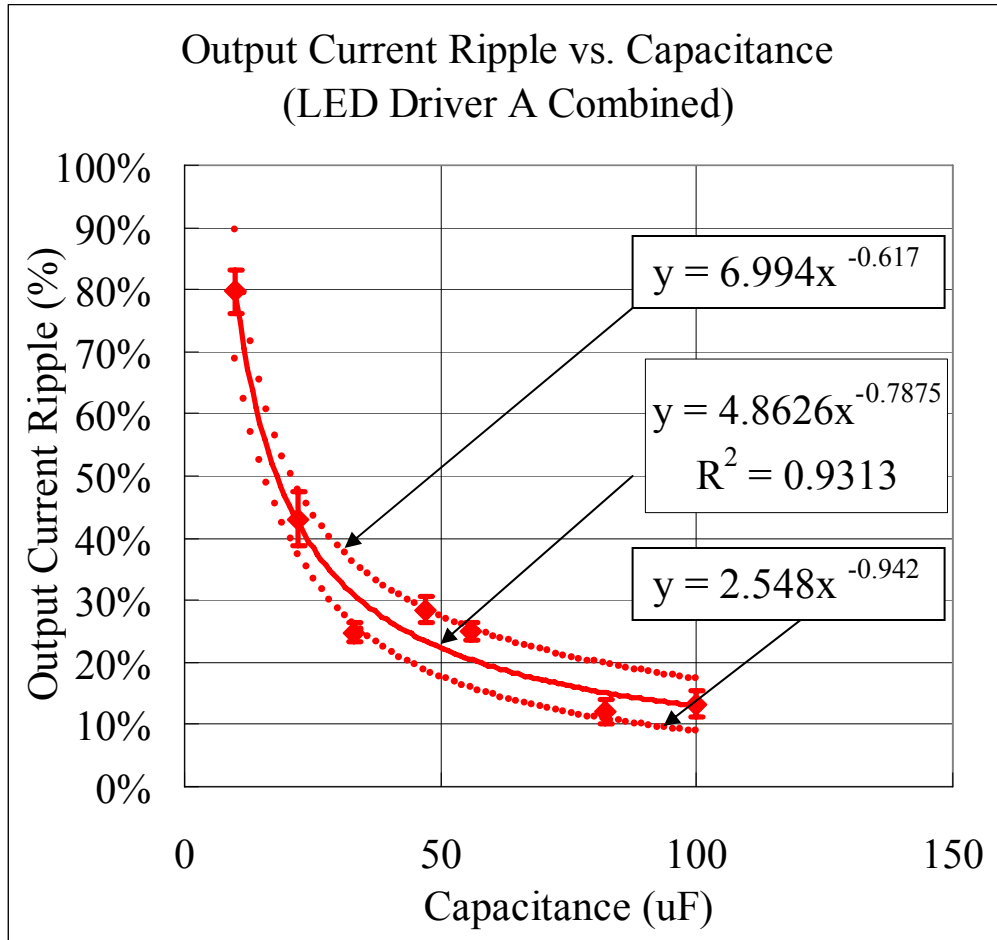
Fig 10-6 shows the relationship between capacitance and output current ripple for LED driver A. Performing the first statistical analysis method yields a calculated correlation coefficient of - 0.821, which is greater than 0.754 in absolute value (threshold for  $p = 0.05$ ,  $N = 7$ ). This proves that there is a statistically reliable negative correlation between current ripple and capacitance for the LED driver A. Notice that this set of data can be well fit using power function in the form of  $y = ax^b$ . The 95% confidence level calculation yields the range of parameter  $a$  and  $b$ .

$$2.548 \leq a \leq 6.994 ,$$

$$-0.942 \leq b \leq -0.617 .$$

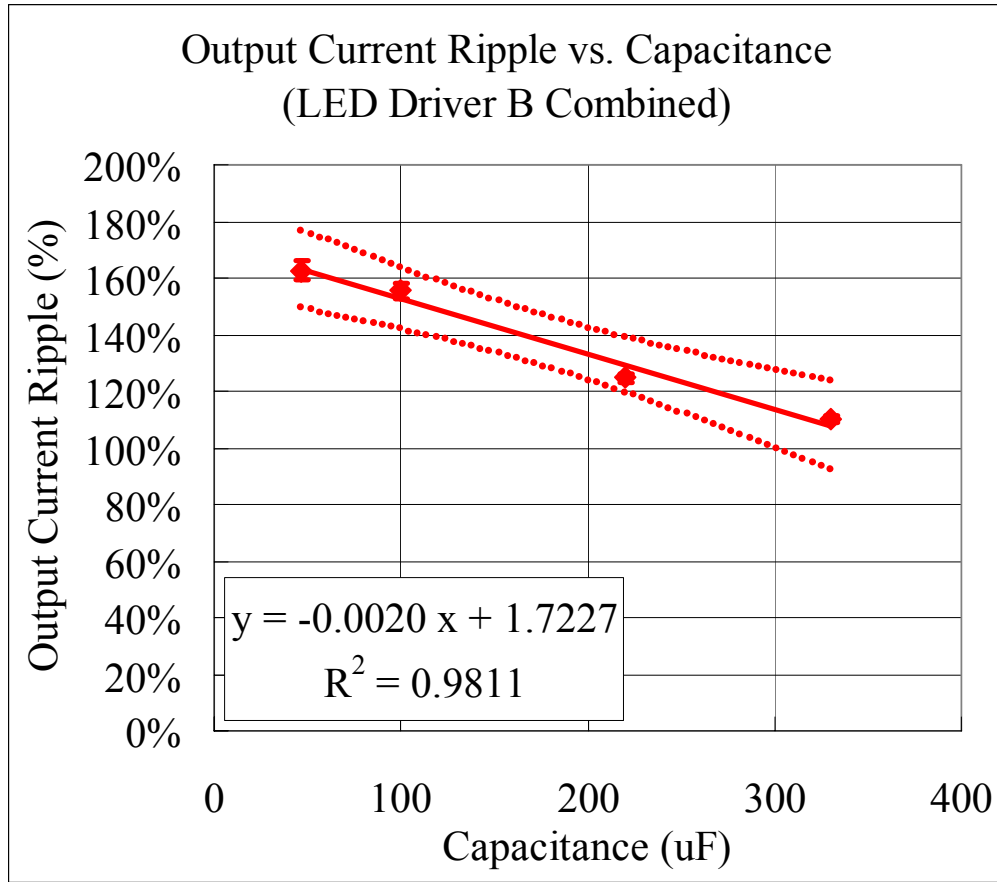
Given  $10 \leq x \leq 100$ , the 1<sup>st</sup> derivative  $y' = abx^{b-1} < 0$ .

This suggests that as capacitance decreases, there is a reliable increase of the current ripple for LED driver A. This verifies hypothesis 2 for LED driver A.



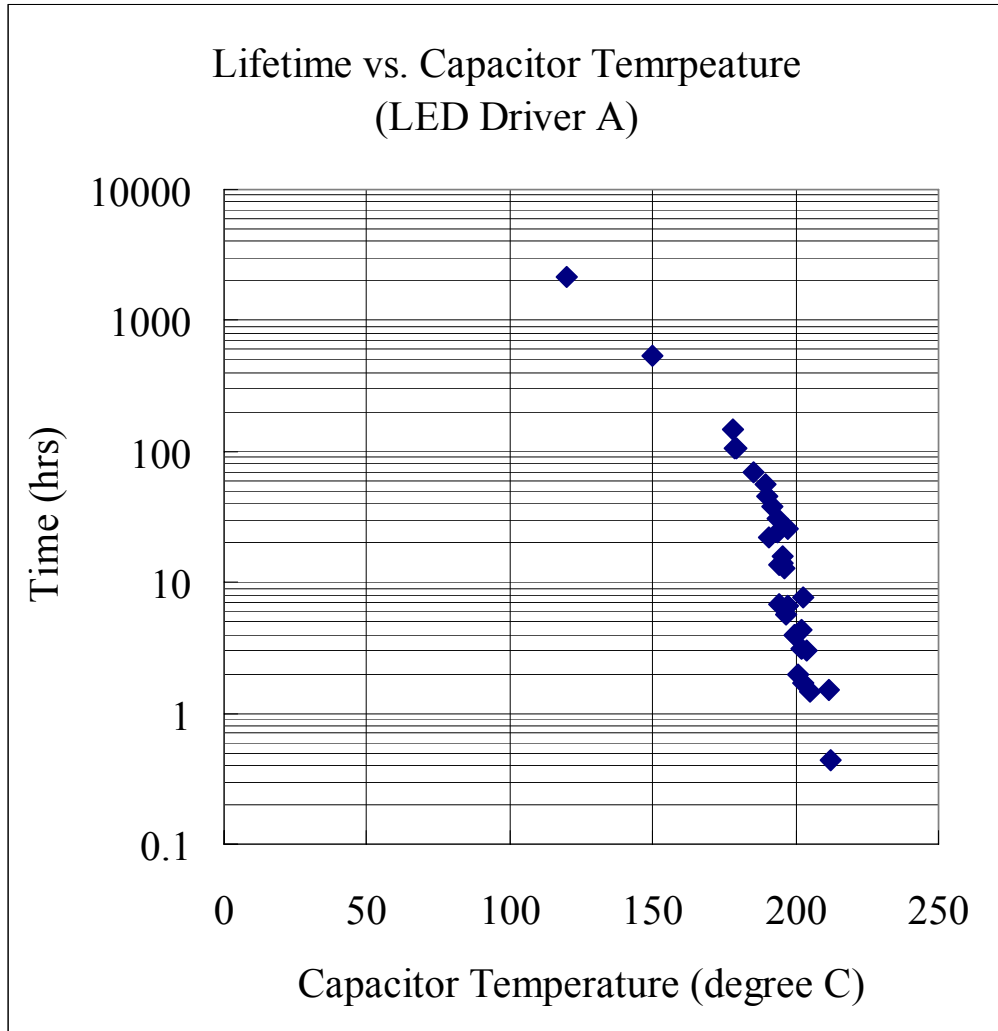
**Fig 10-6 Relationship between output current ripple and capacitance for LED driver A (Dotted lines represent 95% confidence level boundaries.)**

Fig 10-7 shows the relationship between capacitance and output current ripple for LED driver B. Performing the first statistical analysis method yields a calculated correlation coefficient of - 0.991, which is greater than 0.950 in absolute value (threshold for  $p = 0.05$ ,  $N = 4$ ). This proves that there is a statistically reliable negative correlation between current ripple and capacitance for the LED driver B. using a linear curve fit, the 95% confidence level calculation shows that, the slope upper limit is - 0.0011, and the slope lower limit is - 0.0028, both of which are negative, suggesting that as capacitance decreases, there is a reliable increase of the current ripple for LED driver B. This verifies hypothesis 2 for LED driver B.



**Fig 10-7 Relationship between output current ripple and capacitance for LED driver B (Dotted lines represent 95% confidence level boundaries.)**

Fig 10-8 shows the relationship between LED driver A's useful lifetime and its capacitor temperature. Using the first statistical analysis method shows that the calculated correlation coefficient is  $-0.876$ , whose absolute value is greater than  $0.349$  ( $p = 0.05$ ,  $N = 32$ ). This confirms that there is a statistically reliable negative correlation between useful life and capacitor temperature for LED driver A. This verifies hypothesis 3 for LED driver A.



**Fig 10-8 Lifetime profile of LED driver A**

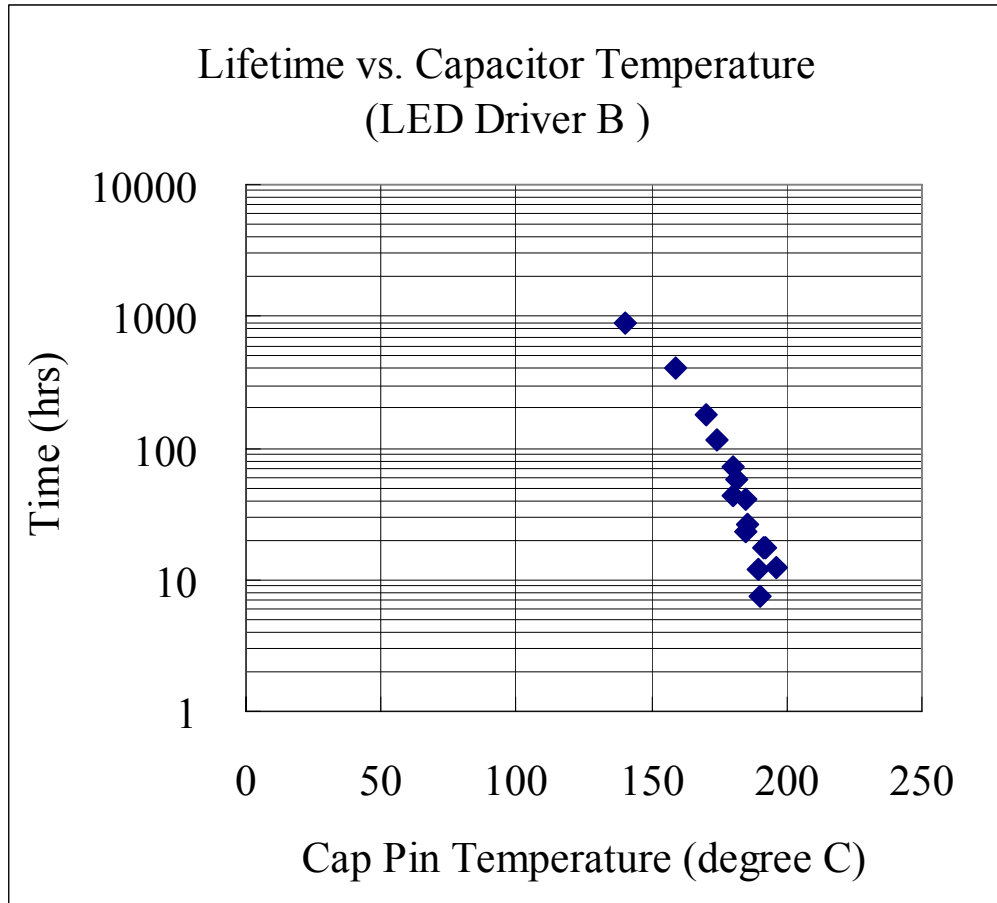


**Fig 10-9 Lifetime profile of LED driver B**

Fig 10-9 shows the relationship between LED driver B’s useful lifetime and its capacitor temperature. Using the first statistical analysis method shows that the calculated correlation coefficient is  $-0.942$ , whose absolute value is greater than  $0.497$  ( $p = 0.05$ ,  $N = 15$ ). This confirms that there is a statistically reliable negative correlation between useful life and capacitor temperature for LED driver B. This verifies hypothesis 3 for LED driver B.